Neural correlates of early- and late-stage learning in the hippocampus and postrhinal cortex

Valerie Joy Estela-Pro
B.S. Lehigh University 2011

Submitted in partial fulfillment of the requirements for the Degree of Doctor of Philosophy in the Department of Neuroscience at Brown University

Providence, Rhode Island
February, 2021

Signature page

This dissertation by Valerie Estela-Pro is accepted in its present form by the Department of Neuroscience as satisfying the dissertation requirements for the degree of Doctor of Philosophy.

Date: _____ _____
Rebecca D. Burwell, PhD, Advisor

Recommended to the Graduate Council

Date: _____ _____
Barry W. Connors, PhD, Reader

Date: _____ _____
Christopher I. Moore, PhD, Reader

Date: _____ _____
Stephanie R. Jones, PhD, Reader

Date: _____ _____
Jeffrey S. Taube, PhD, Outside Reader

Approved by the Graduate Council

Date: _____ _____
Andrew G. Campbell, PhD, Dean of the Graduate School

Curriculum Vitae

VALERIE ESTELA-PRO

EDUCATION

Ph.D.	Neuroscience	**Brown University** (Providence, RI) Neuroscience Department	**GPA: 4.0/4.0**	2014 - 2020
BSc	Biology	**Lehigh University** (Bethlehem, PA) Department of Biology	**GPA: 3.3/4.0**	2007-2011

GRANTS AND FELLOWSHIPS

NIH F99/K00 DSPAN Scholar	National Institutes of Health (USA)	2018 – 2024
NSF Graduate Research Fellow	National Science Foundation (USA)	2015 – 2018
Hispanic Scholarship Award	Hispanic Scholarship Fund (USA)	2016

RESEARCH EXPERIENCE

Graduate	**Brown University** (RI, USA) Rebecca Burwell, PhD	2014 - 2020
Industry	**WIL Research LLC** (OH, USA)	2011 - 2014
Undergraduate	**Lehigh University** (PA, USA) Murray Itzkowitz, PhD	2010 - 2011

PUBLICATIONS

A.N. Bloch, **V.J. Estela**, J.M. Leese, M. Itzkowitz, Male mate preference and size-assortative mating in convict cichlids: a role for female aggression?, Behavioural Processes, Available online 18 July 2016, ISSN 0376-6357, http://dx.doi.org/10.1016/j.beproc.2016.07.010. (http://www.sciencedirect.com/science/article/pii/S0376635716301632)

IN PREPARATION

V.J. Estela, R.D. Burwell. The rodent postrhinal cortex: a review
V.J. Estela, R.D. Burwell. Postrhinal interactions with the hippocampus during a location bi-conditional task
V.J. Estela, S.G. Trettel, R.D. Burwell. Potentially novel oscillation patterns in rats during a complex discrimination task

TEACHING AND MENTORING EXPERIENCE

Guest Lecturer	Psych 345: Physiological Psychology Undergraduate course, Rhode Island College, RI I designed and delivered a guest lecture on learning and memory in this upper level psychology course	Fall 2017
Teaching Associate	The Secret Lives of Animals: A view into their brains and behaviors Middle - high school course, STEM II Program, Brown University, RI I designed and taught both lectures and labs in this 2-week immersive course together with 2 other graduate students in the Neuroscience department.	July 2017
Senior Scholar	Designing and Delivering Scientific Presentations Graduate Student module, IMSD Program, Brown University, RI Helped teach other graduate students best practices in both poster and oral presentations	March 2017
Teacher/Mentor	Brown Science Prep High school student program, Brown University, RI Wrote, edited, and taught lessons from across STEM fields to high schoolers participating in this program	September 2016 - Present
Teaching Assistant	Neural Systems (NEUR1030) Undergraduate course, Brown University, RI In this upper level neuroscience course, I prepared and delivered lectures and quizzes, facilitated discussions on class material, and graded exams (115 students, 1½ hour classes)	Fall 2015
Teaching Assistant	Reflective Teaching Seminar Graduate certificate course, Sheridan Center, Brown University, RI I led a workshop section for a year-long, graduate-level certificate course. I prepared materials and facilitated discussions (15 students, 2-hour sessions)	September 2015 - Dec 2016
Graduate Mentor	African American, Latino, Asian/Asian American, and Native American (ALANA) College student program, Brown University, RI Mentored minority undergraduate students in an effort to inform undergraduate students about the possibilities within the sciences and to encourage diversity within the STEM fields.	August 2014 - May 2015

TEACHING CERTIFICATES

(Sheridan Center for Teaching and Learning, Brown University)

Teaching Consultant Program Certificate IV	As a consultant for the Sheridan Center, I observe classrooms across university departments and provide feedback for instructors (~2/month)	2015-Present
Reflective Teaching Seminar Certificate I	In this year-long seminar, I learned about core principles of teaching, like course/syllabus design, grading & evaluation, and theories of learning.	2014-2015

TALKS

Dept. Seminars	"Navigating the development of a novel behavioral task"	**Brown University** (RI)	2018
	"Characterizing representations in the postrhinal cortex during a location bi-conditional spatial memory task"	**Woods Hole Marine Biological Laboratory** (MA)	2018
	"Representations in the postrhinal cortex during a spatial discrimination [illegible]"	**Brown University** (RI)	2018
	"Emergence of object-location conjunctive coding in the postrhinal [illegible]"	**Brown University** (RI)	2017
	"Object-context conjunctive coding in episodic memory"	**Brown University** (RI)	2016
Conference Talks	"Novel oscillatory events during a cognitively demanding task"	**NIH Blueprint Diversity Conference**	2020
	"Representations in the postrhinal cortex during a spatial discrimination task"	**SACNAS Regional Meeting** (MA)	2018
	"Emergence of object-location conjunctive coding in the postrhinal cortex and hippocampus"	**SACNAS Regional Meeting** (MA)	2017
Outreach	"Let's talk about BRAINS!"	**K-12 classrooms** (20+, RI)	2016 - 2018
	"E.D.G.E: Encouraging Diversity and Growth in Education"	**Orange County High School** (VA)	2015

POSTER PRESENTATIONS

Estela VJ, Burwell RD (2018) "Characterizing representations in the postrhinal cortex during a location bi-conditional spatial memory task" Society for Neuroscience 48th Annual Meeting, San Diego, CA

Estela VJ, Farovik A, Burwell RD (2017) "Object-location conjunctive coding in the parahippocampal network" Society for Neuroscience 47th Annual Meeting, Washington DC

Estela VJ, Burwell RD (2017) "Emergence of object-location conjunctive coding in the postrhinal cortex and hippocampus" Brown University Neuroscience Graduate Program Annual Retreat, Bristol, RI

Estela VJ, Burwell RD (2016) "Emergence of object-location conjunctive coding in the postrhinal cortex and hippocampus" Society for Neuroscience 46th Annual Meeting, San Diego, CA

Estela VJ, Burwell RD (2016) "The science of what happens where: The role of the perirhinal cortex in object-location conjunctive coding" Brown University Neuroscience Graduate Program Annual Retreat, Bristol, RI

Estela VJ, Burwell RD (2016) "The science of what happens where: The role of the perirhinal cortex in object-location conjunctive coding" 2nd Annual Young Scholars Conference, Providence RI

Estela VJ, Udawatta M, Dortch A, Burwell RD (2015) "Sex- and Light Phase- Based Differences in Spontaneous Object Recognition Performance" Brown - NIH Graduate Partnership Program Retreat, Woods Hole, MA

Estela VJ, Udawatta M, Dortch A, Burwell RD (2015) "Sex- and Light Phase- Based Differences in Spontaneous Object Recognition Performance" Brown University Neuroscience Graduate Program Annual Retreat, Bristol, RI

Estela VJ, Leese JM, Itzkowitz M (2011) "The influence of female size on male aggression and mate preference in the convict cichlid" 8th annual Lehigh Valley Ecology and Evolution Symposium, Bethlehem, PA

OUTREACH / ADVOCACY

Community Coordinator	**Graduate Women in Science and Engineering (GWiSE)** (Brown University, RI) We aim to foster an inclusive and supportive community for the women graduate students throughout the STEM fields at Brown. We organize events both within Brown for the students as well as outreach opportunities within the greater Providence community.	January 2017 - Present
Secretary	**Society for the Advancement of Chicanos/Hispanics and Native Americans in Science (SACNAS)** (Brown University, RI) SACNAS is an inclusive organization designed to support the success of Chicanos/Hispanics and Native Americans in advanced STEM degrees. We provide social and professional development activities for the community as well as outreach opportunities in local schools to promote diversity in STEM from an early age.	January 2015 - May 2017

Conference Coordinator	**Young Scholars Conference (YSC)** (Brown University, RI) This event promotes the advancement of womxn graduate students and postdoctoral researchers through scientific engagement, professional development workshops, and feedback from faculty members at Brown.	January 2017 -October 2018

UNIVERSITY SERVICE

Student Representative	**Neuroscience Graduate Program** (Brown University, RI) I was the liaison between students in our graduate program and the faculty directors. I held town hall-style meetings for our students and brought any concerns to the directors anonymously. I also served on the admissions committee for our graduate program and started a mentoring program pairing our incoming first-year students with upper-year students to ease the transition process into graduate school.	May 2017 - May 2018
Retreat Organizer	**Neuroscience Graduate Program** (Brown University, RI) I organized a student-focused retreat for our graduate students at the Marine Biological Labs in Woods Hole, MA. Activities included an improve ice breaker that I designed, a "Cohort Q&A" that provided the opportunity for students in different stages of their graduate career to ask more advanced students questions, a AAAS Science communication work shop, and a "Faculty Journeys" session where Brown faculty members talked about their life/career paths that brought them to Brown.	October 2017
Panelist	**CareerLAB** (Brown University, RI) I served on a panel with 2 other graduate students to talk about the admissions process to graduate school and navigating the first few years	Fall 2017
Recruitment Travel Coordinator	**Neuroscience Graduate Program** (Brown University, RI) I coordinated travel for our recruitment weekend, including individual pick-ups and drop offs of each recruit as well as group movements between scheduled items	Spring 2017
SfN Social Coordinator	**Neuroscience Department** (Brown University, RI) I coordinated the Brown Neuroscience Social at the Society for Neuroscience (San Diego). This included soliciting funding and participation from multiple groups within Brown including the Brown Institute for Brain Science, the Neuroscience Department, and the Neuroscience Graduate	Fall 2016

	Program as well as advertising to all current and past students and alumni.	
Retreat Organizer	**Neuroscience Graduate Program** (Brown University, RI) I organized the annual Neuroscience Graduate Program retreat at the Haffenreffer Estate in Bristol, RI. This included catering, talks from Brown and NIH faculty members and students, a poster session, and activities.	Fall 2015
Social Coordinator	**Neuroscience Graduate Program** (Brown University, RI) I facilitated labs hosting Friday socials to encourage socializing within the program and outside of a single lab. I also fundraised among students and faculty members to fund these socials	Spring 2015 -Fall 2017

AWARDS AND HONORS

- Winner of the B C OF SIGMA XI Prize (2018)
- Sigma Xi Society Nomination (2017): An international honor society of science and engineering
- Winner of Best Undergraduate Presenter Award at the Lehigh Valley Ecology and Evolution Symposium (2011): Given to the undergraduate presenter who conducted and discussed the best executed and most comprehensive study.
- Lehigh Scholar Award (2007-2011): Awarded to students who maintain a 3.0 GPA or better and excelled academically and demonstrated leadership abilities.

Acknowledgements

First and foremost, I'd like to thank my mentor, Rebecca Burwell. She has provided me with all of the skills and tools necessary to fulfill my dream of becoming a professor, and I am truly grateful for all of the work, time, and effort she has put into me to get me to where I am today.

I would also like to thank past and current members of the Burwell lab, without whom this project would not have been possible. Inês Tomás Pereira and Victoria Heimer-McGinn were the first people who introduced me to the lab. It was through working with them initially that I fell in love with the research and the lab, and without their guidance, both scientific and personal, I would not have made it through graduate school. I would also like to thank Kevin Li, an undergraduate researcher who worked incredibly hard with me through the especially bumpy beginning of this research, working with me through issues as they arose and being patient with me as I learned to mentor. I'd like to thank Fang-Chi Yang for setting the bar incredibly high as well as helping me try to reach it, and I'd also like to thank Eunkyu Hwang for always helping me figure out answers to my questions and keeping me sane while we were on this crazy ride together. Thank you also to Taylor Wise who made bad days easier and good days better. Thank you to Sean Trettel for the extensive help on the new drives and helping to figure out our cool new data. Finally, an extra huge thank you to Devon Poeta for keeping the lab running perfectly, training me in practically everything, and keeping me going through my many failures so I could eventually make it to where I am today.

Thank you to my committee members Chris Moore, Barry Connors, and Stephanie Jones for all the help and guidance throughout the years. I would not have become the scientist I am now without your wisdom and advice. I would also like to thank Jeffrey Taube for agreeing to be my outside thesis reader during a very hectic and uncertain time.

I'd like to thank the NSGP program for the support and opportunities they have provided. I owe any of my current and future successes to the fact that they were willing to believe in me.

I'd like to thank my friends, near and far, for all the love and support they provided through the many ups and downs of graduate school. The visits, phone calls, and check-ins are what kept me going. I'd like to especially thank Robyn St. Laurent and Veronica Ryan for their constant support and the innumerable times they helped me through every kind of problem.

Finally, I'd like to thank my family. Your love, support, and encouragement made this possible. Thank you especially to my grandparents; there is no question, I would not be here without you. Thank you, most of all, to my incredible husband. You encouraged me to follow my dream when it was just a crazy idea, and you have done more than I ever imagined one person could do for another to help get me through this. Thank you.

Preface

The rodent postrhinal cortex, homologous to the primate parahippocampal cortex, has an important role in the medial temporal lobe memory network for spatial, episodic, and associative memory, but there is a lack of consensus about the precise function of this region and how its functions differ from those of the hippocampus. By one view, the postrhinal cortex is a simple conduit for spatial information, and the hippocampus both configures a representation of context and then employs that representation in associative learning and episodic memory. Here I provide evidence for the alternative view that the postrhinal cortex, itself, represents environmental contexts and monitors such contexts for changes. By that view, the hippocampus is provided a representation of context by the postrhinal cortex in the service of associative learning and episodic memory.

A number of anatomical and functional studies have compared or dissociated the POR from other medial temporal lobe involved in learning, memory, and memory-guided behavior, but there are no in-depth reviews, particularly covering the last two decades of research. Thus, in the first chapter, I provide a detailed review of the anatomical and functional connectivity as well as the proposed behavioral functions of this region in rodents.

The second chapter reports the results of an electrophysiological study in behaving rats in which I recorded single cells and local field potentials in both the postrhinal cortex and the hippocampus. Neuronal correlates of cells in both regions exhibited a pattern of activity thought to be a signature of context representations. Importantly, this signature appeared earlier in the postrhinal cortex suggesting that

context is represented there and transmitted to the hippocampus for associative learning and episodic memory.

In the third chapter, I report the discovery of a novel phenomenon in the rodent brain, a brain oscillation that exhibits strong similarities to alpha oscillations as they have recently been described in the human brain. To our knowledge, this is the first demonstration of alpha in the rodent brain.

Finally, in the last chapter, I discuss the findings and propose that the postrhinal cortex and the hippocampus can be functionally differentiated during associative learning and that the differences lie in when and where environmental context is represented.

Table of Contents

Chapter 4: Conclusions: Functional differentiation of the hippocampus and postrhinal cortex during associative learning

List of Tables

Chapter 2

List of Figures

Chapter 1

Chapter 2

Chapter 3

Chapter 4

CHAPTER 1

THE POSTRHINAL CORTEX: AN IN DEPTH ANATOMICAL AND FUNCTIONAL REVIEW

Abstract

The parahippocampal cortex has an important role within the medial temporal lobe memory network for spatial and episodic memory, but the precise function of this region remains unclear. Fortunately, the rodent postrhinal cortex (POR) provides a structural and connectional homolog to the parahippocampal cortex that is defined in non-human primates and humans. This important homology allows for direct comparisons between functions found in rodents and those proposed in humans, while allowing for the use of powerful tools not yet available in human research. Although there have been many papers anatomically and functionally comparing or dissociating the POR from other important areas within the medial temporal lobe that are involved in learning, memory, and memory-guided behavior, there are no in-depth reviews, particularly covering the last two decades of research. Here, we review the anatomical and functional connectivity of this area in rats, examine the previously proposed behavioral functions of this region, and suggest a model of this region's role that accounts for the wide array of observations. Finally, we use these observations to elucidate the functions of the human parahippocampal cortex.

Introduction

The medial temporal lobe (MTL) is implicated in both episodic memory and spatial learning. Based on lesion studies utilizing extensive behavioral tests combined with anatomical studies, the regions within the MTL are well identified and, to a certain extent, functionally dissociated. The POR is understood to be a key component in the MTL memory system since its initial anatomical and connectional dissociation from the perirhinal cortex (Burwell et al., 1995; Deacon et al., 1983), but its specific function within this system remains unclear. Previous reviews focused on differentiating the POR from other regions within the MTL, such as the hippocampus and perirhinal cortex (Aggleton et al., 2012), the entorhinal cortices (Eichenbaum et al., 2007), and the retrosplenial cortex (Bucci & Robinson, 2014), but an analysis of the proposed functions of the POR, itself, has yet to be done. This is problematic as the proposed functions of the POR vary widely, with little to no consensus on a framework that bridges the observations. Here, we review the evidence from anatomical and functional studies of the rat POR and propose a unified theory of how the POR contributes to the hippocampal memory system.

Anatomy of the POR

Location and Structure

The POR is located near the caudal pole of the rat brain. It is bordered rostrally by the perirhinal cortex (PER) from which it was originally separated (Figure 1.1A, D). The POR is further bordered dorsally by visual association cortex, ventrally by the medial entorhinal cortex (MEC; Burwell, Witter, and Amaral, 1995), and medially by agranular retrosplenial cortex at its most caudal extent (Vogt & Miller, 1983). Interestingly, in both

rodents and primates, the parasubiculum inserts itself between the POR and MEC (Figure 1.1D-E).

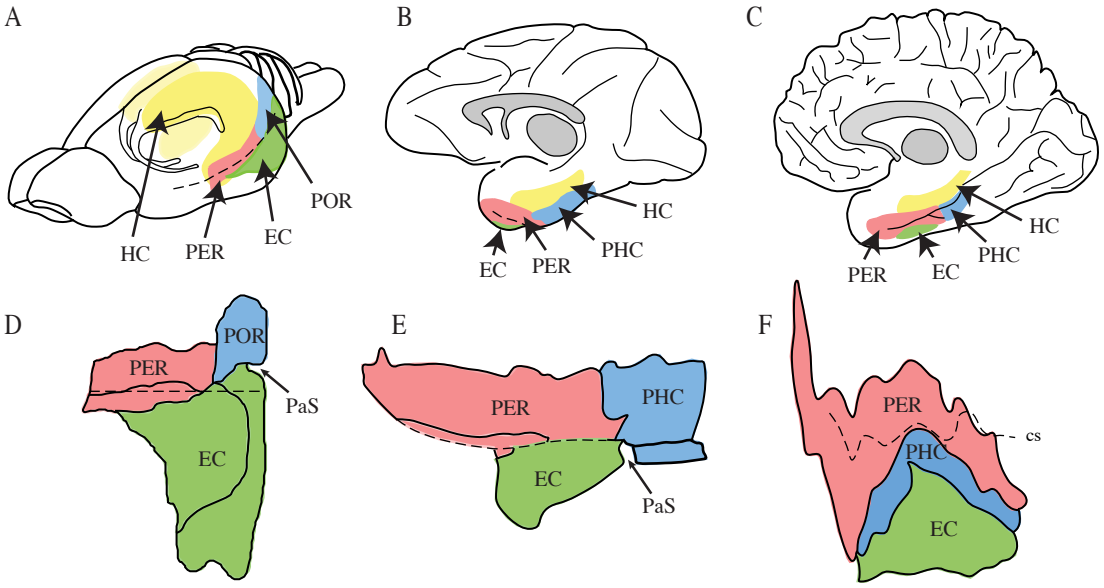

Figure 1.1 Schematics and surface views are shown for the parahippocampal region. A. Oblique surface view of the rat brain showing perirhinal (PER) areas 35 and 36 in red, the postrhinal cortex (POR) in blue, and the entorhinal cortex (EC) in green, and the hippocampus (HC) in yellow. (B) Mid-sagittal schematic of the monkey brain showing the PER, EC, and HC using the same color scheme. The parahippocampal cortex (PHC), the primate homolog of the rodent POR, is shown in blue. C. Mid-sagittal schematic of the human brain showing the PER, PHC, EC, and HC using the same color scheme. D-F. Shown are unfolded maps of the PER, POR/PHC, and EC for the rodent (D), monkey (E), and human (F) brains. Adapted from Burwell (2000). PaS=parasubiculum.

Cytoarchitecturally, the POR can be identified by the presence of ectopic layer II cells in layer I at the region's border with the PER and MEC (Figure 1.2). A more densely packed layer II as compared to that of the PER further defines the POR, as does its deep layers, which contain elongated cells oriented radially as compared to the elongated cells oriented horizontally in the PER.

Three main cell types have been recorded in the POR, including two major inhibitory classes and a single, functionally restricted class of pyramidal cells (Sills et al., 2012). Fast-spiking cells, composed entirely of multipolar nonpyramidal cells, and low

threshold-spiking cells, composed mainly of multipolar and bitufted dendrites make up the two inhibitory classes of cells found in the POR. Interestingly, there is a specific lack of parvalbumin expressing fast-spiking cells in the ventral portion of the POR, distinguishing it from surrounding cortical regions (Sugden, 2015; Beaudin et al., 2012; de Curtis and Paré, 2004). The more homogenous pyramidal cells make up the third class of regular-spiking cells (Sills et al., 2012). Interestingly, no intrinsically bursting pyramidal neurons were seen in the POR, which is similar to what is seen in the entorhinal cortices, but specifically different from what is seen in the PER.

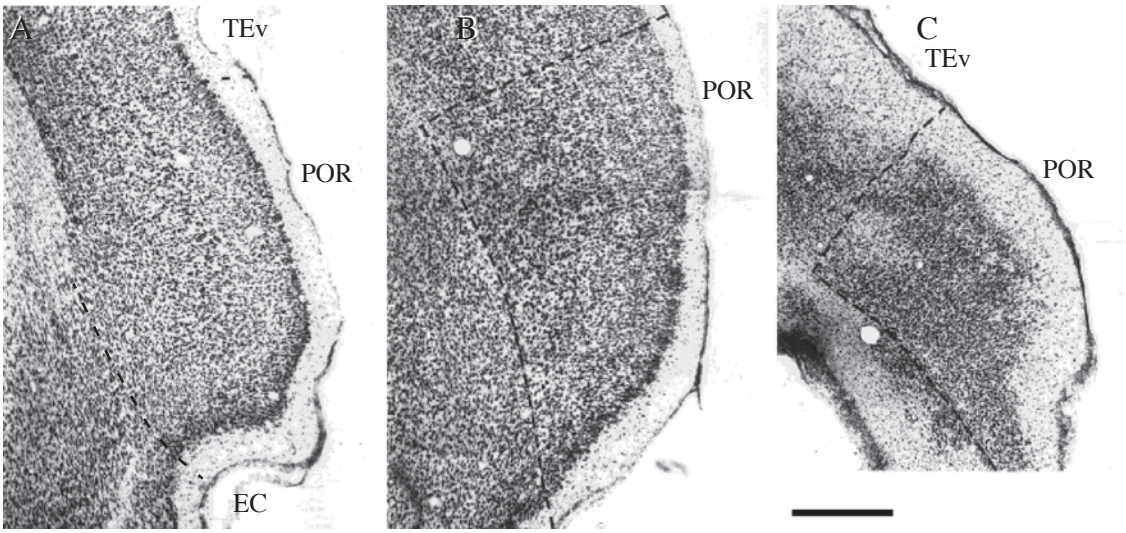

Figure 1.2 Nissle-stained coronal sections showing the POR and adjacent cortical regions at three rostro-caudal levels (Burwell, 2001): -7.64 mm, -8.34, and -9.16 relative to Bregma. Scale bar = 500 um. Abreviations: TEv, ventral temporal cortex; EC, entorhinal cortex. Figure adapted from Burwell (2000).

POR Afferents

Cortical Afferents

A schematic of the major connections of the POR is shown in Figure 1.3. Approximately two-thirds of the afferent connections to the POR come from cortical regions, with a large portion of these originating in visual association and visuospatial areas (Burwell & Amaral, 1998b). Specifically, about half of the cortical projections to

the POR originate in the occipital regions including the lateral and medial visual association areas as well as primary visual cortex (Burwell & Amaral, 1998b). Further, the POR is heavily reciprocally innervated by the posterior parietal cortex, which is known to be important in movement planning, spatial reasoning, and attention, as well as the ventral temporal association areas, which receive projections from motion detection regions and object recognition regions, and are thought to be involved in the interpretation of dynamic moving objects. The retrosplenial cortex, especially the dorsal retrosplenial cortex, also heavily innervates the POR. This region is known to be important for using surrounding visual cues to accomplish tasks. Both the lateral entorhinal and the medial entorhinal regions are reciprocally connected to the POR as well. Finally, there is a weak projection from the frontal regions to the POR, primarily arising in the secondary motor region (Burwell & Amaral, 1998a), and the dorsal and ventral anterior cingulate cortices (Hwang et al., 2018). This pattern of afferents again suggests that the POR receives mainly visual and visuospatial information from the cortical regions.

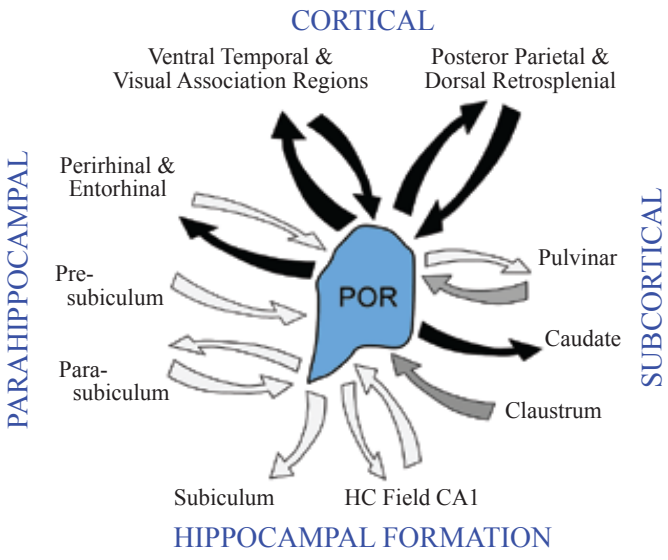

Figure 1.3 Schematic summarizing the cortical, subcortical, hippocampal. and parahippocampal afferent and efferent connections of the postrhinal cortex (POR). Toward the top are the cortical efferents and afferents. On the left are the connections with the structures in the parahippocampal regions. on the right are the stronges connections with subcortical connections. On the bottom are connections with hippo-campal formation structures. Note, strong connections are represented by black arrows, moderate connections are denoted by dark gray arrows, and weak connections are indicated by the light gray arrows. Adapted from Furtak, Wei, Agster, & Burwell, 2007.

Subcortical Afferents

The subcortical connections to the POR are relatively weak, with the exceptions of the dorsal thalamic group and the claustrum. The largest subcortical input to the POR comes from the laterodorsal and lateral posterior areas of the thalamus, with these connections accounting for approximately two fifths of the total subcortical input to the POR (Tomás Pereira et al., 2016). The lateral posterior nucleus, homolog of the pulvinar in the primate brain provides the strongest thalamic connections with the POR. These areas of the thalamus are known to be involved in visual association, visual integration, and spatial cognition. The POR also receives a strong input from the claustrum. This connection accounts for about one fifth of the subcortical input to the POR. The claustrum connects the cortical and subcortical areas of the brain and is thought to play an important role in integrating consciousness. The lateral and basolateral nuclei of the amygdala provide moderate inputs to the POR as well. These amygdalar nuclei are known to be important in contextual fear conditioning. The medial septum also moderately projects to the POR. This nucleus has been found to play an important role in generating theta waves in the hippocampus via inhibitory pacemaking. The hypothalamus also has weak projections to the POR, primarily from the mamillary bodies and the lateral zone. In contrast, the basal ganglia and the olfactory regions provide little to no input to the POR (Tomás Pereira et al., 2016).

Hippocampal Afferents

The majority of hippocampal inputs to the POR come from the presubiculum, particularly the dorsal presubiculum (Agster & Burwell, 2013). These afferents account for approximately seventy percent of the total hippocampal input to POR. Contribution from hippocampus proper to the POR comes almost entirely from dorsal CA1, with a small portion of afferents coming from ventral CA1. There is very little input from CA2 or CA3 to POR and even less direct input from the dentate gyrus. Interestingly, dorsal hippocampus provides substantially more output to the POR than to the other parahippocampal areas such as the perirhinal or entorhinal cortices (Agster & Burwell, 2013).

Parahippocampal Afferents

The parahippocampal region comprises the perirhinal cortex (PER), the POR, the lateral and medial entorhinal cortices (LEC and MEC, and the pre- and para-subiculum (Scaplen, Agster, & Burwell, 2017). The majority of parahippocampal inputs to the POR come from the PER and the entorhinal cortex (Burwell & Amaral, 1998). The POR projects most strongly to the caudal PER, but it does project to the entire rostrocaudal extent. Likewise, the POR projects most strongly to the MEC, but also to the caudal LEC. Of the other parahippocampal structures, the POR projects strongly to caudal parasubiculum as well as the dorsal presubiculum, sometimes also called postsubiculum (Agster & Burwell, 2013).

POR Efferents

Subcortical Efferents

Despite the extremely weak input from the basal ganglia to the POR, the output from the POR to the basal ganglia, specifically the caudoputamen, makes up about one third of the subcortical output from the POR. The dorsal striatum is important in movement planning, and especially in the learning of habitual behavior (Kroemer et al., 2016). The POR also strongly innervates both the dorsal and ventral thalamic groups, with an especially strong reciprocal connection to the lateral posterior nucleus. The POR moderately innervates the amygdala, primarily targeting the lateral amygdala, basolateral amygdala, and central amygdala nuclei. Projections from POR to claustrum are relatively weak, compared to the amount of input received from the area as well as compared to the amount of input claustrum receives from other parahippocampal areas such as the perirhinal and entorhinal cortices. POR input to the septal nuclei is similarly weak, with minimal labeling exclusively in the lateral septal nuclei. Finally, the hypothalamus and olfactory regions had similarly weak input received from the POR (Agster et al., 2016).

Cortical Efferents

Cortically, the POR is more heavily connected with caudal regions than rostral ones. The strongest connections from the POR innervate the dorsal retrosplenial, posterior parietal, visual, and ventral temporal regions, suggesting that the main targets of POR information are visual and visuospatial areas. The strongest projections from the POR terminate in the occipital region, specifically the primary visual cortex and the medial and lateral visual association areas (Agster & Burwell, 2009). Temporally, the POR heavily innervates the ventral temporal association area (Agster & Burwell, 2009) as well as the medial entorhinal cortex (Burwell & Amaral, 1998a; Naber et al., 1997).

These efferents are made up mainly of excitatory projections, which indicates the potential for efficient high-volume information transfer (Koganezawa et al., 2015). The POR also projects to the caudal portion of the lateral entorhinal cortex. For both projections to the entorhinal areas, the POR projects mainly to the lateral band, which in turn projects to the dorsal hippocampus. POR also provides substantial input to cingulate regions, preferentially targeting retrosplenial areas, with moderate innervation to the dorsal retrosplenial area and light innervation to the ventral retrosplenial area. The POR also strongly projects to the posterior parietal cortex, with caudal regions of the POR projecting more strongly than rostral regions (Agster & Burwell, 2009). POR projections to the piriform, insular, and frontal regions were minimal. Frontal projections that do arise come mainly from the deep layers of POR and target the ventrolateral orbitofrontal region (Delatour & Witter, 2002).

Hippocampal Efferents

Just as the majority of hippocampal inputs to the POR were from subicular regions, a majority of the POR outputs to the hippocampus are also to the subicular areas. The POR projects strongest to the caudal parasubiculum, followed closely by the dorsal subiculum and presubiculum. POR projects moderately to both dorsal and ventral CA1, and dorsal dentate gyrus. Projections from the POR to dorsal and ventral CA2 and ventral subiculum are very weak, with little to no projections to dorsal and ventral CA3 or ventral dentate gyrus (Agster & Burwell, 2013).

Parahippocampal Efferents

The parahippocampal efferents largely reciprocate the afferents. The POR projects most strongly to the PER and the entorhinal cortex (Burwell & Amaral, 1998). The POR primarily targets caudal PER, but it targets the entire rostrocaudal extent of the PER. POR projects most strongly to the MEC and the caudal LEC. Tee POR projects strongly to caudal parasubiculum and to dorsal presubiculum (Agster & Burwell, 2013).

Function of the POR

Historically, the POR was understood as a gateway for neocortical visuospatial information to get to the hippocampus (Eacott et al., 1994; Squire et al., 2004), with the dorsal visual stream (the "where pathway") targeting the POR. Likewise, the ventral visual stream (the "what pathway") was viewed as targeting the PER. By this view, the perirhinal cortex projects object information to the lateral entorhinal cortex, which then passes it on to the hippocampus. On the other hand, the postrhinal cortex sends spatial information to the medial entorhinal cortex, which also passes it on to the hippocampus making up the "where" pathway extension. At the end of these pathways, the hippocampus would then bind the object information and the spatial information for the purpose of episodic memory (Eichenbaum, 2000; Eichenbaum et al., 2007; Knierim et al., 2006). This view, however, ignores the cross-talk between these two pathways, such as direct and reciprocal connections between the PER and the POR (Burwell & Amaral, 1998a; Furtak et al., 2007) and direct connections from POR to CA1 (Agster & Burwell, 2013; Naber et al., 2001)(Figure 1.4). Further, this view understates the roles of the regions upstream of the hippocampus by presenting them as simple relay areas. In fact,

the POR has been shown to play an important role in many processing functions that extend well beyond relaying sensory information.

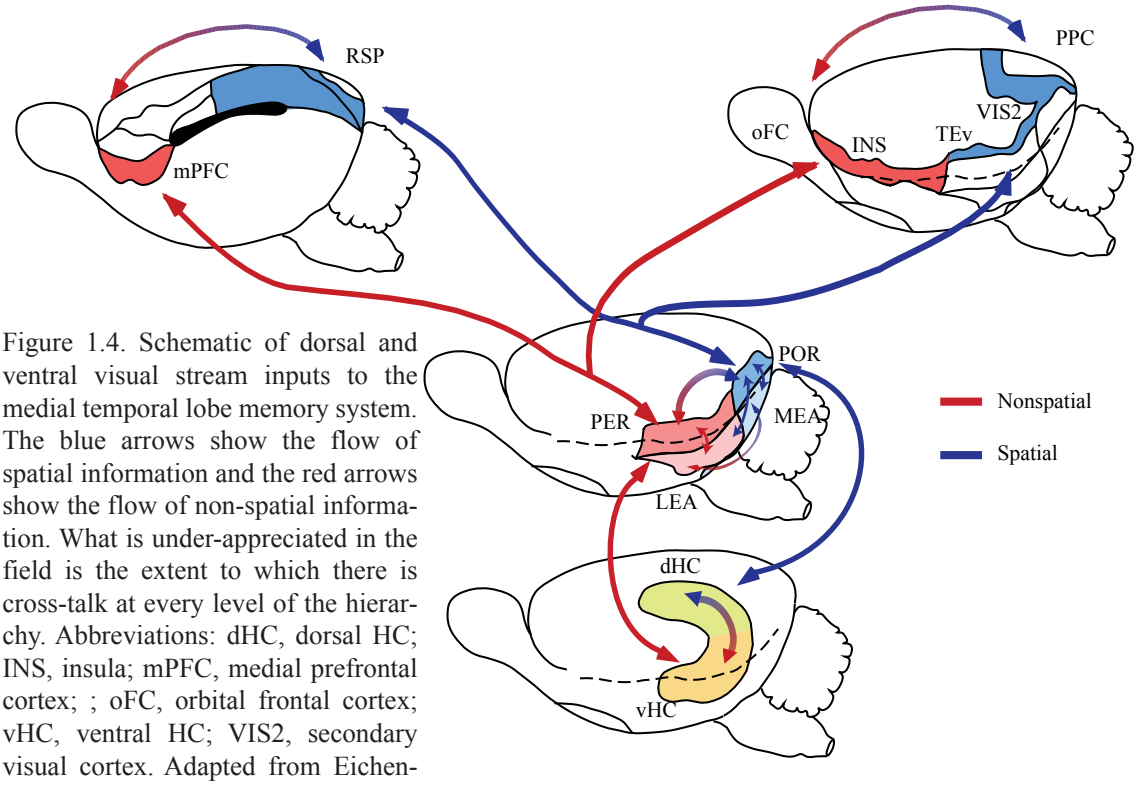

Figure 1.4. Schematic of dorsal and ventral visual stream inputs to the medial temporal lobe memory system. The blue arrows show the flow of spatial information and the red arrows show the flow of non-spatial information. What is under-appreciated in the field is the extent to which there is cross-talk at every level of the hierarchy. Abbreviations: dHC, dorsal HC; INS, insula; mPFC, medial prefrontal cortex; ; oFC, orbital frontal cortex; vHC, ventral HC; VIS2, secondary visual cortex. Adapted from Eichenbaum, 2000, Nat. Rev. Neurosci.

Attentional processes

The link between memory and attention has long been apparent. Appropriate attentional orienting to a stimulus is required for mnemonic processing, but the signal that subserves this process has yet to be identified (Posner et al., 1984). Currently, two systems are suggested for mediating attentional mechanisms. The anterior network is proposed to mediate "top-down" attention by enhancing the neural processing of sensory input, thus increasing the signal-to-noise ratio and facilitating attentional bias. This network primarily includes frontal regions implicated in attention (Posner et al., 1998). In contrast, the posterior network is proposed to mediate "bottom-up" attentional

mechanisms that are driven by target salience and sensory context that in turn trigger attentional processing by higher cortical areas (Posner et al., 1998). This posterior network primarily includes parietal and inferotemporal regions, and these regions are known to be especially important in visuospatial attentional tasks. The POR is heavily interconnected with the regions of the posterior network (Burwell & Amaral, 1998b), and these connections combined with its other subcortical, cortical, and hippocampal connections position the POR to be an ideal region to aid in directing attention for memory. There is evidence to suggest that it does just that. For example, damage to the POR produced deficits in attentional orienting in a conditioned orienting task (Bucci & Burwell, 2004). Further, there is evidence that the POR modulates attention in response to changes in the environmental context. In a cue rotation paradigm, POR cells were shown to remap quickly and unpredictably following cue rotation, and did not return to their baseline firing maps when the cues were returned to their original positions, but rather remapped again (Burwell & Hafeman, 2003). This suggests that POR cells are attending to changes in environmental context, and because of the position of the POR within different networks, this could in turn bias attention in higher cortical areas.

Spatial memory and navigation

There is a fair amount of disagreement in the field about the involvement of the POR in spatial memory and navigation. It has been reported that combined cytotoxic lesions of the PER and POR led to deficits in spontaneous object recognition, but spared function of spatial working memory in a T-maze task (Aggleton et al., 1997). Similarly, combined *N*-methyl-D-aspartate (NMDA) lesions of the PER and POR also disrupted

object discrimination but spared performance on the Morris water maze task as well as the standard radial arm maze task (Bussey et al., 1999). Further, rats with these combined lesions of the PER and POR were reported to outperform controls in a spatially guided T-maze task when the retention delay was increased to 60s (Bussey et al., 2000). These studies convergently suggest that whereas the PER and POR are important in object discrimination and retention, they are not necessary for spatial memory. When the lesions were focused specifically on the POR, the results diverged. Liu and Bilkey (2002) reported that NMDA lesions centered on the POR produced deficits in both the reference memory versions and working memory versions of the Morris water maze task and the radial arm maze task, as well as producing deficits in delay-nonmatching-to-place versions of the radial arm maze and T-maze. Through these experiments they suggested that the POR in fact has a delay-independent role in spatial processing, and that a possible explanation for the discrepancies was that the effect of a combined lesion was not necessarily equal to the sum of the deficits produced by the individual components. Conversely, neurotoxic lesions that were focused on the POR were shown to cause deficits in contextual fear conditioning (Bucci et al., 2000) and contextual discrimination (Bucci et al., 2002), while having no impact on performance on the water maze (Burwell et al., 2004). Further, this group reported that combined lesions of the PER, POR, and entorhinal cortices failed to impair place learning.

Although these results may seem at odds with one another, it is possible that the differences arise from either the interpretation of the data and/or experimental differences. Both sets of studies appear to show that POR lesioned animals perform more poorly on initial tests of spatial memory, but that with repetition, the animals are able to

closely match sham performance. This suggests that either POR is potentially important in the initial learning process of spatial information, or that some aspect of the spatial environment that is generally used to create a representation of space for navigation is missing, but can be overcome with additional exposure to the environment. In addition, an analysis of the inconsistencies in PER lesion studies of the impact of PER damage on water maze performance indicated that both task differences and strain differences accounted for inconsistencies (Aggleton, Kyd, and Bilkey, 2004).

Scene perception, contextual learning and memory

One candidate for the aspect of the spatial environment that the POR represents that is subsequently used in navigation is the environmental context. As previously stated, while lesions centered on the POR do not always affect spatial navigation, they do reliably cause deficits in contextual fear conditioning (Bucci et al., 2000) and contextual discrimination (Bucci et al., 2002). In these experiments, rats were trained to differentiate between two contexts: one paired with a shock, and one without. Animals with sham lesions were able to differentiate between the two contexts by the third day of training, as shown by decreased freezing in the non-shock paired context, while animals with POR lesions tended to freeze more in both contexts, showing an inability to distinguish the two contexts. A similar conclusion can be drawn from subsequent studies that found that animals with POR lesions tended to freeze less across all contexts following successful fear conditioning training, with the result being a tendency for animals with POR lesions to overgeneralize rather than differentiate between contexts (Burwell et al., 2004; Peck & Taube, 2017). Additionally, through a series of lesion experiments the importance of the

postrhinal cortex in contextual scene representation was demonstrated (Eacott & Gaffan, 2005; Gaffan et al., 2004; Norman & Eacott, 2005). In these experiments, rats with postrhinal lesions were shown to exhibit deficits in recognizing the context for which objects appeared, without deficits for the objects themselves. Further, the POR has been shown to respond to changes in the spatial relationship between objects and their background context (Howard et al., 2011), which combines the observed attentional function of the POR with the representation of environmental context (Figure 1.5).

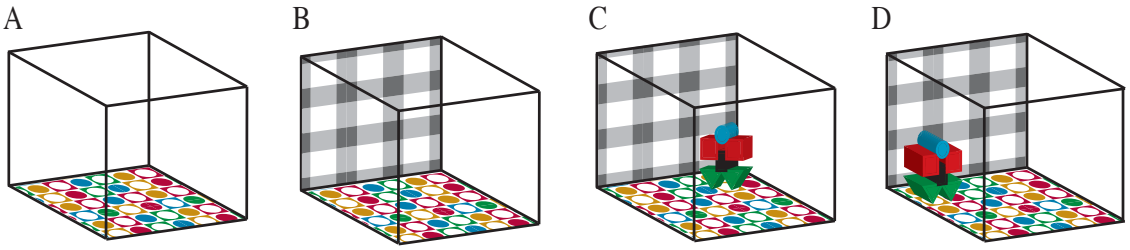

Figure 1.5. Illustration of how the POR might be involved in the processing of information in the local environmental context. A. POR may encode the features of local contexts, such as a small room with a pattern on the floor. B. Based on Burwell and Hafeman (2003), POR may signal changes such as an altered pattern on the wall. C. POR also appears to encode the spatial layout of objects in the local context. D. As suggested by Howard et al. (2011), POR may also signal when there are changes in the spatial layout of objects, e.g., the transition from c to d. With permision from Ho and Burwell (2014).

Associations and conjunctions

The function of the POR has also been suggested to be of a more associative nature, despite being located upstream of the hippocampus which has long been thought to be the sole conjunction location within the MTL. Both allocentric and egocentric representations have been observed in the POR, as have cells that respond conjunctively to two or more different spatial representations within an environment (LaChance et al., 2019). In these experiments, neurons recorded from the POR were shown to encode three distinct aspects of the environment: “Center-bearing” cells encoded the egocentric bearing of the center of the arena; “center-distance” cells showed tuning to the animal’s

distance to the center of the arena in both positive and negative linear responses; and head direction cells were observed, with these cells responding to the direction of the rats head in an allocentric reference frame. Interestingly, more than half (51%) of recorded cells that encoded one of these variables also showed conjunctive coding to at least one other spatial variable. These conjunctions were suggested to contribute to the perception of a spatial layout of a scene. Importantly, this is consistent with the POR encoding the spatial layout of objects and features in the local spatial context.

If the POR is important for encoding context, it should not be surprising to observe responses to both non-spatial visual information, such as objects and features of a scene or context, and spatial visual information, such as the spatial layout of such objects in a scene or physical space. Accordingly, the POR has also been seen to respond at comparable levels to both spatial and non-spatial tasks via immediate-early gene activation (Beer et al., 2013), with this group further suggesting that the POR responded to both spatial and object information. Similarly, POR cells that responded preferentially to an object when it was in a particular location, or object-location conjunction cells, have also been reported (Furtak et al., 2012).

Taken together, these data suggest that the POR appears to have an important role in representing the local environmental context, inclusive of the objects, their positions, and changes in those positions.

Neuronal oscillations in the POR

In addition to the proposed functions of individual neurons and neuronal networks, another aspect of brain activity to be considered is the local field potential

(LFP). Oscillatory activity bands in the rodent have been broadly described and defined, and the most widely accepted band definitions in the rodent include delta (~0-4 Hz), theta (~4-12 Hz), beta (~13-30 Hz), and gamma (>30 Hz; Buzsaki & Draguhn, 2004). Oscillatory band definitions in humans are similar, except that in humans, theta is generally defined as 4-8 Hz and there is an alpha band defined at 8-12 Hz (Lever et al., 2014). Therefore, the theta frequency band in rodents is comparatively broad as the frequencies analogous to alpha in the human brain are instead included within the theta band. The theta rhythm is a large amplitude, relatively slow (4–12 Hz), and highly regular rhythm that has been shown to play an important role in navigation as well as spatial and episodic memory processing (Buzsaki, 2005). The rodent hippocampal network literature focuses primarily on two frequencies — theta and gamma. Two types of theta have been described: Type 1 theta (6-12 Hz) is positively correlated with running speed and is atropine resistant; Type 2 theta (4-9 Hz) is more closely associated with immobility and is blocked with the administration of atropine (Bland, 1986). The vast majority of studies of theta in rats focus on the hippocampal theta rhythm and its role in navigation and spatial memory, thus focusing predominantly on Type 1 movement-associated theta (6-12 Hz). Theta rhythms in the hippocampus correlate with theta in many cortical and subcortical hippocampal efferent and afferent structures, including the entorhinal cortex (Mitchell & Ranck Jr., 1980), medial septum (Nerad & McNaughton, 2006), amygdala (Seidenbecher et al., 2003), parasubiculum (Glasgow & Chapman, 2007), and prefrontal cortex (Jones & Wilson, 2005). Functionally, the theta rhythm in rodents has been shown to correlate with the intake of sensory information during exploratory movements such as whisking and sniffing, with each theta cycle serving as a

mechanism to temporally segment the samples of stimuli from the environment (Kepecs et al., 2005).The second main rhythm studied in the HC, gamma oscillations, are thought to temporally link the activity of distributed cells both within and between regions (Colgin & Moser, 2010). These oscillations are relatively fast (>30 Hz), and unlike theta rhythms, which tend to remain relatively stable throughout active behaviors, gamma oscillations tend to occur in bursts at particular times within the theta cycle (Bragin et al., 1995; Colgin et al., 2009). Functionally, these high frequency gamma oscillations are thought to be ideally suited to coordinate operations on a time scale that is beyond the range of conscious perception, such as rapidly selecting inputs, grouping neurons into functional ensembles, and retrieving memories necessary to perform the current task (Colgin & Moser, 2010).

For the POR, only two studies have examined the occurrence or function of theta or gamma. The first study reported that theta power differed across task epochs, with theta power being higher during "task-relevant" epochs compared to "task-irrelevant epochs". In addition, theta power increased following incorrect trials compared to correct trials (Furtak et al., 2012). Both of these findings suggest an attentional function of theta, possibly as an error signal. Phase locking of cells to theta was also examined, and it was found that a proportion of cells (38% of recorded cells) were phase-locked to theta, with putative pyramidal cells typically being locked to the tough of theta and putative fast-spiking cells being locked mainly to the peak of theta (Furtak et al., 2012). This suggests theta is an important mechanism in the POR for information transfer, and the similarities between POR theta and HC theta suggest that it is likely an important information relay mechanism between the POR and other regions including the HC. Phase locking of cells

with gamma was also examined in the referenced study, with large proportions of cells being phase locked to both low gamma and high gamma, although there were no task-related differences seen with respect to gamma power or phase-locking.

The second study examined the instantaneous amplitude and shape of theta oscillations in the POR as they relate to running speed (Ghosh et al., 2020). Theta in the POR was found to mimic theta in the HC in that it is temporally asymmetrical, with the falling phase of theta cycles lasting longer than the subsequent rising phase. These reported results suggest that the amplitude and waveform shape of individual theta cycles might be governed by partially independent mechanisms, highlighting the importance of examining single cycles in order to understand the behavioral correlates of cortical theta rhythms.

Proposed Role within MTL

Based on the data reviewed above, we propose that the rodent POR does not subserve attention, location, scene perception, or contextual encoding individually, but that it is involved in all of these processes in a conjunctive manner. Specifically, we suggest that the POR acts as an important part of the posterior attentional network to signal changes in the local environmental context, encoding these changes as conjunctions of the various aspects of the context. This includes conjunctions of allocentric and egocentric spatial orientation (LaChance et al., 2019) as well as conjunctive representations of the objects, patterns, and locations that together make up the local physical environment (Furtak et al., 2012).

Interestingly, the human homologue of the POR, the parahippocampal cortex (PHC), has been hypothesized to similarly not mediate scenes or places alone, but rather to encode contextual associations (Bar & Aminoff, 2003). Specifically, the PHC mediating both spatial and non-spatial contextual associations has been proposed as the framework to bridge the understanding of how the area is involved in both spatial information processing and episodic memory (Bar et al., 2008). That these areas are so consistent across species suggests that a similar conclusion should be drawn about the framework of function of the POR.

Conclusion

Here we outline the cortical, subcortical, and hippocampal connectivity of the POR, as well as the numerous behavioral functions in which the POR has been implicated. Taken together, the behavioral evidence supports a view of postrhinal and parahippocampal function that is consistent with the anatomical and functional evidence (Figure 1.6). We suggest the POR combines object and feature information from the PER with spatial information from RSC, PPC, secondary visual cortex, and the pulvinar to represent the spatial layout of objects and features in specific environmental contexts. As well as maintaining a representation of the current context, the POR also has an attentional component in that it monitors the context for changes and updates that representation when changes occur. The representation is made available to other regions for the binding of events with context to form episodes that are located in time, for guiding context-relevant behavior, and for recognizing objects in scenes and contexts.

This attentional aspect is further seen in the LFPs recorded within the POR, especially in the observed function of theta.

We propose that the HC is one of the regions that relies heavily on the representations of context from the POR, specifically for the purposes of associative learning and episodic memory. In the remainder of this thesis I address how the POR and the HC differentially participate in the early and late stages of associative learning.

References

Aggleton, J., Kyd, R., & Bilkey, D. (2004). When is the perirhinal cortex necessary for the performance of spatial memory tasks? *Neuroscience & Biobehavioral Reviews*, *28*(6), 611–624. https://doi.org/10.1016/j.neubiorev.2004.08.007

Aggleton, J. P., Keen, S., Warburton, E. C., & Bussey, T. J. (1997). Extensive cytotoxic lesions involving both the rhinal cortices and area TE impair recognition but spare spatial alternation in the rat. *Brain Research Bulletin*, *43*(3), 279–287. https://doi.org/10.1016/s0361-9230(97)00007-5

Aggleton, J. P., Vann, S. D., Oswald, C. J., & Good, M. (2000). Identifying cortical inputs to the rat hippocampus that subserve allocentric spatial processes: A simple problem with a complex answer. *Hippocampus*, *10*(4), 466–474. https://doi.org/10.1002/1098-1063(2000)10:4<466::AID-HIPO13>3.0.CO;2-Y

Aggleton, John P., Brown, M. W., & Albasser, M. M. (2012). Contrasting brain activity patterns for item recognition memory and associative recognition memory: Insights from immediate-early gene functional imaging. *Neuropsychologia*, *50*(13), 3141–3155. https://doi.org/10.1016/j.neuropsychologia.2012.05.018

Agster, K. L., & Burwell, R. D. (2008). Anatomy of the Hippocampus and the Declarative Memory System. In *H. E. Eichenbaum (Ed.), Sys and Neurosci: Vol. Vol. 3* (1st ed., pp. 47–66). Elsevier.

Agster, K. L., & Burwell, R. D. (2009). Cortical efferents of the perirhinal, postrhinal, and entorhinal cortices of the rat. *Hippocampus*, *19*(12), 1159–1186. https://doi.org/10.1002/hipo.20578

Agster, K. L., & Burwell, R. D. (2013). Hippocampal and subicular efferents and afferents of the perirhinal, postrhinal, and entorhinal cortices of the rat. *Behavioural Brain Research*, *254*, 50–64. https://doi.org/10.1016/j.bbr.2013.07.005

Agster, K. L., Tomás Pereira, I., Saddoris, M. P., & Burwell, R. D. (2016). Subcortical connections of the perirhinal, postrhinal, and entorhinal cortices of the rat. II. efferents: SUBCORTICAL EFFERENTS OF PERIRHINAL, POSTRHINAL, & ENTORHINAL CORTICES. *Hippocampus*, *26*(9), 1213–1230. https://doi.org/10.1002/hipo.22600

Bar, M., Aminoff, E., & Schacter, D. L. (2008). Scenes Unseen: The Parahippocampal Cortex Intrinsically Subserves Contextual Associations, Not Scenes or Places Per Se. *Journal of Neuroscience*, *28*(34), 8539–8544. https://doi.org/10.1523/JNEUROSCI.0987-08.2008

Bar, Moshe, & Aminoff, E. (2003). Cortical analysis of visual context. *Neuron*, *38*(2), 347–358. https://doi.org/10.1016/s0896-6273(03)00167-3

Beaudin, S. A., Singh, T., Agster, K. L., & Burwell, R. D. (2013). Borders and Comparative Cytoarchitecture of the Perirhinal and Postrhinal Cortices in an F1 Hybrid Mouse. *Cerebral Cortex*, *23*(2), 460–476. https://doi.org/10.1093/cercor/bhs038

Beer, Z., Chwiesko, C., Kitsukawa, T., & Sauvage, M. M. (2013). Spatial and stimulus-type tuning in the LEC, MEC, POR, PrC, CA1, and CA3 during spontaneous item recognition memory: Spatial and Stimulus-Type Tunings in Recognition Memory. *Hippocampus*, *23*(12), 1425–1438. https://doi.org/10.1002/hipo.22195

Bragin, A., Jando, G., Nadasdy, Z., Hetke, J., Wise, K., & Buzsaki, G. (1995). Gamma (40-100 Hz) oscillation in the hippocampus of the behaving rat. *The Journal of Neuroscience*, *15*(1), 47–60. https://doi.org/10.1523/JNEUROSCI.15-01-00047.1995

Bucci, D. J., Phillips, R. G., & Burwell, R. D. (2000). Contributions of postrhinal and perirhinal cortex to contextual information processing. *Behavioral Neuroscience*, *114*(5), 882–894. https://doi.org/10.1037//0735-7044.114.5.882

Bucci, David J., & Burwell, R. D. (2004). Deficits in Attentional Orienting Following Damage to the Perirhinal or Postrhinal Cortices. *Behavioral Neuroscience*, *118*(5), 1117–1122. https://doi.org/10.1037/0735-7044.118.5.1117

Bucci, David J., & Robinson, S. (2014). Toward a conceptualization of retrohippocampal contributions to learning and memory. *Neurobiology of Learning and Memory*, *116*, 197–207. https://doi.org/10.1016/j.nlm.2014.05.007

Bucci, David J., Saddoris, M. P., & Burwell, R. D. (2002). Contextual fear discrimination is impaired by damage to the postrhinal or perirhinal cortex. *Behavioral Neuroscience*, *116*(3), 479–488.

Burgess, C. R., Ramesh, R. N., Sugden, A. U., Levandowski, K. M., Minnig, M. A., Fenselau, H., Lowell, B. B., & Andermann, M. L. (2016). Hunger-Dependent Enhancement of Food Cue Responses in Mouse Postrhinal Cortex and Lateral Amygdala. *Neuron*, *91*(5), 1154–1169. https://doi.org/10.1016/j.neuron.2016.07.032

Burwell, R. D., & Amaral, D. G. (1998a). Perirhinal and postrhinal cortices of the rat: Interconnectivity and connections with the entorhinal cortex. *The Journal of Comparative Neurology*, *391*(3), 293–321. https://doi.org/10.1002/(sici)1096-9861(19980216)391:3<293::aid-cne2>3.0.co;2-x

Burwell, R. D., & Amaral, D. G. (1998b). Cortical afferents of the perirhinal, postrhinal, and entorhinal cortices of the rat. *The Journal of Comparative Neurology*, *398*(2), 179–205. https://doi.org/10.1002/(sici)1096-9861(19980824)398:2<179::aid-cne3>3.0.co;2-y

Burwell, R. D., & Hafeman, D. M. (2003). Positional firing properties of postrhinal cortex neurons. *Neuroscience*, *119*(2), 577–588. https://doi.org/10.1016/s0306-4522(03)00160-x

Burwell, R. D., Saddoris, M. P., Bucci, D. J., & Wiig, K. (2004). Corticohippocampal Contributions to Spatial and Contextual Learning. *Journal of Neuroscience*, *24*(15), 3826–3836. https://doi.org/10.1523/JNEUROSCI.0410-04.2004

Burwell, Rebecca D. (2006). The Parahippocampal Region: Corticocortical Connectivity. *Annals of the New York Academy of Sciences*, *911*(1), 25–42. https://doi.org/10.1111/j.1749-6632.2000.tb06717.x

Burwell, Rebecca D., Bucci, D. J., Sanborn, M. R., & Jutras, M. J. (2004). Perirhinal and postrhinal contributions to remote memory for context. *The Journal of Neuroscience: The Official Journal of the Society for Neuroscience*, *24*(49), 11023–11028. https://doi.org/10.1523/JNEUROSCI.3781-04.2004

Burwell, Rebecca D., Witter, M. P., & Amaral, D. G. (1995). Perirhinal and postrhinal cortices of the rat: A review of the neuroanatomical literature and comparison with findings from the monkey brain. *Hippocampus*, *5*(5), 390–408. https://doi.org/10.1002/hipo.450050503

Bussey, T. J., Duck, J., Muir, J. L., & Aggleton, J. P. (2000). Distinct patterns of behavioural impairments resulting from fornix transection or neurotoxic lesions of the perirhinal and postrhinal cortices in the rat. *Behavioural Brain Research*, *111*(1–2), 187–202. https://doi.org/10.1016/s0166-4328(00)00155-8

Bussey, T. J., Muir, J. L., & Aggleton, J. P. (1999). Functionally dissociating aspects of event memory: The effects of combined perirhinal and postrhinal cortex lesions on object and place memory in the rat. *The Journal of Neuroscience: The Official Journal of the Society for Neuroscience*, *19*(1), 495–502.

Buzsaki, G. (2004). Neuronal Oscillations in Cortical Networks. *Science*, *304*(5679), 1926–1929. https://doi.org/10.1126/science.1099745

Buzsáki, G. (2005). Theta rhythm of navigation: Link between path integration and landmark navigation, episodic and semantic memory. *Hippocampus*, *15*(7), 827–840. https://doi.org/10.1002/hipo.20113

Colgin, L. L., Denninger, T., Fyhn, M., Hafting, T., Bonnevie, T., Jensen, O., Moser, M.-B., & Moser, E. I. (2009). Frequency of gamma oscillations routes flow of information in the hippocampus. *Nature*, *462*(7271), 353–357. https://doi.org/10.1038/nature08573

Davies, M., Machin, P., Sanderson, D., Pearce, J., & Aggleton, J. (2007). Neurotoxic lesions of the rat perirhinal and postrhinal cortices and their impact on biconditional visual discrimination tasks. *Behavioural Brain Research*, *176*(2), 274–283. https://doi.org/10.1016/j.bbr.2006.10.005

Deacon, T. W., Eichenbaum, H., Rosenberg, P., & Eckmann, K. W. (1983). Afferent connections of the perirhinal cortex in the rat. *The Journal of Comparative Neurology*, *220*(2), 168–190. https://doi.org/10.1002/cne.902200205

Decurtis, M., & Pare, D. (2004). The rhinal cortices: A wall of inhibition between the neocortex and the hippocampus. *Progress in Neurobiology*, *74*(2), 101–110. https://doi.org/10.1016/j.pneurobio.2004.08.005

Delatour, B., & Witter, M. P. (2002). Projections from the parahippocampal region to the prefrontal cortex in the rat: Evidence of multiple pathways. *The European Journal of Neuroscience*, *15*(8), 1400–1407.

Eacott, M. J., Gaffan, D., & Murray, E. A. (1994). Preserved recognition memory for small sets, and impaired stimulus identification for large sets, following rhinal cortex ablations

in monkeys. *The European Journal of Neuroscience*, *6*(9), 1466–1478. https://doi.org/10.1111/j.1460-9568.1994.tb01008.x

Eacott, M. J., & Gaffan, E. A. (2005). The roles of perirhinal cortex, postrhinal cortex, and the fornix in memory for objects, contexts, and events in the rat. *The Quarterly Journal of Experimental Psychology. B, Comparative and Physiological Psychology*, *58*(3–4), 202–217. https://doi.org/10.1080/02724990444000203

Eichenbaum, H. (2000). A cortical-hippocampal system for declarative memory. *Nature Reviews. Neuroscience*, *1*(1), 41–50. https://doi.org/10.1038/35036213

Eichenbaum, H., Yonelinas, A. P., & Ranganath, C. (2007). The Medial Temporal Lobe and Recognition Memory. *Annual Review of Neuroscience*, *30*(1), 123–152. https://doi.org/10.1146/annurev.neuro.30.051606.094328

Furtak, S. C., Ahmed, O. J., & Burwell, R. D. (2012). Single Neuron Activity and Theta Modulation in Postrhinal Cortex during Visual Object Discrimination. *Neuron*, *76*(5), 976–988. https://doi.org/10.1016/j.neuron.2012.10.039

Furtak, S. C., Wei, S.-M., Agster, K. L., & Burwell, R. D. (2007). Functional neuroanatomy of the parahippocampal region in the rat: The perirhinal and postrhinal cortices. *Hippocampus*, *17*(9), 709–722. https://doi.org/10.1002/hipo.20314

Gaffan, E. A., Healey, A. N., & Eacott, M. J. (2004). Objects and positions in visual scenes: Effects of perirhinal and postrhinal cortex lesions in the rat. *Behavioral Neuroscience*, *118*(5), 992–1010. https://doi.org/10.1037/0735-7044.118.5.992

Ghosh, M., Shanahan, B. E., Furtak, S. C., Mashour, G. A., Burwell, R. D., & Ahmed, O. J. (2020). *Instantaneous amplitude and shape of postrhinal theta oscillations differentially*

encode running speed [Preprint]. Neuroscience. https://doi.org/10.1101/2020.06.03.130609

Glasgow, S. D., & Chapman, C. A. (2007). Local Generation of Theta-Frequency EEG Activity in the Parasubiculum. *Journal of Neurophysiology*, *97*(6), 3868–3879. https://doi.org/10.1152/jn.01306.2006

Howard, L. R., Kumaran, D., Olafsdottir, H. F., & Spiers, H. J. (2011). Double Dissociation between Hippocampal and Parahippocampal Responses to Object-Background Context and Scene Novelty. *Journal of Neuroscience*, *31*(14), 5253–5261. https://doi.org/10.1523/JNEUROSCI.6055-10.2011

Hwang, E., Willis, B. S., & Burwell, R. D. (2018). Prefrontal connections of the perirhinal and postrhinal cortices in the rat. *Behavioural Brain Research*, *354*, 8–21. https://doi.org/10.1016/j.bbr.2017.07.032

Jones, M. W., & Wilson, M. A. (2005). Theta Rhythms Coordinate Hippocampal–Prefrontal Interactions in a Spatial Memory Task. *PLoS Biology*, *3*(12), e402. https://doi.org/10.1371/journal.pbio.0030402

Kepecs, A., Uchida, N., & Mainen, Z. F. (2006). The Sniff as a Unit of Olfactory Processing. *Chemical Senses*, *31*(2), 167–179. https://doi.org/10.1093/chemse/bjj016

Kinnavane, L., Amin, E., Olarte-Sánchez, C. M., & Aggleton, J. P. (2017). Medial temporal pathways for contextual learning: Network c-*fos* mapping in rats with or without perirhinal cortex lesions. *Brain and Neuroscience Advances*, *1*, 239821281769416. https://doi.org/10.1177/2398212817694167

Knierim, J. J., Lee, I., & Hargreaves, E. L. (2006). Hippocampal place cells: Parallel input streams, subregional processing, and implications for episodic memory. *Hippocampus*, *16*(9), 755–764. https://doi.org/10.1002/hipo.20203

Koganezawa, N., Gisetstad, R., Husby, E., Doan, T. P., & Witter, M. P. (2015). Excitatory Postrhinal Projections to Principal Cells in the Medial Entorhinal Cortex. *Journal of Neuroscience*, *35*(48), 15860–15874. https://doi.org/10.1523/JNEUROSCI.0653-15.2015

Kroemer, N. B., Burrasch, C., & Hellrung, L. (2016). To work or not to work. In *Progress in Brain Research* (Vol. 229, pp. 125–157). Elsevier. https://doi.org/10.1016/bs.pbr.2016.06.009

LaChance, P. A., Todd, T. P., & Taube, J. S. (2019). A sense of space in postrhinal cortex. *Science*, *365*(6449), eaax4192. https://doi.org/10.1126/science.aax4192

Liu, P., & Bilkey, D. K. (2002). The effects of NMDA lesions centered on the postrhinal cortex on spatial memory tasks in the rat. *Behavioral Neuroscience*, *116*(5), 860–873. https://doi.org/10.1037/0735-7044.116.5.860

Mitchell, S. J., & Ranck, J. B. (1980). Generation of theta rhythm in medial entorhinal cortex of freely moving rats. *Brain Research*, *189*(1), 49–66. https://doi.org/10.1016/0006-8993(80)90006-2

Naber, P. A., Caballero-Bleda, M., Jorritsma-Byham, B., & Witter, M. P. (1997). Parallel input to the hippocampal memory system through peri- and postrhinal cortices. *Neuroreport*, *8*(11), 2617–2621. https://doi.org/10.1097/00001756-199707280-00039

Naber, P. A., Witter, M. P., & Lopes da Silva, F. H. (2001). Evidence for a direct projection from the postrhinal cortex to the subiculum in the rat. *Hippocampus*, *11*(2), 105–117. https://doi.org/10.1002/hipo.1029

Nerad, L., & McNaughton, N. (2006). The septal EEG suggests a distributed organization of the pacemaker of hippocampal theta in the rat. *European Journal of Neuroscience*, *24*(1), 155–166. https://doi.org/10.1111/j.1460-9568.2006.04902.x

Nishio, N., Tsukano, H., Hishida, R., Abe, M., Nakai, J., Kawamura, M., Aiba, A., Sakimura, K., & Shibuki, K. (2018). Higher visual responses in the temporal cortex of mice. *Scientific Reports*, *8*(1), 11136. https://doi.org/10.1038/s41598-018-29530-3

Norman, G., & Eacott, M. J. (2005). Dissociable effects of lesions to the perirhinal cortex and the postrhinal cortex on memory for context and objects in rats. *Behavioral Neuroscience*, *119*(2), 557–566. https://doi.org/10.1037/0735-7044.119.2.557

Passetti, F., Chudasama, Y., & Robbins, T. W. (2002). The frontal cortex of the rat and visual attentional performance: Dissociable functions of distinct medial prefrontal subregions. *Cerebral Cortex (New York, N.Y.: 1991)*, *12*(12), 1254–1268. https://doi.org/10.1093/cercor/12.12.1254

Peck, J. R., & Taube, J. S. (2017). The postrhinal cortex is not necessary for landmark control in rat head direction cells: Postrhinal Cortex Lesions and Landmark Control. *Hippocampus*, *27*(2), 156–168. https://doi.org/10.1002/hipo.22680

Posner, M. I., Rothbart, M. K., & The American Association for Research into Nervous and Mental Diseases. (1998). Attention, self–regulation and consciousness. *Philosophical Transactions of the Royal Society of London. Series B: Biological Sciences*, *353*(1377), 1915–1927. https://doi.org/10.1098/rstb.1998.0344

Posner, M. I., Walker, J. A., Friedrich, F. J., & Rafal, R. D. (1984). Effects of parietal injury on covert orienting of attention. *The Journal of Neuroscience: The Official Journal of the Society for Neuroscience*, *4*(7), 1863–1874.

Qi, X., Du, Z. J., Zhu, L., Liu, X., Xu, H., Zhou, Z., Zhong, C., Li, S., Wang, L., & Zhang, Z. (2019). The Glutamatergic Postrhinal Cortex–Ventrolateral Orbitofrontal Cortex Pathway Regulates Spatial Memory Retrieval. *Neuroscience Bulletin*, *35*(3), 447–460. https://doi.org/10.1007/s12264-018-0325-4

Ramos, J. M. J. (2013). Differential contribution of hippocampus, perirhinal cortex and postrhinal cortex to allocentric spatial memory in the radial maze. *Behavioural Brain Research*, *247*, 59–64. https://doi.org/10.1016/j.bbr.2013.03.017

Scaplen, K. M., Agster, K. L., & Burwell, R. D. (2017). Anatomy of the Hippocampus and the Declarative Memory System. In *J. H. Byrne (Ed.), Concise Learning and Memory* (1st ed.). Academic Press.

Seidenbecher, T. (2003). Amygdalar and Hippocampal Theta Rhythm Synchronization During Fear Memory Retrieval. *Science*, *301*(5634), 846–850. https://doi.org/10.1126/science.1085818

Sills, J. B., Connors, B. W., & Burwell, R. D. (2012). Electrophysiological and morphological properties of neurons in layer 5 of the rat postrhinal cortex. *Hippocampus*, *22*(9), 1912–1922. https://doi.org/10.1002/hipo.22026

Squire, L. R., Stark, C. E. L., & Clark, R. E. (2004). The medial temporal lobe. *Annual Review of Neuroscience*, *27*, 279–306. https://doi.org/10.1146/annurev.neuro.27.070203.144130

Sugden, A. U. (2015). *Diverse subtypes of fast-spiking inhibitory neurons in neocortex*. (Unpublished doctoral dissertation). Brown University, Providence, RI https://doi.org/10.7301/Z0QC01WF

Tomás Pereira, I., Agster, K. L., & Burwell, R. D. (2016). Subcortical connections of the perirhinal, postrhinal, and entorhinal cortices of the rat. I. afferents: SUBCORTICAL

AFFERENTS OF PERIRHINAL, POSTRHINAL, AND ENTORHINAL CORTICES. *Hippocampus*, *26*(9), 1189–1212. https://doi.org/10.1002/hipo.22603

Vogt, B. A., & Miller, M. W. (1983). Cortical connections between rat cingulate cortex and visual, motor, and postsubicular cortices. *The Journal of Comparative Neurology*, *216*(2), 192–210. https://doi.org/10.1002/cne.902160207

CHAPTER 2

CONJUNCTIVE CODING IN THE HIPPOCAMPUS AND POSRHINAL CORTEX DURING LEARNING OF A COMPLEX BI-CONDITIONAL TASK

Valerie J. Estela[1], Sean G. Trettel[2], Rebecca D. Burwell[1,2]

VJE performed all experiments and analysis with the following exceptions: LFP and phase locking analysis for this chapter was acquired with the help of SGT. VJE wrote the chapter with input from RDB.

[1]Neuroscience Graduate Program, Brown University, Providence, Rhode Island 02912, USA
[2]Department of Cognitive, Linguistic and Psychological Sciences, Brown University, Providence, Rhode Island 02912, USA

Abstract

Remembering the context in which events occur is a hallmark of episodic memory. Structures in the medial temporal lobe (MTL), specifically the perirhinal (PER) and postrhinal (POR) cortices and the hippocampus (HC), are implicated in representing contexts and contextual learning, such as associating a particular context with a particular event. There are, however, open questions about the functional differentiation of these structures. The study reported in this chapter was designed to dissociate the contributions of the POR and the HC to the association of an event with a particular context. Briefly, we found that both HC and POR have specific yet different responses to the different task related epochs, and importantly, that HC and POR have specifically different time frames in which object-location conjunctions emerge during the learning of a task.

Introduction

The formation of episodic memories requires a network capable of representing objects within a complex context, allowing for recollection of events in time and space. These contexts are not simply places, rather they are spatial locations usually containing items and patterns and having other characteristics, for example portals or particular geometries. It should not be surprising that a network of brain regions is necessary for both forming representations of contexts and using those representations to guide behavior and cognition and for learning and memory. Structures in the medial temporal lobe (MTL), specifically the perirhinal (PER) and postrhinal (POR) cortices and the hippocampus (HC), are implicated in these processes, but exactly how is not completely understood. These same brain regions show alterations in multiple disorders and diseases. For example, symptom severity in PTSD is positively correlated with increased regional cerebral blood flow in the HC and parahippocampal cortex (PHC, primate homologue of POR; Shin, et al., 2014). Hippocampal and PHC disruption are further implicated in depression (Drevets, et al., 2008). Specifically, object-location associative learning, which depends on these regions, is disrupted in patients with Alzheimer's disease (Fowler, et al., 2002) and schizophrenia (Wood, et al., 2002; Burglen, et al., 2004). Understanding these areas of the brain and how they contribute to context-guided behavior and to cognitive function is crucial to developing new, more effective ways of treating the cognitive symptoms of these disorders.

There is a wide consensus based on diverse methods including lesion and imaging studies that the hippocampus is necessary for episodic memory (O'Keefe & Nadel, 1978; Eichenbaum, 2000). Historically, the perirhinal cortex (PER), postrhinal cortex (POR),

and medial and lateral entorhinal cortices (MEA, LEA) were understood as gateways for neocortical information to the hippocampus. Researchers believed that these medial temporal lobe (MTL) areas all made similar contributions to episodic memory (Eacott, et al., 1994; Squire, et al., 2004). More recently, it has been shown that individual cortical areas can be functionally differentiated (Eichenbaum & Lipton, 2008; Jarrard, et al., 2004; Murray, et al., 2007) with the PER involved in object recognition, the POR in contextual discrimination, and the entorhinal cortices (EC) in spatial and working memory. The predominant view of the MTL represents the connections between the parahippocampal regions and the HC as extensions of the "what" and the "where" visual processing pathways. The "what" pathway is thought to be PER→LEA→HC, while the "where" pathway is POR→MEA→HC (Eichenbaum, 2000; Knierim, et al., 2006; Eichenbaum, et al., 2007; Figure. 2.1). This view, however, ignores the cross-talk between these two pathways, such as direct and reciprocal connections between the PER and the POR (Burwell & Amaral, 1998; Furtak, et al., 2007) and direct connections from POR to CA1 (Naber, et al., 2001, Agster & Burwell, 2013).

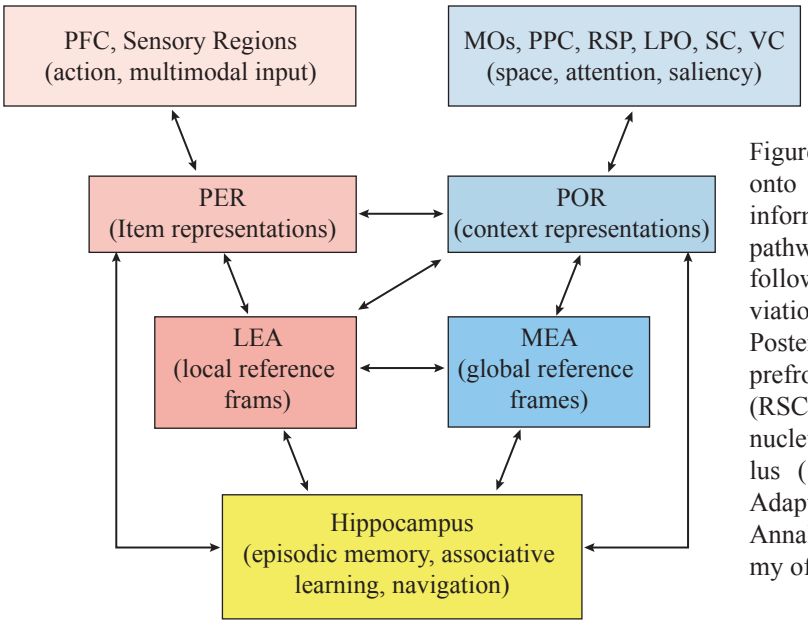

Figure 2.1. Pathways converging onto the hippocampus. Object information follows the red pathway, spatial information follows the blue pathway. Abbreviations: rodent dlPFC (MOs) Posterior parietal (PPC), prefrontal (PFC), retrosplenial (RSC), thalamic lateral posterior nucleus (LPO), superior colliculus (SC), visual cortex (VC). Adapted from Burwell, 2006, the Annals of the New York Academy of Sciences.

This view also overstates the function of the HC as the sole processor of the system. Though the HC is generally implicated in contextual learning, it does not appear to be necessary in all cases (reviewed in Holland and Bouton, 1999). For example, extensive pretraining lesions of the HC do not cause consistent behavioral deficits in contextual fear conditioning (Maren et al., 1997; Frankland et al.,1998, Gewirtz et al., 2000). Conversely, damage to the POR reliably produces deficits in tasks requiring contextual learning. For example, the POR is necessary for contextual discrimination (Bucci et al., 2002) and for contextual fear conditioning, whether damaged before training or up to 100 days after training (Bucci et al., 2000; Burwell et al., 2004). Further, POR damage also causes deficits in contextual learning paradigms that do not involve aversive stimuli (Eacott and Gaffan, 2005; Norman and Eacott, 2005).

Anatomical and electrophysiological data also support a role for POR in contextual processing. The POR receives a majority of its input from visual, visual-spatial, and spatial attention regions, especially the retrosplenial cortex (RSC), the

posterior parietal cortex (PPC), and the lateral posterior nucleus of the thalamus (LPO) along with visual association cortices (Burwell and Amaral, 1998; Furtak et al., 2007). The remaining major input to POR arises in the PER (Burwell and Amaral, 1998), ideally positioning it for a role in combining object, location, and spatial attention signals. Electrophysiologically, single unit recording studies show that whereas both the HC and POR have cells that respond preferentially to certain locations within a given environment (O'Keefe, 1976; Burwell and Hafeman, 2003), these cells respond differently when spatial cues are altered. When both proximal and distal cues are rotated in opposite directions, approximately half of HC cells rotate concurrently with one subset (Shapiro et al., 1997). In contrast, a large majority of POR location fields (84%) adopted new spatial correlates immediately when experimental cues were rotated, but did so neither predictably nor concordantly (Burwell and Hafeman, 2003). This suggests that POR might be responsible for monitoring and signaling immediate changes to the local environmental context.

Using an odor-based conditional discrimination task, Komorowski and colleagues were able to show that as an animal learned an association, object-location cells emerged in the HC, eventually becoming more prevalent than place cells (Komorowski, et al., 2009). These are cells that show selectivity for a particular object only when it is in a particular location. Because the binding of objects in contexts is crucial to the development of an episode, we can interpret the formation of an object-location conjunction as a conduit for the formation of an episodic memory. Surprisingly, these conjunction cells were also discovered upstream of the HC in the POR. This was unexpected as previous paradigms suggested the HC to be the only region within the

parahippocampal system to have single units with conjunctive representations. Interestingly, these conjunction cells in the POR were observed in a simple, concurrent object discrimination task in which the location of the object within the environment was not behaviorally relevant (Furtak, et al., 2012). Thus, it appeared that object-location correlates develop automatically in POR, in comparison to their emergence with learning in the HC. To further compare object-location conjunctions in the POR and HC, it was necessary to record in these regions in rats performing a discrimination task that mimicked both the Komorowski, et al. (2009) and the Furtak, et al. (2012) tasks.

To achieve this, we developed the location biconditional discrimination (locBCD) task. The locBCD task is formally more like the Komorowski, et al. (2009) task, but is primarily visual like the Furtak, et al. (2012) task. This locBCD task requires a rat to learn that one in a pair of objects is correct in the East wing of a bowtie-shaped recording area, and the other in the same pair is correct in the West. The floor projection apparatus is used with the bow-tie shaped maze such that East is delineated by one floor pattern (dots) and West is delineated by a different floor pattern (stripes) (Fig 2.2). This set up is ideal for our purpose because it capitalizes on the natural propensity of rats to explore objects and the natural propensity to attend to items and objects on the ground. The task also optimizes reliance on the POR since the majority of cortical inputs to POR are visual and visuospatial. Additionally, this task is fully automated increasing the number of trials that can be performed by an animal in a given session. Importantly, the rules of the task are the same as the Komorowski item-in-place task, though the primary modalities are different. Thus, the design of the locBCD task allows for observing object-location conjunctions in both the HC and the POR.

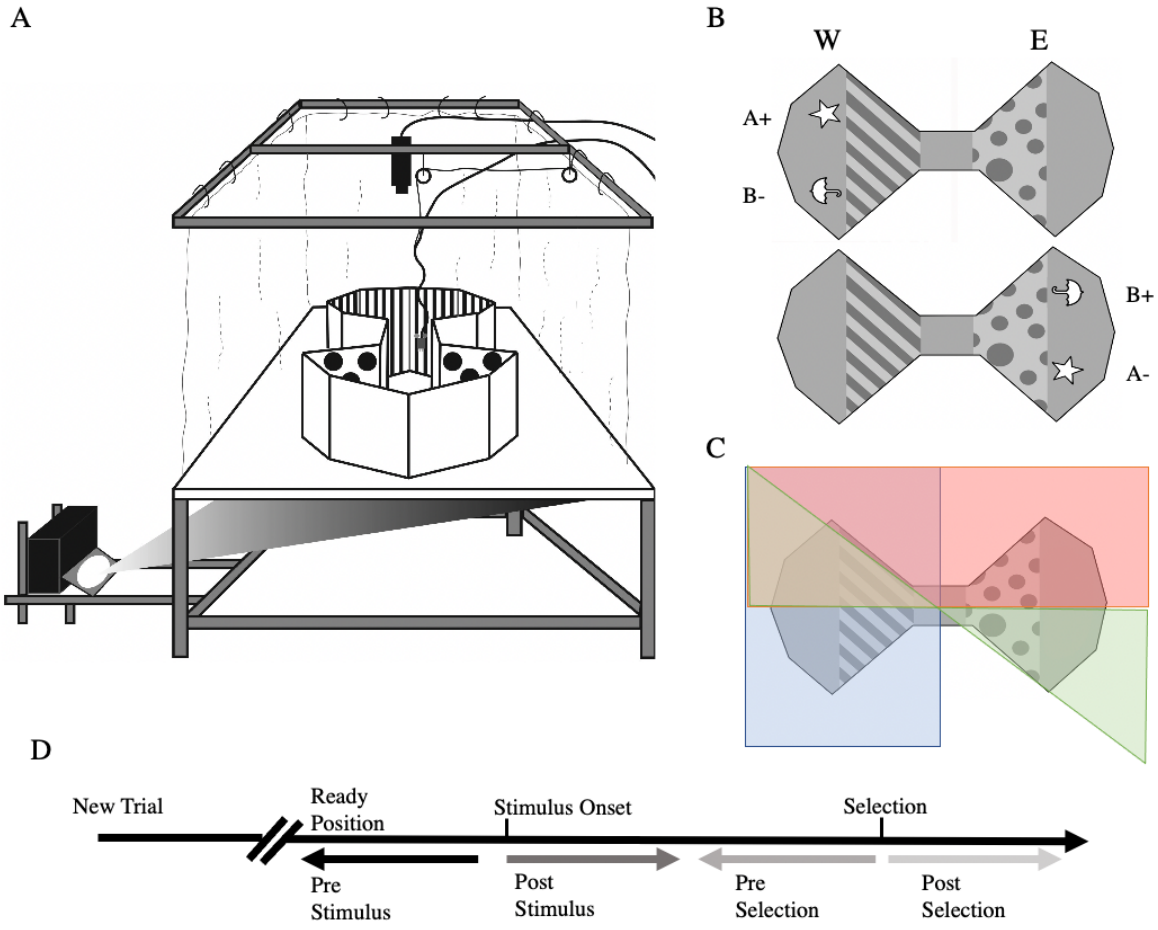

Figure 2.2. The Location Bi-conditional (locBCD) task. A. Schematic of the floor projection maze with the bowtie-shaped enclosure used for the task. B. Top down view of west vs. east trials. Trials were initiated when the rat stopped in the ready position (middle of the maze) and faced one side of the maze (either west or east). After a variable period, two objects appeared. One object was correct in the west and the other in the east regardless of left vs right location. The animal made a selection by approaching one of two objects. Correct choices were rewarded with intracranial stimulation of the medial forebrain bundle. C. Representative portions of the maze as analyzed; blue = allocentric west, red = allocentric north, green = egocentric right. D. Epochs examined within the locBCD task. PreStimulus and PostStimulus represent the 500ms epochs before and after stimulus onset, respectively. PreSelection and PostSelection represent the 500ms epochs before and after object selection, respectively. Panel A adapted from Jacobson, et al., 2014, JOVE.

Using the locBCD task on the floor projection maze, we aimed to address three main questions: 1. How do spatial and non-spatial correlates of the HC and POR differ during this complex task? 2. Does the relative timing of the emergence of object location

conjunctions differ in the POR compared to the HC? and 3. What does this suggest for the overall function of the POR?

Experimental procedures

Subjects

Subjects were 5 male Long-Evans rats (Charles Rivers Laboratories, Wilmington, MA). Rats were initially pair housed in a 12:12 hr light:dark cycle with ad libitum access to water. After surgery, rats were singly housed. Four of the rats were housed in paired cages with a porous divider in order to have contact with the former cage mate. After arriving in the colony, animals were handled several days per week until the beginning of behavioral training. Prior to training, rats were placed on a feeding schedule to maintain body weight at 85%–90% of free feeding weight. Because the task relied on light to be performed, animals were tested during the light portion of their light cycle to avoid disturbing the animals' circadian rhythms. All procedures were in accordance with appropriate institutional animal care and use committee and NIH guidelines for the care and use of animals in research.

Apparatus

Rats were tested on the floor projection apparatus described previously (Furtak et al., 2009; Jacobson et al., 2014). This apparatus exploits the natural tendency of rats to attend to items located in the lower portion of their visual field and permits automated control over the task. The set-up consisted of a bowtie shaped maze (115 x 70 x 45 cm) on top of a clear Plexiglas subfloor (147.32 cm × 111.80 cm and 1.25 cm thick) covered

by Dual Vision Fabric (Da-Lite Screen Company, Warsaw, IN), a fabric specifically designed for rear screen projection. A thin Plexiglas sheet (0.32 cm) covered the fabric for protection. Visual stimuli were projected onto the floor from below using an LCD projector (WT610 projector, NEC Corporation). The floor projection maze was interfaced with two PC systems used for location tracking, behavioral control, and neuronal data acquisition. Tracking was accomplished with a single camera using CinePlex Studio (v3.4.1; Plexon, Inc.) which tracked LEDs that were attached to the headstage of the animal at the beginning of each session. Based on the location of the rat, this system presented visual stimuli, collected behavioral data, and controlled delivery of intracranial stimulation (ICS) of the medial forebrain bundle for reward.

Behavioral Training

Animals were implanted prior to the start of behavioral training. The training paradigm began 7 days post-surgery with habituation to the room, habituation to the maze, and habituation to the connected cables. Habituations started with the animal being placed into one blocked-off side of the maze with all visual and olfactory cues available along with several 40 mg food pellets (Bioserve, Frenchtown, NJ). After 10 minutes, animals were removed, the maze was cleaned, and remaining food pellets were counted as a measure of habituation to the novel environment. After a 5 minute delay, this procedure was repeated for the animal in the opposite side of the maze. Once animals were eating 90-100% of the pellets on each side, the maze was opened so they could travel between the two sides and habituate to the maze in full. Next, optimization of ICS levels was used to create a conditioned place preference for the start zones,

simultaneously training the animals to stop in the correct zones and wait for a variable amount of time. Once stopping reliably, animals were trained to approach a 2D object that is presented on the floor following the variable wait period (900 - 1300ms) to receive a reward. Once approaching stimuli consistently, animals were then transitioned to a training pair of objects, and began the process of learning the bi-conditional rule. Limits were set to ensure that observed preferences were minimized. Animals could not complete more than 5 trials on a given side of the maze without being forced to complete a trial on the opposite side. Similarly, correction trials were used to eliminate left/right side biases. Animals that demonstrated a preference for going to a particular side received correction trials that forced them to complete the same choice, with the correct answer on their non-preferred side. Finally, to avoid the possibility of using an alternating strategy, animals could only complete 10 trials in an alternating fashion before being forced to perform 2 trials on the same side of the maze.

To reach criterion, an animal needed to correctly complete 8 out of 10 consecutive trials. Due to the difficult nature of the task, multiple trials to criterion were recorded as was the percent correct for every 50 trials. After an animal reached criterion on a pair or no longer showed interest, he was subsequently presented with a new pair in the following session. In all phases of shaping and training in which two objects were presented, the left versus right location of the correct stimulus was counterbalanced in randomized trials.

Surgery and Histology

Animals were premedicated with diazepam (2–5 mg/kg; i.p.), glycopyrrolate (0.05 mg/kg; s.c.), carprofen (5 mg/kg; s.c.), and butorphanol tartrate (0.5 mg/kg; s.c.) to decrease risk of seizures, counteract respiratory effects of anesthesia, and to control pain. Under surgical levels of isoflurane anesthesia (1.0%–2.5%) electrodes were stereotaxically implanted targeting POR (-0.1mm anterior to and 4.4mm lateral to lambda, 16°angle laterally) and HC (-3.6mm posterior to and 2.9mm lateral to bregma). An ICS electrode was implanted contralaterally to the HC bundle (-2.2 posterior to and 2.0 lateral to bregma). The implanted microdrive assembly was produced in-house and consisted of 24 individually drivable tetrodes (25mm nichrome wires, A-M Systems, Inc., Carlsborg, WA). Two silver ground wires were wrapped around anchor screws placed in the skull. The electrodes were lowered 0.5mm from the cortical surface and the entire hyperdrive was secured with dental cement and anchor screws. Rats were allowed 7 days to recover prior to behavioral training. At the end of the experiment, animals were given an overdose of Beuthanasia-D (100 mg/kg, i.p.), electrode tip placements were marked with a small lesion, the animals were perfused, and the brains were extracted and prepared for histology and subsequent localization of electrodes. The brains were post-fixed for 24 h in 4% formalin and then transferred to a 30% sucrose solution until sectioning. The brains were sectioned at 40 μm and stained for Nissl material with thionin. The locations of electrode tips were reconstructed with a light microscope and localized in HC or POR as defined by Burwell (2001). During recording, microdrivers were generally driven down slowly (~43.75μm/day) as the animal learned to perform the task. Total distance advanced ranged from 1.59mm to 2.91mm in HC and 3.32mm to 4.28mm in POR.

Electrophysiology

The Omniplex D Neural Data Acquisition (Plexon, Inc.) system was used to record neuronal activity during performance of the task. Single unit activity was filtered at .77 - 6000Hz and digitized at 40Hz. Waveforms were extracted by real-time thresholding (PlexControl, Plexon, Inc.) and stored for offline isolation using Offline Sorter (Plexon, Inc.). Timestamps and behavioral event markers were extracted using Neuroexplorer (Plexon, Inc.). Local field potential (LFP) activity was filtered at 0.7-170Hz and digitized at 1kHz. Power was obtained using multi-taper spectral analysis of the LFP (Neuroexplorer, Plexon, Inc.).

Single Neuron Activity Analysis

Spikes associated with putative individual cells were isolated offline based on waveform characteristics and using a variety of partially automated and manual techniques (Offline Sorter, Plexon, Inc.). Spikes were categorized as either pyramidal or fast-spiking using both the calculated peak-to-trough time as well as the average waveform shape. Cells naturally clustered into two groups with respect to the peak-to-trough time, with fast-spiking cells having narrow spike-widths of less than 200 μs and pyramidal cells having wider spike-widths of greater than 300 μs. The result was a dataset for each putative pyramidal and fast-spiking cell containing timestamps corresponding to spike times and behaviorally relevant event markers. These datasets were further analyzed using Neuroexplorer (NEX, Nex Technologies, Madision, AL, USA), SPSS (IBM Corporation, Somers, NY, USA), and Matlab (Mathworks, Natick,

MA, USA). Firing rates for each cell were analyzed for behavioral correlates using factorial analysis of variance (fANOVA), with firing rate as the dependent variable. For each cell, we first computed the mean firing rate (spikes/s) for each of four epochs in each trial. The epochs included the pre-stimulus and post-stimulus epochs, which consisted of the 500 ms periods immediately before and after stimulus onset, respectively, and the pre-selection and post-selection epochs, which were the 500 ms periods immediately before and after the rat selected a target by approaching the location. The length of these epochs were chosen based on the peak activity times seen previously using similar tasks within this floor projection maze setup (Furtak et al., 2012; Jacobson et al., 2014; Yang et al., 2017).

In the first set of analyses, we analyzed correlates of stimulus onset and choice. The dependent variable was the mean firing rates for each epoch. The between-trial variable was outcome (correct response vs. incorrect response), and the two within-trial variables were stimulus onset (pre-stimulus vs. post stimulus) and selection time (pre-selection vs. post-selection).

For the second set of analyses, we examined neural correlates associated with the location of the stimulus. Again, the dependent variable was mean firing rate. Location was the between-trial variable for all analyses, but trials were pooled differently. Two analyses assessed allocentric correlates. In the first, we compared east vs. west locations, i.e. NE and SE vs. NW and SW. In the second, we compared north vs. south locations, i.e. NE and NW vs. SE and SW. To assess egocentric correlates we compared left vs. right locations, i.e. NE and SW vs. NW and SE. Analyses for allocentric location and egocentric location correlates were conducted separately for the post-stimulus, pre-

selection, and post-selection. The pre-stimulus epoch was not analyzed for location analysis because the animal is always in the middle of the maze and there was no stimulus in view.

For the analysis of object-location conjunctions, we examined neural correlates of cells associated with a particular object, a given location of the stimulus, and/or a combination of the two, or a "conjunction". The dependent variable was firing rate. There were two between-trial variables, object (1 or 2) and location (NW, SW, NE, SE). To examine the timing of the occurrence of object-location conjunctions in the locBCD task, we first separated the data by session. Each session took place on a different day. Analyses were conducted separately for the post-stimulus, pre-selection, and post-selection. The pre-stimulus epoch was not analyzed as there was no object present. We then assessed numbers of cells responsive to object, location, and object-location conjunctions. Because the locBCD task was difficult for the rats to master and typically took multiple sessions for a rat to acquire the rule, following epoch analysis we next separated all of the sessions into "Early", "Mid", and "Late" sessions based on individual performance of the task. Early sessions were determined based on a criterion of the rat not having more than a single instance of trials to criterion reached in a given session. Mid sessions were sessions in which the animal reached criterion more than once, but not more than once consecutively. Late sessions were after an animal had reach criterion at least twice consecutively in a single session. In the final analysis of these conjunctions, we analyzed sessions from the four animals with dual-site implants in which a new object pair was introduced. This analysis more closely matches that done by Komorowski, et al.

(2009), in which they separated each session by trial block and examined conjunction emergence within a single session.

Local Field Potential Analysis

Continuous data, or local field potentials (LFPs), as well as timestamps for behaviorally relevant event markers and spike times were extracted and exported to Matlab (Mathworks, Natick, MA) from Neuroexplorer (NEX, Plexon, Inc.). The Chronux toolbox for Matlab was used for the multitaper spectral analysis of the LFP. The spectrum of each of the LFPs recorded from the both the HC and the POR was calculated over the entire session for each electrode.

The oscillatory bands used in this analysis are defined as follows: Theta = 6-10 Hz; Alpha = 10-15 Hz; Slow Gamma = 35-55 Hz; Fast Gamma = 65-100 Hz. To determine theta phase, we first applied a band-pass filter (2-50 Hz) and subsequently used this filtered signal to find peaks and troughs as well as ascending and descending zero crossings of theta waves. Peaks (180°) of theta waves were identified as local maxima and troughs (0°) as local minima. Ascending points (90°) were identified as the zero crossings of the signal between the trough and peak, and descending points (270°) were identified as the zero crossings of the signal between peak and trough. The waveform-based theta phase was then obtained by interpolating phase values between these specified phase quadrants (as done in Belluscio et al. 2012). For gamma and alpha phases, the time-varying power in each particular frequency band was calculated using a Morlet wavelet analysis (as done in Colgin et al. 2009) with a width parameter of 19. For spike assignments to oscillatory cycles, the start time of the cycle was defined as the time

of the peak. The next peak represented the end time of that cycle. Spikes occurring within the start and end peak were assigned to the cycle. Circular statistics were applied to test if cells were significantly phase-locked to theta, alpha, slow gamma, or fast gamma ($P < 0.05$).

Results

Histology

Implanted electrodes were localized via examination and measurement of Nissl-stained brain regions. Methodology created based loosely on the Cavalieri method (Altunkaynak et al., 2009) was used to measure tetrode tracks on sequential brain slices and then matched to the anterior-posterior and medial-lateral relative locations of the electrodes in the implanted bundle. Specifically, a grid with 500 μm boxes was created based on the scale bar for the microscope images acquired, and overlaid on each section. Each column was numbered starting with the most medial box at 1. For HC slices, electrodes were localized within a 90º grid of columns as electrodes were implanted at a 0º angle, or 90º to the surface of the skull/brain. For POR slices, electrodes were localized within a 16º grid of columns as electrodes were implanted at a 16º angle to the surface of the skull/brain. Observed electrode locations were recorded for each individual section. Pictures of the implanted electrode bundle were then used to match tracks of electrodes based on anterior-posterior and medial-lateral relative locations.

Using this procedure, a total of 163 putative cells were identified in the HC and 166 putative cells were identified in the POR. Hippocampal electrodes were located between -1.56mm and -3.20mm posterior to bregma and between 0.8mm-2.5mm lateral

to the midline (Figure 2.3A). Some electrode tips/tracks that were localized within the sections appeared to be above the cell layer of the HC. Generally, when electrodes are above the cell layer, there is little to no recordable activity. Because of the localization, spike widths and amplitudes were compared between cells recorded on those electrodes and those that were localized to within the cell layer. Doing this, we found that neither the spike widths nor the amplitudes were significantly different between the two populations of cells (spike width: $p = 0.09$; amplitude: $p = 0.41$) suggesting that although some electrode tracks were only found above the cell layer, the recordings most likely came from within the cell layer. Based on this, we combined the two populations and are calling them both "HC cells". Postrhinal electrodes were located between -7.38mm and -9.24mm posterior to bregma (Figure 2.3B). All five animals yielded isolated units, with 3 animals having identified units in HC and 4 animals having units in POR. Each cell was recorded for a single session on separate days.

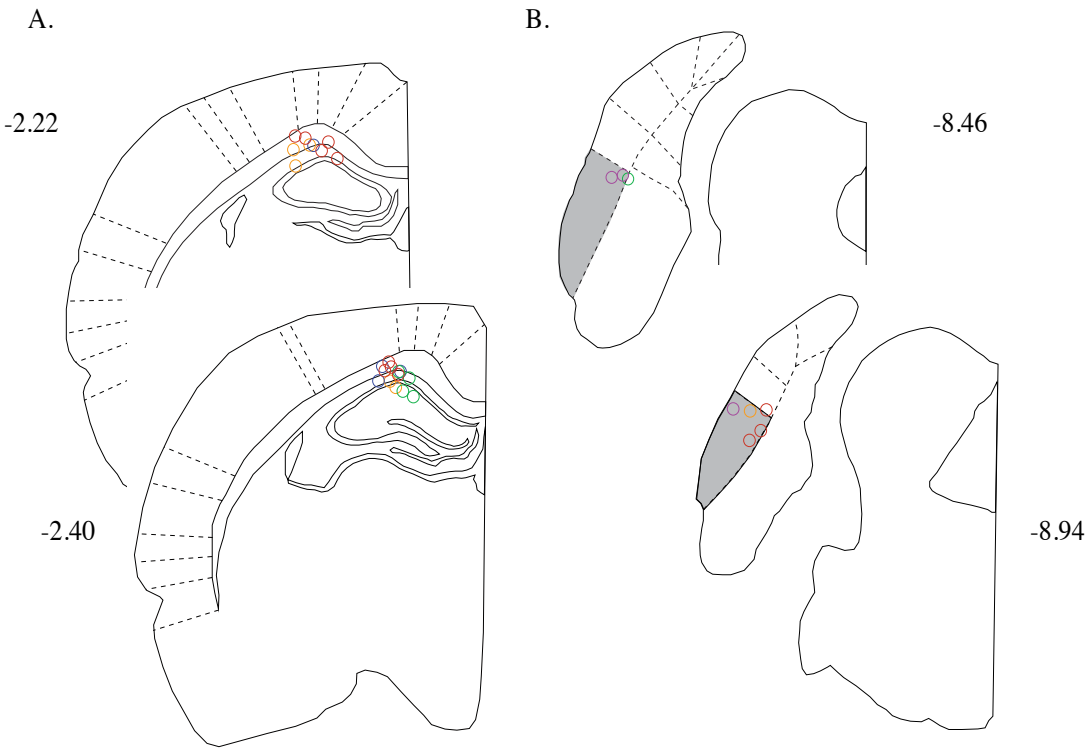

Figure 2.3. Estimated locations of implanted tetrodes. Tetrodes are color coded by animal. A. Histology from animals with dual-site HC and POR implants showing HC tetrodes. Coronal sections shown at Bregma - 2.22 mm and Bregma -2.40 mm. B. Histology from animals with dual-site HC and POR implants showing POR tetrodes. Coronal sections shown at Bregma – 8.46 mm and Bregma -8.94 mm. Dual-site implants: red: 19-012, green: 19-013, blue: 19-014, orange: 19-015. Single site POR implants: purple: 17-024

Behavioral Performance

Because this was a very difficult task for the rats to learn, their averaged performance when looking either across or within trials appears to stay around chance (Figure 2.4A, B) and suggests that learning of the rule did not occur. However, because the task was difficult, the performance needs to be examined in more nuanced ways. One way we attempted to do this was to examine performance with respect to the animal reaching trials to criterion (TTC, at least 10 correct in the previous 12 consecutive trials). For these analyses, a session is defined as the set of trials performed on a given day.

Therefore, when comparing across sessions we are comparing across all days of the experiment, split into Early, Mid, and Late sessions based on number of sessions completed. Early sessions included the first 7 sessions an animal ran, Mid sessions included the next 7 sessions the animal ran, and Late sessions included any remaining sessions. When comparing across trials, we are comparing the trials performed on a single day, with each session split equally into thirds based on the number of trials performed that day, creating Initial trials (first third of trials performed that day by that animal), Mid trials (second third of trials), and Ending trials (final third of trials performed that day). When we examine the animals' performance in this way, we can see that as the animals performed more sessions, although their average accuracy did not increase, the number of TTC reached did, with the lowest number of TTC being reached during Early sessions (4), increasing during mid sessions (6.2), and the highest number of TTC being reached during Late sessions (7.5; Figure 2.4A). If we look instead within sessions, we see that at the beginning of a given session, animals reached TTC an average of 3.8 times during Initial Trials, dropped to an average of 3 times during the middle third of trials, and had the highest number of TTC within a given session during Ending Trials with 4.8 averaged. This data suggests that while it didn't appear that the rule was firmly learned and transferred from day to day, there was likely some recollection of the task from the previous session.

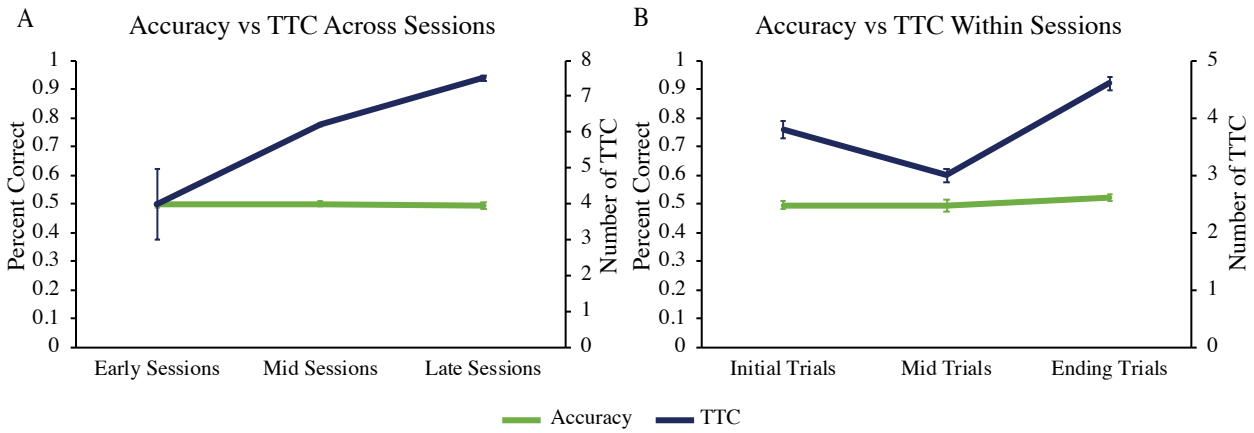

Figure 2.4. Performace and trials to criterion across and within sessions. A. Accuracy and number of trials to criterion reached averaged across all five animals for each of the three defined categories of sessions: Early, Mid, and Late. B. Accuracy and number of trials to criterion reached averaged across all five animals for each of the three defined categories of trials within a given session: Initial, Mid, and Ending. Error bars are SEM.

Epoch analysis

To begin examining the functions of the hippocampus and postrhinal cortex during the locBCD task, we first investigated whether cells in the HC and POR responded differently to the two main events in the task: stimulus onset and selection. Neuronal responses to stimulus onset were analyzed by comparing average firing rates for the 500 ms before stimulus onset to the 500 ms following stimulus onset. Responses to selection were similarly analyzed by comparing the 500 ms before selection to the 500 ms following selection. Of the 163 recorded HC cells, 86% (140) were identified as pyramidal cells and 14% (23) were identified as fast-spiking (Table 2.1). Of the 166 recorded POR cells, 93% (154) were identified as pyramidal cells and 7% (12) were identified as fast-spiking. Epoch analysis showed that overall, the HC responded significantly more to the different epochs than POR. Of the cells recorded, 82% of all HC cells (134) and 66% of all POR cells (111) showed an epoch correlation ($X^2 = 10.1803$, $p<0.05$). This difference was mimicked within the pyramidal cell classification, with

81% (113) of the 140 HC pyramidal cells showing an epoch correlate, while only 64% (99) of the 154 POR pyramidal cells showed any epoch correlate ($X^2 = 9.8412$, $p<0.05$; Table 2.1). Within the fast-spiking cell classification, 91% (21) of the 23 HC fast-spiking cells showed any epoch correlate, while 100% (12) of the 12 POR fast-spiking cells showed any epoch correlate, but these were not statistically different ($X^2 = 0.0109$, $p>0.05$).

Table 2.1. Selectivity of HC and POR pyramidal and fast spiking neurons during task epochs

Epochs	Cell Correlate	HC Percent (#)		POR Percent (#)	
		Pyramidal 86% N = 140	**Fast Spiking 14% N = 23**	**Pyramidal 93% N = 154**	**Fast Spiking 7% N = 12**
All Epochs	Any Correlate	81% (113)	91% (21)	64% (99)	100% (12)
Peri-stimulus	Stim Onset	25* (42)	3 (5)	14 (23)	1 (2)
	Outcome	4 (6)	0 (0)	7 (12)	1 (1)
	Stim Onset x Outcome	3 (5)	1 (2)	10* (16)	1 (2)
	Single Stim Epoch Response⁺	92 (44)	83 (5)	79 (33)	75 (3)
	Multiple Stim Epoch Responses⁺	8 (4)	17 (1)	21 (9)	25 (1)
Peri-selection	Selection	39* (65)	8 (14)	22 (37)	4 (7)
	Outcome	40 (66)	8 (13)	32 (54)	6 (10)
	Selection x Outcome	33 (54)	8 (13)	30 (50)	7 (11)
	Single Selection Epoch Response⁺	46 (48)	38 (8)	55 (50)	17 (2)
	Multiple Selection Epoch Responses⁺	54 (57)	62 (13)	45 (41)	83 (10)
Stimulus and Selection		**30% (40)**	**4% (6)**	**31% (34)**	**4% (4)**

⁺percent of cells out of those of that cell type responsive during that epoch; *p<0.05 compared to region counterpart

Peri-Stimulus

During the peri-stimulus epoch, 34% (48) of the 140 HC pyramidal cells and 26% (6) of fast-spiking HC cells were responsive. In the POR, 27% (42) of the 154 POR pyramidal cells and 33% (4) of the POR fast-spiking cells were responsive.

Of the 48 HC pyramidal cells responsive during the peri-stimulus epoch, 92% (44) had a single response while 8% (4) had multiple responses. Of the 6 fast-spiking HC cells responsive during the peri-stimulus epoch, 83% (5) had a single response and 17% (1) had multiple responses. For POR, of the 42 POR pyramidal cells responsive during

the peri-stimulus epoch, 79% (33) had a single response while 21% (9) had multiple responses. Of the 4 POR fast-spiking cells responsive during the peri-stimulus epoch, 75% (3) had a single response and 25% (1) had multiple responses.

During the peri-stimulus epoch 25% (42 cells) of 140 HC pyramidal cells and 14% (23) of the 154 POR pyramidal cells responded to stimulus appearance, while 3% (5) of the 23 HC fast-spiking cells and 1% (2) of the 12 POR fast-spiking cells responded to stimulus appearance.

In response to outcome of the trial, 4% (6) of HC pyramidal cells and 7% (12) of POR pyramidal cells had changes in firing rate that appeared to differ based on correct vs. incorrect, while no HC fast-spiking cells and only 1% (1) POR fast-spiking cell responded to outcome.

An interaction between stimulus and outcome was seen in only 3% (5) of the HC pyramidal cells but in 10% (16) of the POR pyramidal cells. An interaction was seen in 1% (2) fast-spiking cells in both HC and POR.

Comparing between the two regions within the peri-stimulus epoch, HC pyramidal cells showed a significantly higher occurrence of response to stimulus onset compared to the POR ($X^2 = 9.6646$, $p<0.05$) while the POR had significantly more pyramidal cells that responded to the interaction of stimulus presentation and outcome of the trial ($X^2 = 9.5929$, $p<0.05$).

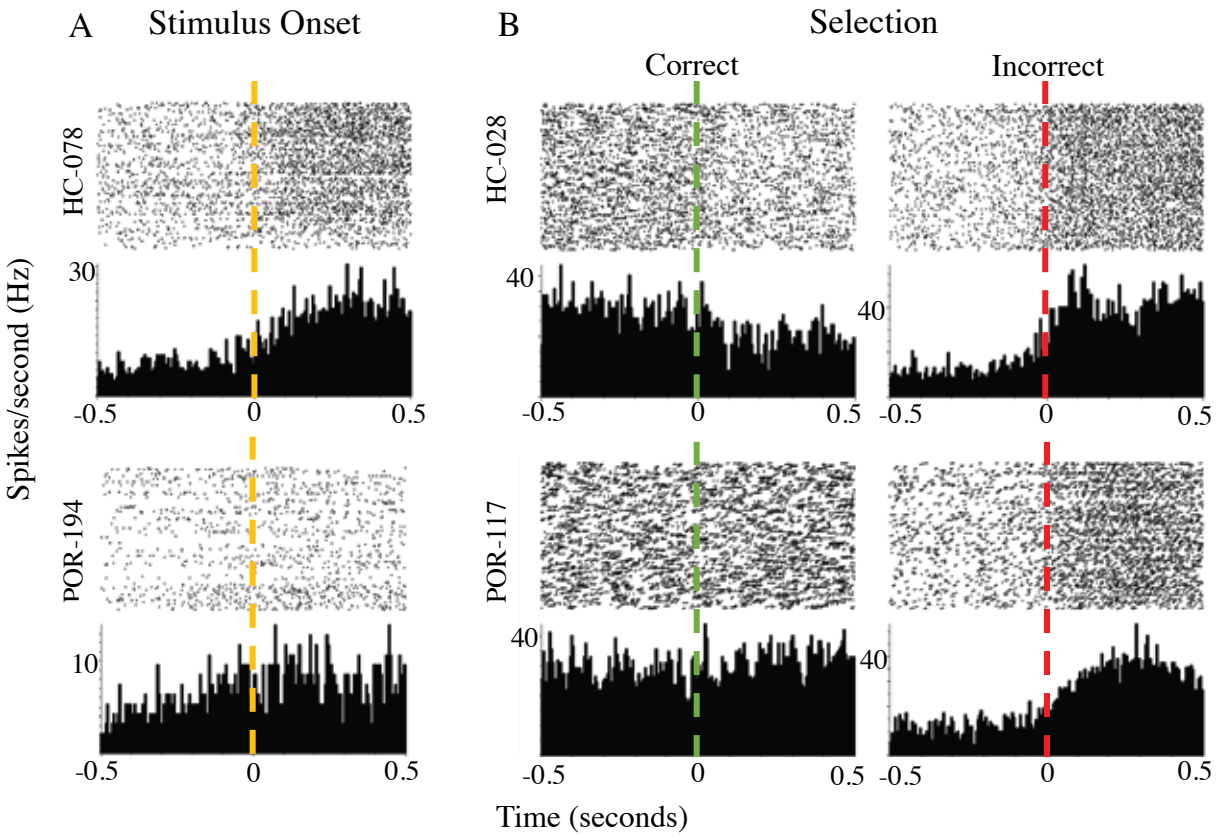

Figure 2.5. Raster and histogram plots for example selective cells. A. Example of one pyramidal HC (top) and one pyramidal POR cell (bottom) responsive to stimulus onset. B. The upper panel shows an example of a pyramidal HC cell responsive to outcome during the selection epoch. The lower panel shows an example of a pyramidal POR cell responsive to outcome during the selection epoch. Both are examples of cells that responded more to incorrect responses.

Peri-Selection

Of the 105 HC pyramidal cells responsive during the peri-selection epoch, 46% (48) had a single response while 54% (57) had multiple responses. Of the 21 fast-spiking HC cells responsive during the peri-selection epoch, 38% (8) had a single response and 62% (13) had multiple responses. For POR, of the 91 POR pyramidal cells responsive during the peri-selection epoch, 55% (50) had a single response while 45% (41) had multiple responses. Of the 12 POR fast-spiking cells responsive during the peri-selection epoch, 17% (2) had a single response and 83% (10) had multiple responses.

During the peri-selection epoch 39% (65 cells) of 140 HC pyramidal cells and 22% (37) of the 154 POR pyramidal cells responded to choice, while 8% (14) of the 23 HC fast-spiking cells and 4% (7) of the 12 POR fast-spiking cells responded to selection.

In response to outcome of the trial, 40% (66) of HC pyramidal cells and 32% (54) of POR pyramidal cells had changes in firing rate that appeared to differ based on correct vs. incorrect, while 8% (13) HC fast-spiking cells and 6% (10) POR fast-spiking cell responded to outcome.

An interaction between selection and outcome was seen in 33% (54) of the HC pyramidal cells and in 30% (50) of the POR pyramidal cells. An interaction was seen in 8% (13) of the HC fast-spiking cells and in 7% (11) of POR fast-spiking cells.

Comparing between the two regions within the peri-selection epoch, HC pyramidal cells showed a significantly higher occurrence of response to overall selection compared to the POR ($X^2 = 16.2439$, $p<0.05$, see Figure 2.5 for examples).

Location analysis

To form a full representation of context, spatial information is a necessary component, and therefore we also set out to examine whether the HC and POR represented special information differently during the locBCD task. We expected both the HC and POR to represent space, but not necessarily in the same way. To accomplish this, we analyzed cells for allocentric and egocentric correlates. An allocentric correlate would be, for example, a cell that fired more when the animal or the object to be chosen was in

the NW, SW, NE, or SE quadrant of the maze. A cell with a lower resolution allocentric correlate might fire differently when the animals or the chosen object was in the West vs. East or North vs. South (Figure 2.2D, Figure 2.5). A cell with an egocentric location correlate would fire differentially when the object to be chosen was on the animal's left, for example, regardless of the East/West side of the maze.

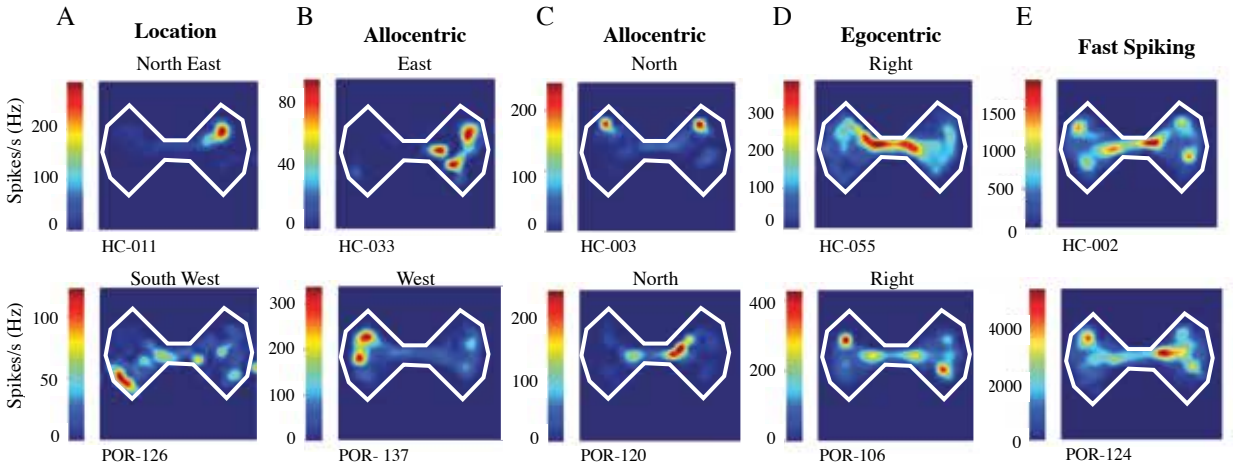

Figure 2.6. Example spatial plots for HC (top) and POR (bottom). A. Example of a location correlate in HC (North East) and POR (South West). B. Example of an East/West Allocentric spatial correlate in HC (East) and POR (West). C. Example of a North/South Allocentric spatial correlate in HC (North) and POR (North). D. Example of an Egocentric spatial correlate in HC (right) and POR (right). A-D. Examples of pyramidal cell firing patterns. E. Example of a fast spiking cell from HC (top) and POR (bottom).

Neuronal firing rates were analyzed during the three epochs in which location information was relevant: post stimulus epoch (500ms before stimulus onset), the pre-selection epoch (500ms before selection), and the post-stimulus epoch (500ms after selection). Location selectivity was evident for all three epochs for both HC and POR and in both pyramidal and fast-spiking cell types. To initially analyze allocentric spatial responses, East trials were compared to West trials, and North trials were compared to South trials. For the second analysis, cells were considered allocentric if they had any allocentric response. Egocentric right responses were compared to egocentric left responses.

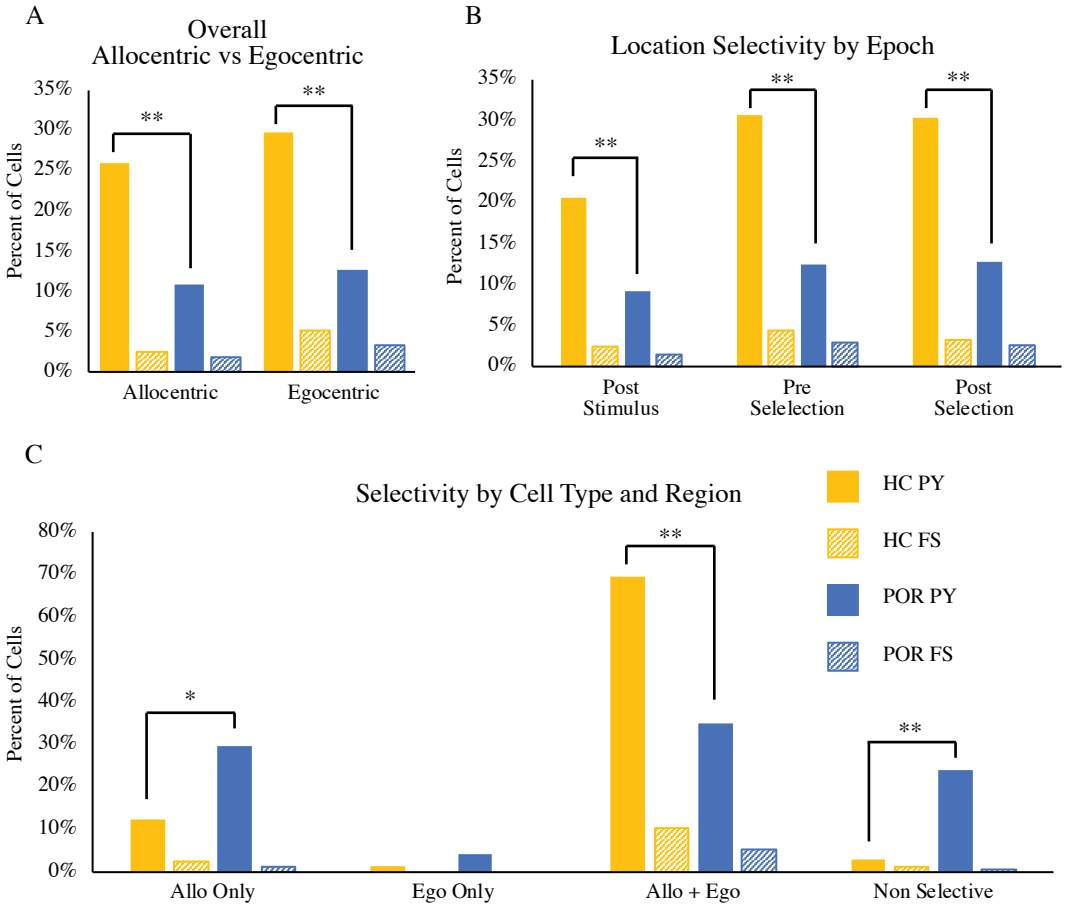

Figure 2.7. Location selectivity by cell type and region. A. Location selectivity separated by cell type and epoch. Percentages out of total PY or FS cells within a given region. B. Allocentric compared to egocentric selectivity. Data was collapsed across epochs as there were no observed differences. C. Selectivity separated by response. Again, data was collapsed across epochs as there were no observed differences. *p<0.05. **p<0.001.

Overall, HC cells were more selective than POR cells for both allocentric and egocentric responses, but only pyramidal cells were significantly more selective (allocentric $X^2 = 31.42$, $p<0.0001$; egocentric $X^2 = 46.56$, $p<0.0001$; Figure 2.7A). When the location selectivity was looked at broken down by epoch, we see that this same trend holds, with HC cells being more selective overall than POR cells, but only pyramidal cells being significantly more selective (post-stim $X^2 = 20.73$, $p<0.0001$; pre-selection $X^2 = 20.48$, $p<0.0001$; post-selection $X^2 = 29.67$, $p<0.0001$; Figure 2.7B).

However, when each spatial representation is examined individually, the POR had significantly more pyramidal cells that were responsive only to allocentric correlates (X^2 = 12.55, p<0.001) and significantly more pyramidal cells that were nonselective for a location correlate (X^2 = 28.39, p<0.0001) while the HC had significantly more pyramidal cells that were both allocentric and egocentric responsive (X^2 = 55.86, p<0.0001, Table2.2; Figure 2.7C).

Table 2.2. Allocentric and Egocentric correlates of HC and POR

Cell Correlate	HC Percent (#)		POR Percent (#)	
Allocentric Only	**15**	**(24)**	**31***	**(51)**
Pyramidal	*12*	*(20)*	*30*	*(49)*
Fast Spiking	*2*	*(4)*	*1*	*(2)*
Egocentric Only	**1**	**(2)**	**4**	**(7)**
Pyramidal	*1*	*(2)*	*4*	*(7)*
Fast Spiking	*0*	*(0)*	*0*	*(0)*
Allocentric + Egocentric	**80***	**(130)**	**40**	**(40)**
Pyramidal	*69*	*(113)*	*35*	*(58)*
Fast Spiking	*10*	*(17)*	*5*	*(9)*
No location correlate	**4**	**(7)**	**25***	**(41)**
Pyramidal	*3*	*(5)*	*24*	*(40)*
Fast Spiking	*1*	*(2)*	*1*	*(1)*
TOTAL	**100%**	**(163)**	**100%**	**(166)**
Pyramidal	***86%***	***(140)***	***93%***	***(154)***
Fast Spiking	***14%***	***(23)***	***7%***	***(12)***

*p<0.05 compared to region counterpart

Conjunction analysis

To address our second main question, we analyzed the emergence of object-location conjunction correlates in both the HC and POR during the locBCD task both

overall as well as separated by cell type. This sort of conjunctive coding might be expected if a region is representing context, i.e., the spatial layout of objects in the environment. However, object-location conjunctive coding might also emerge along with associative learning, for example, learning that an object has a particular meaning in a particular location. In the HC, object-location correlates emerged as an animal learned such an association (Komorowski, et al., 2009). These object-location cells, again, are cells that show selectivity for a particular object only when it is in a particular location (see Figure 2.8 for examples). Object-location conjunction cells were also discovered upstream of the HC in the POR. This was unexpected as previous paradigms suggested the HC to be the sole conjunction location within the parahippocampal system, linking the what and where streams together. Interestingly, these conjunction cells in the POR were observed in a simple, concurrent object discrimination task in which the location of the object in the environment was not behaviorally relevant (Furtak, et al., 2012). This suggests that object-location correlates develop automatically in POR compared with the HC in which they emerge with the learning of a location-based association.

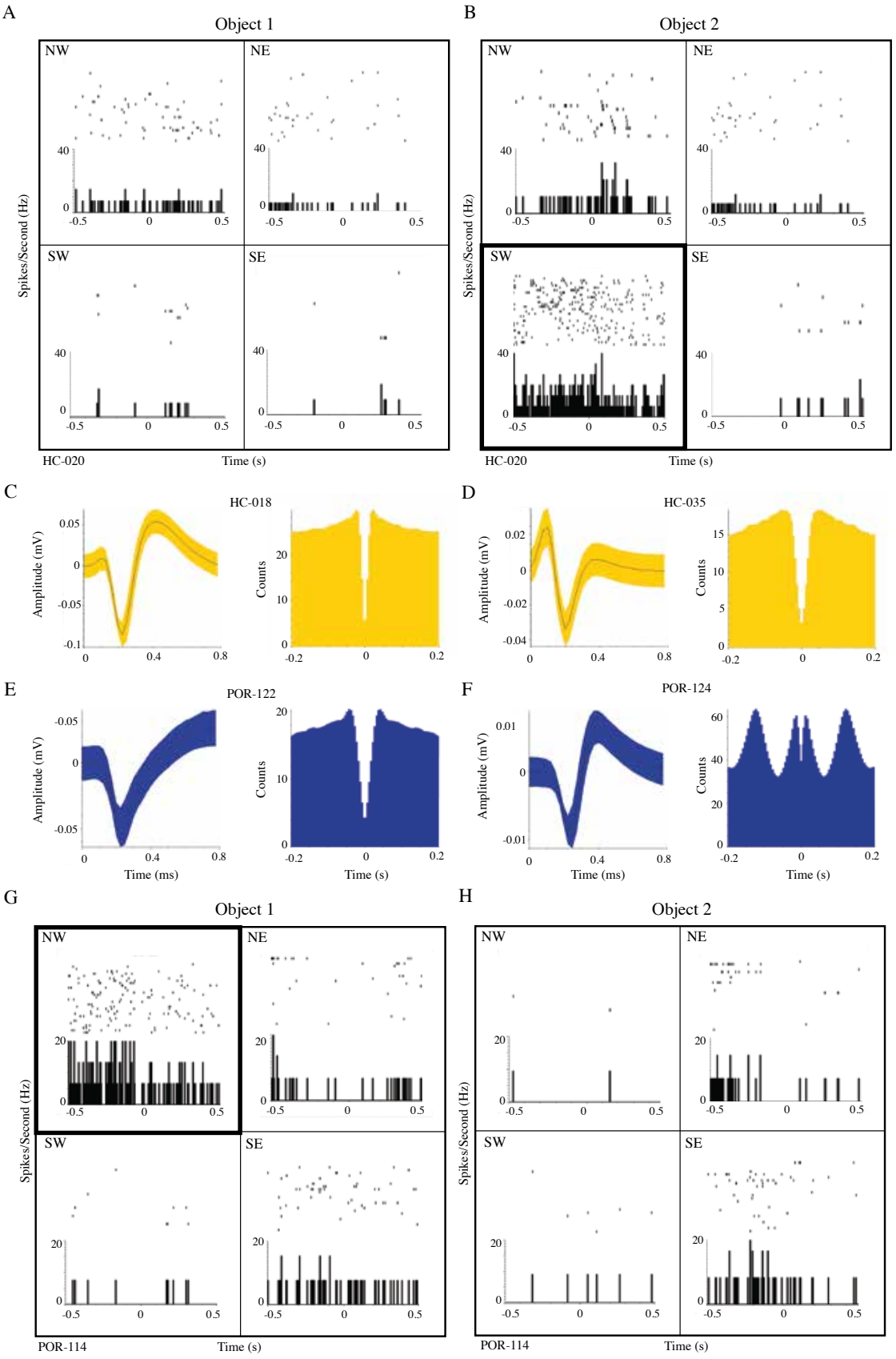
A
Object 1
NW
NE
SW
SE
Spikes/Second (Hz)
HC-020
Time (s)
B
Object 2
NW
NE
SW
SE
Spikes/Second (Hz)
HC-020
Time (s)
C
HC-018
Amplitude (mV)
Counts
D
HC-035
Amplitude (mV)
Counts
E
POR-122
Amplitude (mV)
Time (ms)
Counts
Time (s)
F
POR-124
Amplitude (mV)
Time (ms)
Counts
Time (s)
G
Object 1
NW
NE
SW
SE
Spikes/Second (Hz)
POR-114
Time (s)
H
Object 2
NW
NE
SW
SE
Spikes/Second (Hz)
POR-114
Time (s)

Figure 2.8. Example cells. A & B. Example HC pyramidal cell showing an object-location conjunction within a session. Rasters and histograms shown for responses to object 1 (A) and object 2 (B) in the North West (NW), North East (NE), South West (SW) and South East (SE) positions where objects could appear within the maze. This cell responded most strongly to object 2 when it was in the SW position (outlined in black). C. Example waveform and autocorrelogram for a HC pyramidal cell. D. Example waveform and aurocorrelogram for a HC fast spiking cell. E. Example waveform and autocorrelogram for a POR pyramidal cell. F. Example waveform and aurocorrelogram for a POR fast spiking cell. G & H. Example POR pyramidal cell showing an object-location conjunction within a session. Rasters and histograms shown for responses to object 1 (G) and object 2 (H) in the four possible object locations. This cell responded most strongly to object 1 when it was in the NW position (outlined in black).

To begin studying these object-location conjunctions, we first examined them across the three defined epochs within a given session: post-stimulus, pre-selection, and post-selection. When we do this, we find that in each epoch, HC cells respond significantly more to location than POR cells (post-stimulus: $X^2 = 19.65$, $p<0.0001$; pre-selection: $X^2 = 26.76$, $p<0.0001$; post-selection: $X^2 = 41.23$, $p<0.0001$; Figure 2.9). Whereas object and conjunction representations do not differ significantly between the HC and POR in either the post-stimulus or the pre-selection epochs. However, in the post-selection epoch, the HC shows significantly more responsive cells in both of these categories (object: $X^2 = 5.44$, $p<0.05$; conjunction: $X^2 = 9.63$, $p<0.05$). This is consistent with associative learning, as the animal is physically in the place where the object holds meaning (either rewarded or not rewarded).

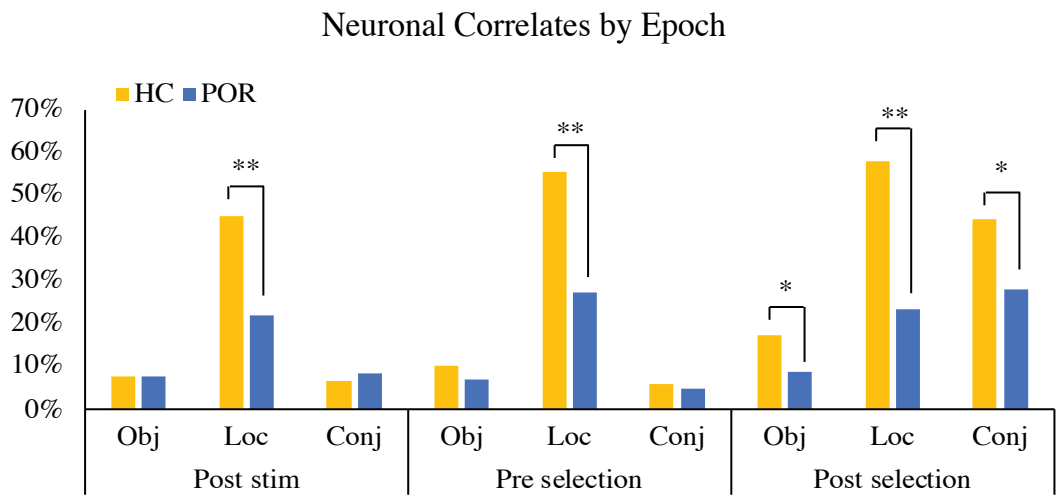

Figure 2.9. Percentages of HC and POR cells responsive object, location, and conjunctions during the three defined epochs. *p<0.05; **p<0.001.

When the cells of each region are separated by cell type, we see that the patterns apparent in the overall cell population were driven by the pyramidal cells, as they show the same significant differences. HC pyramidal cells respond significantly more to location than POR cells across all epochs (post-stimulus: $X^2 = 25.52$, $p<0.0001$; pre-selection: $X^2 = 28.32$, $p<0.0001$; post-selection: $X^2 = 50.72$, $p<0.0001$; Figure 2.10B). Object representations differ significantly only in the post-selection epoch, with HC pyramidal cells responding more ($X^2 = 5.78$, $p<0.05$; Figure 2.10A). Similarly, conjunction representations only differ significantly in the post-selection epoch, with HC pyramidal cells responding more ($X^2 = 12.61$, $p<0.05$; Figure 2.10C). Fast spiking cells did not differ significantly in any epoch for any representation, possibly due to the low numbers.

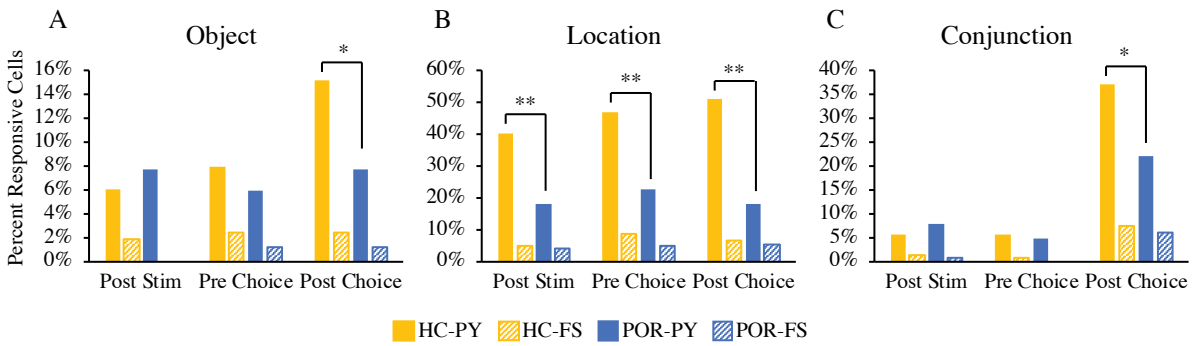

Figure 2.10. Percentages of HC and POR cells separated by pyramidal and fast spiking, responsive to (A) object, (B) location, and (C) conjunctions during the three defined epochs. All comparisons of distributions were non-significant.

Because the locBCD task was difficult for the rats to master and typically took multiple sessions for a rat to acquire the rule, we next separated all of the sessions into "Early", "Mid", and "Late" sessions by blocks, with the first 7 sessions labelled as "Early", the next 7 sessions labelled as "Mid" and any remaining sessions labelled as "Late". These divisions were decided upon based on the average performance of the animals. Generally, animals started reaching criterion more after approximately 7 sessions. When sessions were separated in this way, we unexpectedly found that cells in the HC seem to have object-location conjunctions emerge in earlier sessions than we see them emerging in POR, with the conjunctions eventually becoming more prevalent in POR (Figure 2.11A, C). Specifically, 40% (20 cells) of the 50 HC cells recorded during early sessions showed conjunction representations compared to 16% (9) of the 56 early session POR cells ($X^2 = 7.61$, $p<0.05$). Further, 49% (37) of the 75 mid-session HC cells showed conjunctions, compared to 14% (21) of the 82 mid-session POR cells ($X^2 = 9.46$, $p<0.05$). In the late sessions, 42% (16) of the 38 HC cells showed conjunction correlates

while 61% (17) of the 28 late session POR cells showed conjunction correlates ($X^2 = 2.23$, $p>0.05$).

When the cells of each region are separated by cell type, we again see that the patterns observed in the overall data were mainly driven by pyramidal cells, although there was a strong response from POR FS cells (Figure 2.11B, D). This response was not significantly greater than that of the HC FS cells, again likely due to the low numbers of total FS cells recorded.

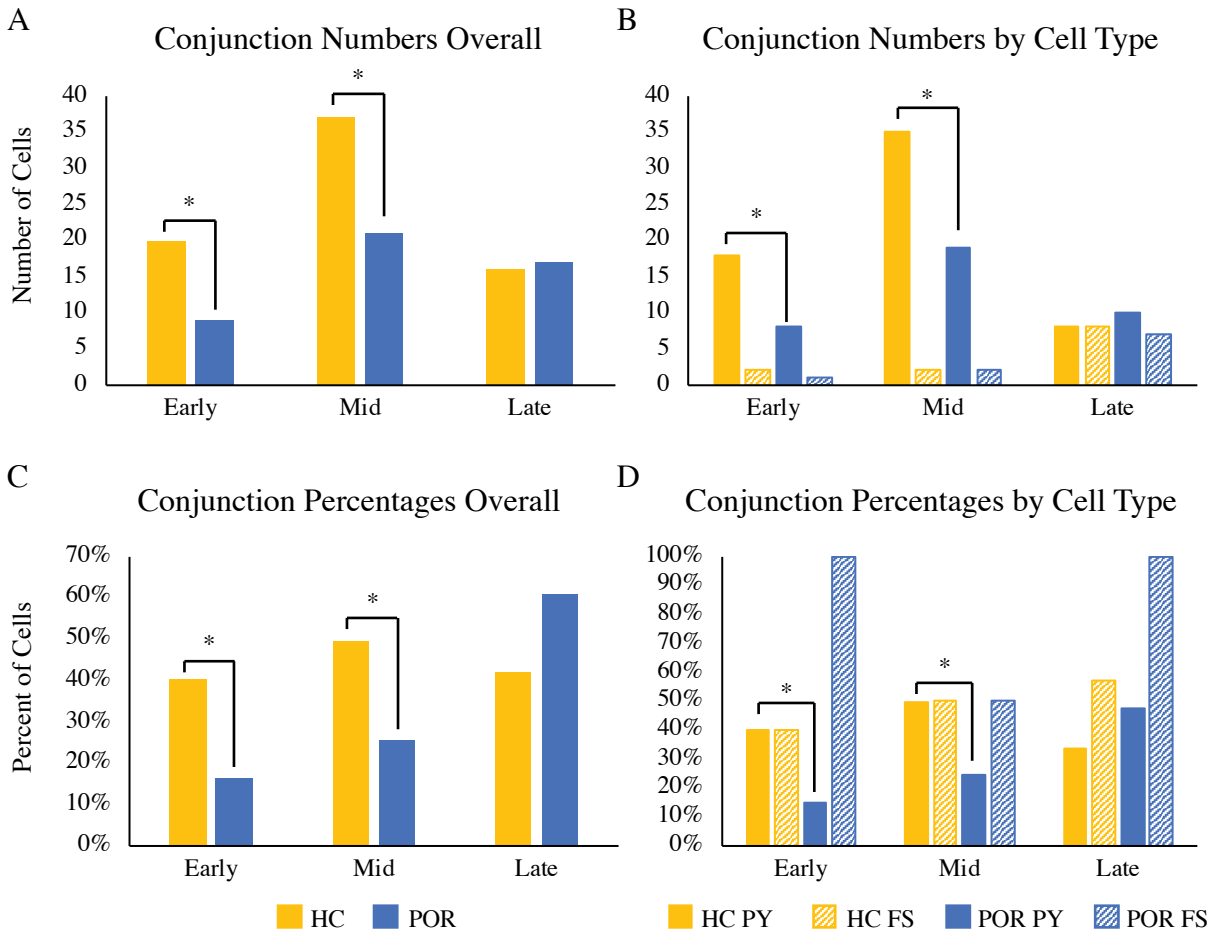

Figure 2.11. Numbers and percentages of object-location conjunction cells across sessions. These cells were responsive to a particular object in a particular location during early, mid, or late sessions. A. Numbers of conjunction cells in HC and POR in Early, Mid, and Late Sessions. B. Numbers of conjunction cells in HC and POR split by cell type. C. Percentages of conjunction cells in Early, Mid, and Late Sessions. D. Percentages of conjunction cells split by cell type. *p<0.05.

In the final analysis, we examined sessions from the four animals with dual-site implants in which a new object pair was introduced. When this analysis was performed by Komorowski, et al. (2009), they found that within each session, object-location conjunctions emerged as the animal learned the association. When we separated our trials in a similar manner, we found that POR cells showed significantly more conjunction correlates in both initial ($X^2 = 14.15$, $p<0.0001$) and ending ($X^2 = 16.99$, $p<0.0001$) trials

of a given session (Figure 2.12A), which closely matches with our prediction that the POR immediately forms context representations including objects-in-locations.

Interestingly, if we separate the cells of each region by cell type, we see that during sessions in which a novel object was presented, POR FS cells responded especially consistently (Initial trials POR FS = 100% [3 FS cells]; Ending trials POR FS = 100% [3 FS cells]; Figure 2.12B). Further, although only HC pyramidal cells showed any conjunctions during Initial trials (5%, 3 PY cells) only HC FS cells showed conjunctions in Ending trials (10%, 1 FS cell; Figure 2.12B).

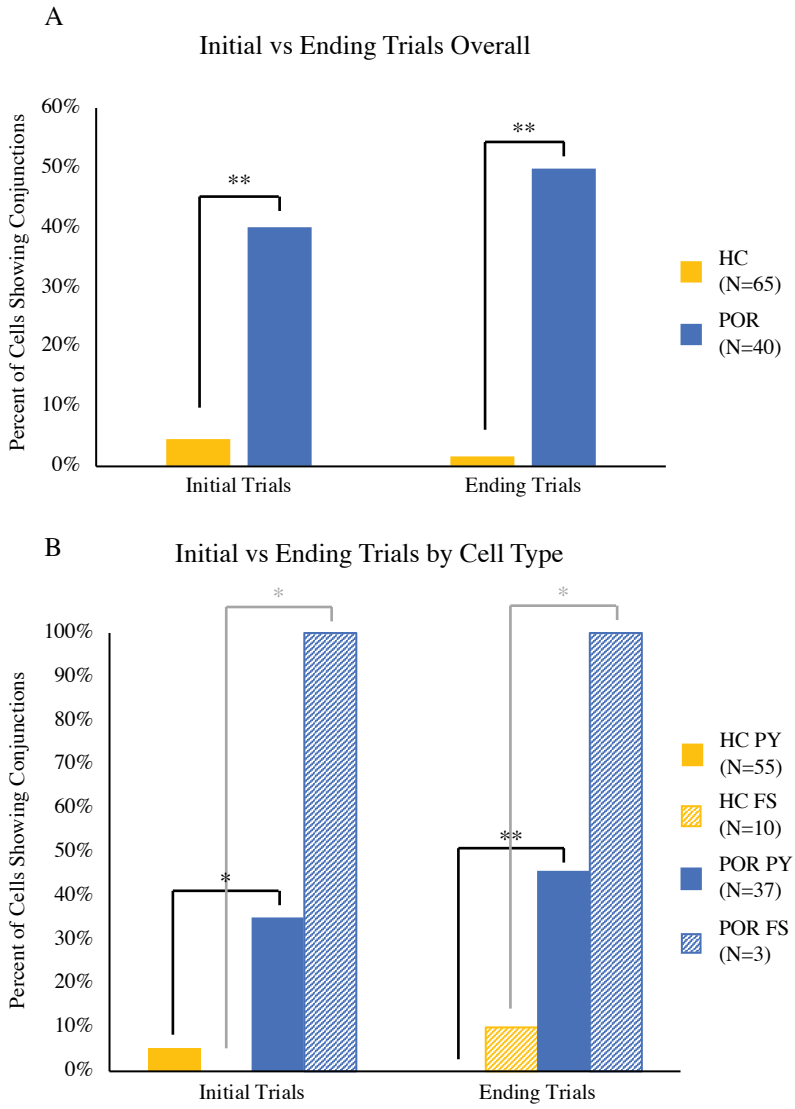

Figure 2.12. Percentages of object-location conjunctions in HC and POR. A. Percentages of all HC and POR cells showing object location conjunctive responses during Initial and Ending trials in a given session in which novel objects were presented. B. Percentages of cells in HC and POR broken down by cell type that showed conjunctions in Initial and Ending trials of a given session in which novel objects were presented. *p<0.05; **p<0.001.

Local field potential analysis

Because brain oscillations, particularly in the theta, gamma, and we propose alpha ranges (see chapter 3), are thought to represent or encode various important aspects of attention, memory, and cognition, we conducted multi-taper spectral analyses of HC and POR LFP signals, focusing on the theta, alpha, and gamma bands. Sessions that had strong theta and in which the tetrodes were localized to the appropriate region were used in this analysis, comparing the cell firing to all localized electrodes. Theta rhythms were

defined as 6–10 Hz oscillations, alpha as 9-12 Hz, and fast gamma as 70–110 Hz. Theta oscillations in the hippocampus are strongly modulated by running speed (reviewed in Buzsaki, 2005) and POR theta oscillations have been shown to be similarly modulated by speed (Furtak et al., 2012) so we first examined both theta and the proposed separated alpha oscillations with respect to velocity. Doing this, we find that both HC and POR theta are significantly positively correlated with running speed (HC theta: $r = 0.497$, $p<0.05$; POR theta: $r = 0.748$, $p<0.05$). Conversely, neither HC alpha or POR alpha are correlated with running speed (HC alpha: $r = 0.212$, $p>0.05$; POR alpha: $r = 0.179$, $p>0.05$). Together, these suggest that the separation of alpha from theta at or around these demarcations is potentially valid.

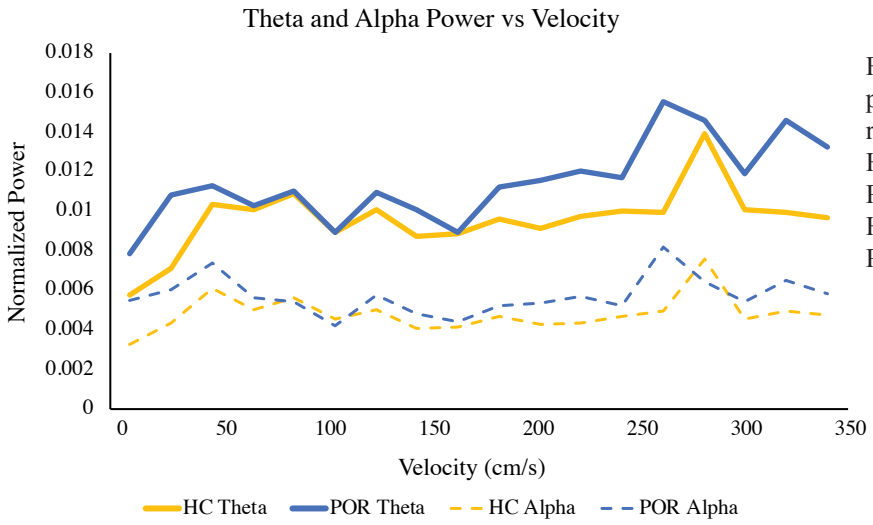

Figure 2.13. Theta and alpha power in the HC and POR with respect to velocity.
HC theta: $r = 0.497$, $p<0.05$.
POR theta: $r = 0.748$, $p<0.001$.
HC alpha: $r = 0.212$, $p>0.05$.
POR alpha: $r = 0.179$, $p>0.05$.

An examination of neuronal synchrony indicated that cells from both HC and POR fired in phase with theta, alpha (see Chapter 3 for a more in-depth analysis of alpha), and fast gamma to varying degrees. Specifically, significantly more HC cells were phase locked to theta than POR cells, with HC having 59% (96 of 163) of cells locked to

theta and POR having 39% (66 of 169) cells locked to theta ($X^2 = 9.96$, $p < .05$; Figure 2.14, Figure 2.15A). Phase locking to alpha or fast gamma did not differ significantly between the HC and POR (alpha: $X^2 = 0.20$, $p > .05$; fast gamma: $X^2 = 2.28$, $p > .05$; Figure 2.15A).

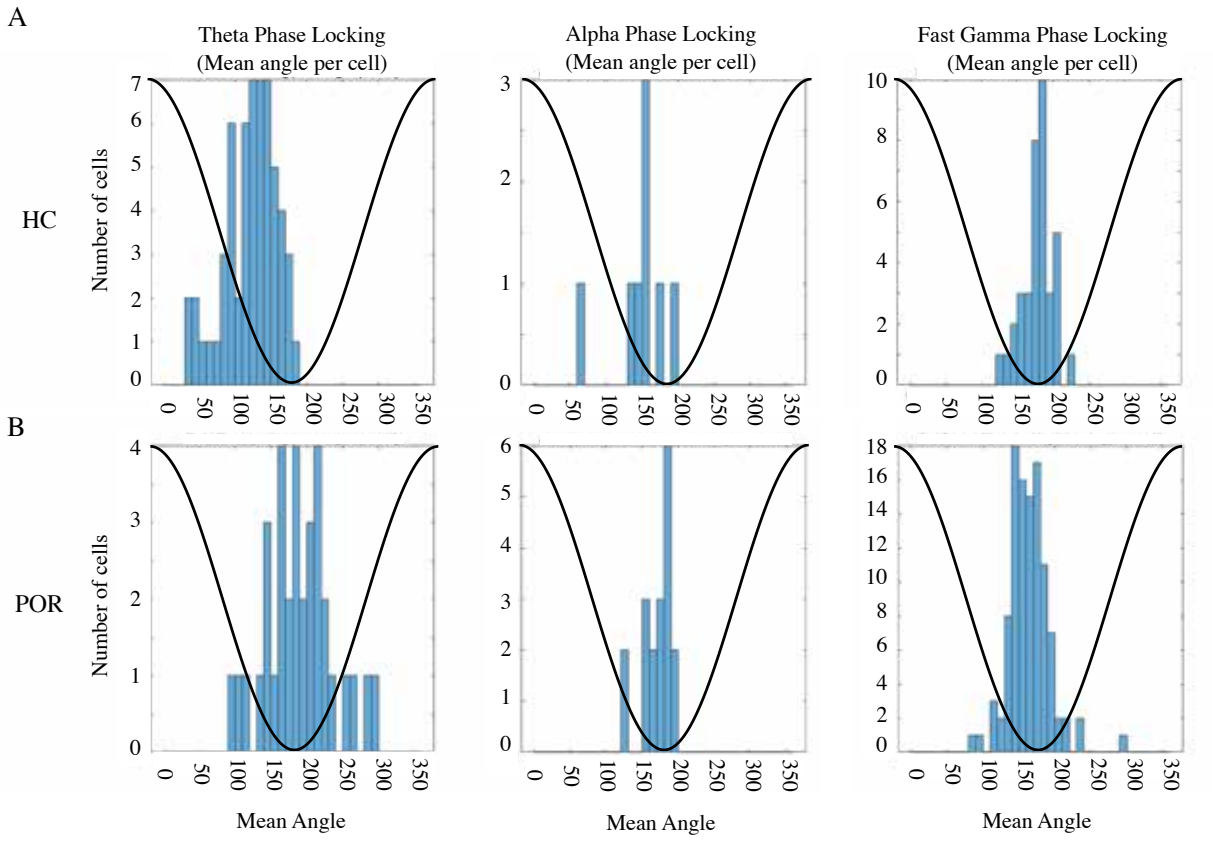

Figure 2.14. A. Phase locking of HC cells to theta, alpha, and fast gamma based on mean angle for each cell. B. Phase locking of POR cells to theta, alpha, and fast gamma based on mean angle for each cell.

When the cells of each region are separated by cell type, we see an interesting trend pop out. Specifically, we see that while HC pyramidal cells are still significantly more phase locked to theta than POR pyramidal cells ($X^2 = 16.50$, $p < .001$; Figure 2.15B), POR fast spiking cells are significantly more phase locked to theta than HC fast spiking cells ($X^2 = 5.90$, $p < .05$; Figure 2.15B). Further, although overall there was not a significant difference between HC and POR with respect to phase locking to alpha in

general for the regions, we see that again, POR fast spiking cells are significantly more phase locked than HC fast spiking cells ($X^2 = 5.90$, $p < .05$; Figure 2.15B). Finally, although the between region comparisons are not significant, we see that both HC and POR show greater percentages of fast spiking cell phase locking to fast gamma than pyramidal cells in either region.

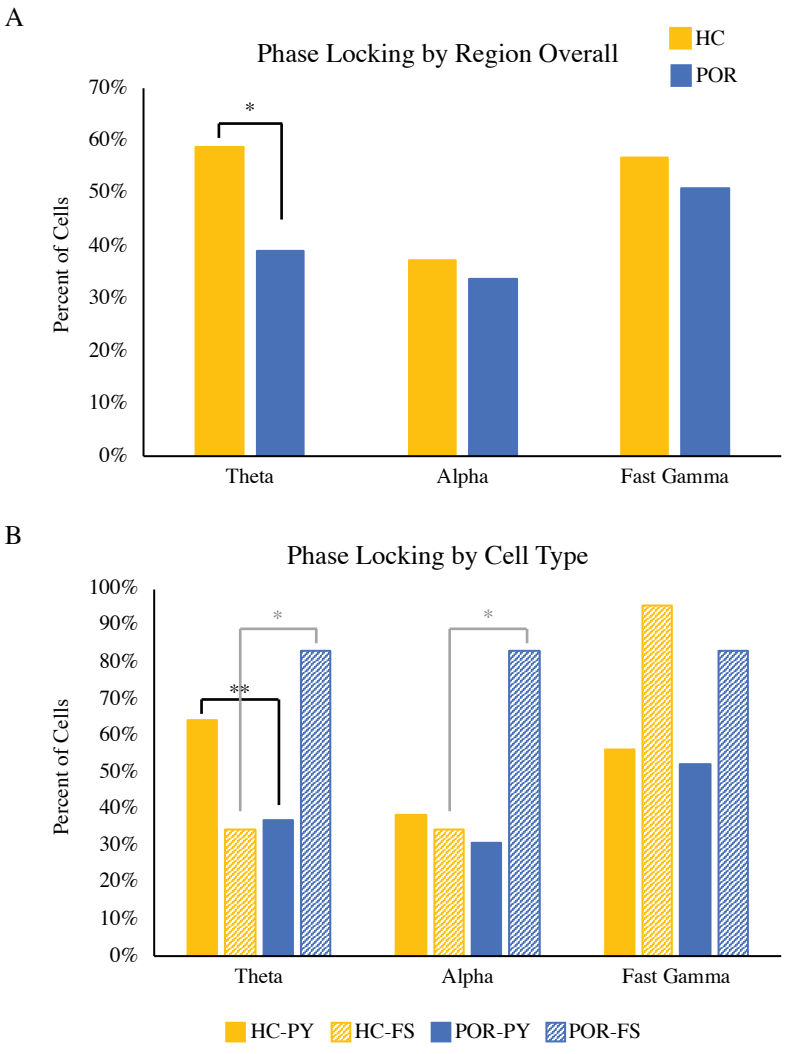

Figure 2.15. Percentages of phase locking in HC and POR. A. Percentages of all HC and POR cells showing phase locing to theta, alpha, or fast gamma. B. Percentages of cells in HC and POR broken down by cell type that showed phase locking to theta, alpha, or fast gamma. *p<0.05; **p<0.001.

Discussion

In this study, we used a novel location bi-conditional task to examine the neuronal correlates of the HC and the POR during learning and execution of complex rule. Both spatial and non-spatial information were presented to the rats to be used in completion of the task, and therefore we were able to examine both spatial and non-spatial correlates throughout the post stimulus, pre selection, and post selection epochs. During this task, the animal was trained to stop in designated "ready" positions for a variable amount of time to trigger a trial. Once the objects appeared, the animal needed to make a decision and approach one of the objects. If correct, the animal received reward via intracranial stimulation of the medial forebrain bundle, and if incorrect, the animal received a short time-out before being allowed to trigger a new trial. The use of the floor projection maze in conjunction with this task design exploited the natural tendency of a rat to explore its environment and to focus on stimuli presented to the lower portion of its visual field (Lashley, 1938). Further, the automatic design of this task allowed for increased trial numbers per session compared to previous manual versions, which is crucial in *in vivo* electrophysiological studies. Using this experimental design, we are able to report on 2 main topics examined: comparative spatial and non-spatial analysis between HC and POR, and the relative timing of conjunction emergence, and we examine these factors with respect to our hypothesis that the POR represents aspects of context in the local physical environment, specifically objects-in-locations, more immediately than does the HC.

First, we have shown that both HC and POR have specific yet different responses to the peri-stimulus and peri-selection epochs. During the peri-stimulus epoch, the HC

had 25% (42) pyramidal cells that represented stimulus onset, while the POR pyramidal cells represented the interaction of stimulus onset and trial outcome more than the HC with 10% (16 cells; see Table 2.1). While subtle, this statistically significant difference is the first indication that the POR is representing contextually relevant conjunctions at a time prior to the HC. In the location analysis, we showed that while the HC had more location representations overall, when broken down into subcomponents, the POR had significantly more allocentric-only representations while the HC had more allocentric-egocentric interactions. Further, we found that these differences were predominately driven by pyramidal cells in both the HC and POR. This finding is not surprising as allocentric-egocentric interactions are likely a large component of what makes place cells so robustly punctate, and based on previous findings we would expect to see more place cells and general location correlates in the HC than in the POR.

In the conjunction analysis, we examined the responsiveness of cells in the HC and POR to the presented objects, the behaviorally relevant locations, and the conjunction of an object in a particular location. We again saw that in every examined epoch, the HC had significantly more location correlates than the POR (Figure 2.9), and this was driven predominantly by the responses of the pyramidal cells (Figure 2.10). Further, in the post selection epoch specifically, the HC also exhibited a greater overall percentage of both object cells [HC: 18% (29); POR: 9% (15); $X^2 = 5.44$, $p<0.05$] as well as object-location conjunction cells [HC: 45% (73); POR: 28% (47); $X^2 = 9.63$, $p<0.05$], and again, these differences were driven by the pyramidal cells in each region. While it is not surprising that the HC has greater representations of these things overall, it is interesting to see object representations in the POR as well as to see a greater percentage of cells in the

POR representing object-location conjunctions [28% (47)] than location alone [23% (39)]. Together, these indicate that the known anatomical connection between the perirhinal cortex, which is known to be important in object discrimination and representation, and the POR is also likely functional.

We next divided the training sessions into early, mid, and late sessions to compare the occurrence of object-location conjunctions between the HC and POR with respect to these time frames. Based on the findings from Komorowski et al. (2009) showing that item-place, or object-location, correlates emerged with the learning of an association in the HC (Komorowski et al., 2009), and the previous work in the POR that indicates the POR represents the environment and changes in the environment very quickly (Burwell and Hafeman, 2003), we expected to see conjunctions in the POR in earlier sessions than we saw them in the HC. This is not what was found (see Figure 2.11). Instead, we found that in early sessions and mid sessions, the HC had significantly more conjunction correlates than the POR. Although not statistically significant, the POR did have more conjunction correlates in the late sessions than HC. Further, while the observed trends appeared to be mostly driven by the pyramidal cells within the regions, we do see a robust response of the fast spiking cells, especially in the POR.

Initially, finding that the HC showed conjunctions significantly more than the POR in earlier sessions was surprising. We expected that because the POR seems to form representations more immediately than the HC, and because the task took multiple sessions to learn the rule, that this division would show conjunctions in POR earlier. However, there are several possible reasons for not observing the predicted result. First, during this time period the rats were learning the task, so the early and middle learning

sessions may not have captured object learning. Alternatively, object learning may have already emerged even though performance did not reach criterion. Second, the tetrodes were being moved downward across sessions. This may not have made much difference in the HC because tetrodes were always in the pyramidal cells layer. In contrast, in the POR, tetrodes were moving from layer to layer. It may be that the location of tetrodes later in training accounts for differences. For these reasons, the second within session analysis of novel pairs is more appropriate.

The second analysis provided the opportunity to compare HC and POR responses to objects in specific locations prior to learning, and this analysis more closely matches that which was done by Komorowski et al. (2009) as they examined conjunction emergence in single sessions as opposed to across multiple sessions. To ensure that we were only analyzing sessions that included trials prior to object learning, for this analysis we limited the sessions to those in which novel pairs were presented to the animals. When only sessions with novel pairs were examined and trials within each session were split into "initial" and "ending" trials, we do, in fact, see a striking difference in the timing of conjunction emergence in the POR and HC (Figure 2.12). In the first half of the session, or initial trials, 40% (16) of the POR cells recorded showed object-location conjunctions, compared to 5% (3) of HC cells ($X^2 = 20.92$, $p<0.0001$). This provides strong evidence that, consistent with our hypothesis, the POR represents object-location conjunctions in the local physical environment on a faster time scale than does the HC. It should be noted that, in the locBCD task, rats do not generally learn which object is correct in a single session. When we separate these populations out by cell type, we see that there is a striking response of fast spiking cells in the POR to object-location

conjunctions when presented with novel objects. However, based on the number of cells recorded, the pyramidal cells within the POR still drove the main differences.

Finally, in our analysis of the local field potentials in HC and POR, we found several interesting results. Previously it was shown that 38% of POR cells were phase locked to theta (Furtak et al., 2012). This is extremely similar to the 39% (66) of POR cells that we found phase locked to theta here. Interestingly, this previous study also found that 64% of POR cells phase locked to slow gamma, while we found no cells in either HC or POR that phase locked to slow gamma. Furtak et al. also found that 93% of POR cells showed significant phase locking to fast gamma, while we observed 53% in the POR and 61% in the HC. Although the results of POR cells phase locking to theta were well reproduced, there was a fair decrease in fast gamma phase locking and a surprising absence of slow gamma phase locking. One possible source of this difference is the increased number of cells recorded from the POR here compared to the previous study (n = 169 vs n = 69, respectively). Therefore, with an increased pool, the effects previously seen may have been somewhat washed out. A second possible source of difference is the quality of the LFP recording, specifically in using tetrodes in this study compared to stereotrodes in the previous study.

Functionally, the observed rhythms and phase-locking have several potential indications. The stable proportion of cells phase-locked to theta in the POR might suggest that the attentional role theta plays is an important component required for the complete representation of context, and here we were able to reproduce this function. Further, the large proportions of fast spiking POR cells phase locked across theta, alpha, and fast gamma compared to their proportions in the HC might signal an interesting function of

inhibition within the POR network compared to the HC. The equivalent phase locking in HC and POR to fast gamma is interesting in light of the theory that MEC, which is upstream of the HC but downstream of the POR, is a main source of fast gamma in the HC (Chrobak & Buzsaki, 1998; Colgin et al., 2009). One possibility this suggests is that the main source of fast gamma is earlier in the network than MEC. Alternatively, this might suggest that directionality, as it typically applies to neuronal signaling, is less strict with respect to oscillation generation, such that "upstream" and "downstream" have less importance.

Summary

Our finding that postrhinal cells show more object-location conjunctions than the hippocampus when animals are presented with a novel object-context problem provides strong evidence for our hypotheses about postrhinal function. These findings are consistent with the view that object-location conjunctive coding in the hippocampus results from associative learning, whereas object-location conjunctive coding in the postrhinal cortex results from representing the spatial layout of objects and features in the local physical environment. Postrhinal context representations are made available to other brain regions for a variety of purposes. In the locBCD task, the postrhinal cortex represents context and monitors the current context for changes, whereas the hippocampus is binding object information from the perirhinal cortex with context information from the postrhinal cortex to form object-location associations.

References

Agster, K. L., & Burwell, R. D. (2013). Hippocampal and subicular efferents and afferents of the perirhinal, postrhinal, and entorhinal cortices of the rat. *Behavioural Brain Research*, *254*, 50–64. https://doi.org/10.1016/j.bbr.2013.07.005

Altunkaynak, B. Z., Altunkaynak, E., Unal, D., & Unal, B. (2009). A novel application for the cavalieri principle: A stereological and methodological study. *The Eurasian Journal of Medicine*, *41*(2), 99–101.

Belluscio, M. A., Mizuseki, K., Schmidt, R., Kempter, R., & Buzsaki, G. (2012a). Cross-Frequency Phase-Phase Coupling between Theta and Gamma Oscillations in the Hippocampus. *Journal of Neuroscience*, *32*(2), 423–435. https://doi.org/10.1523/JNEUROSCI.4122-11.2012

Belluscio, M. A., Mizuseki, K., Schmidt, R., Kempter, R., & Buzsaki, G. (2012b). Cross-Frequency Phase-Phase Coupling between Theta and Gamma Oscillations in the Hippocampus. *Journal of Neuroscience*, *32*(2), 423–435. https://doi.org/10.1523/JNEUROSCI.4122-11.2012

Bucci, D. J., Phillips, R. G., & Burwell, R. D. (2000). Contributions of postrhinal and perirhinal cortex to contextual information processing. *Behavioral Neuroscience*, *114*(5), 882–894. https://doi.org/10.1037/0735-7044.114.5.882

Bucci, D. J., Saddoris, M. P., & Burwell, R. D. (2002). Contextual fear discrimination is impaired by damage to the postrhinal or perirhinal cortex. *Behavioral Neuroscience*, *116*(3), 479–488.

Burglen, F., Marczewski, P., Mitchell, K. J., van der Linden, M., Johnson, M. K., Danion, J.-M., & Salamé, P. (2004). Impaired performance in a working memory binding task in patients with schizophrenia. *Psychiatry Research*, *125*(3), 247–255. https://doi.org/10.1016/j.psychres.2003.12.014

Burwell, R. D., & Amaral, D. G. (1998). Cortical afferents of the perirhinal, postrhinal, and entorhinal cortices of the rat. *The Journal of Comparative Neurology*, *398*(2), 179–205. https://doi.org/10.1002/(sici)1096-9861(19980824)398:2<179::aid-cne3>3.0.co;2-y

Burwell, R.D, & Hafeman, D. M. (2003). Positional firing properties of postrhinal cortex neurons. *Neuroscience*, *119*(2), 577–588. https://doi.org/10.1016/S0306-4522(03)00160-X

Burwell, Rebecca D. (2001). Borders and cytoarchitecture of the perirhinal and postrhinal cortices in the rat: Perirhinal and Postrhinal Borders and Cytoarchitecture. *Journal of Comparative Neurology*, *437*(1), 17–41. https://doi.org/10.1002/cne.1267

Burwell, Rebecca D., Saddoris, M. P., Bucci, D. J., & Wiig, K. A. (2004). Corticohippocampal contributions to spatial and contextual learning. *The Journal of Neuroscience: The Official Journal of the Society for Neuroscience*, *24*(15), 3826–3836. https://doi.org/10.1523/JNEUROSCI.0410-04.2004

Chrobak, J. J., & Buzsáki, G. (1998). Gamma Oscillations in the Entorhinal Cortex of the Freely Behaving Rat. *The Journal of Neuroscience*, *18*(1), 388–398. https://doi.org/10.1523/JNEUROSCI.18-01-00388.1998

Colgin, L. L., Denninger, T., Fyhn, M., Hafting, T., Bonnevie, T., Jensen, O., Moser, M.-B., & Moser, E. I. (2009a). Frequency of gamma oscillations routes flow of information in the hippocampus. *Nature*, *462*(7271), 353–357. https://doi.org/10.1038/nature08573

Colgin, L. L., Denninger, T., Fyhn, M., Hafting, T., Bonnevie, T., Jensen, O., Moser, M.-B., & Moser, E. I. (2009b). Frequency of gamma oscillations routes flow of information in the hippocampus. *Nature*, *462*(7271), 353–357. https://doi.org/10.1038/nature08573

Drevets, W. C., Price, J. L., & Furey, M. L. (2008). Brain structural and functional abnormalities in mood disorders: Implications for neurocircuitry models of depression. *Brain Structure and Function*, *213*(1–2), 93–118. https://doi.org/10.1007/s00429-008-0189-x

Eacott, M. J. (2004). Integrated Memory for Object, Place, and Context in Rats: A Possible Model of Episodic-Like Memory? *Journal of Neuroscience*, *24*(8), 1948–1953. https://doi.org/10.1523/JNEUROSCI.2975-03.2004

Eacott, M. J., & Gaffan, E. A. (2005). The Roles of Perirhinal Cortex, Postrhinal Cortex, and the Fornix in Memory for Objects, Contexts, and Events in the Rat. *The Quarterly Journal of Experimental Psychology Section B*, *58*(3–4b), 202–217. https://doi.org/10.1080/02724990444000203

Eacott, Madeline J., & Norman, G. (2004). Integrated memory for object, place, and context in rats: A possible model of episodic-like memory? *The Journal of Neuroscience: The Official Journal of the Society for Neuroscience*, *24*(8), 1948–1953. https://doi.org/10.1523/JNEUROSCI.2975-03.2004

Eichenbaum, H., Yonelinas, A. P., & Ranganath, C. (2007). The Medial Temporal Lobe and Recognition Memory. *Annual Review of Neuroscience*, *30*(1), 123–152. https://doi.org/10.1146/annurev.neuro.30.051606.094328

Eichenbaum, Howard. (2000). A cortical–hippocampal system for declarative memory. *Nature Reviews Neuroscience*, *1*(1), 41–50. https://doi.org/10.1038/35036213

Eichenbaum, Howard, & Lipton, P. A. (2008). Towards a functional organization of the medial temporal lobe memory system: Role of the parahippocampal and medial entorhinal cortical areas. *Hippocampus*, *18*(12), 1314–1324. https://doi.org/10.1002/hipo.20500

Fowler, K. S., Saling, M. M., Conway, E. L., Semple, J. M., & Louis, W. J. (2002). Paired associate performance in the early detection of DAT. *Journal of the International Neuropsychological Society: JINS*, *8*(1), 58–71.

Frankland, P. W., Cestari, V., Filipkowski, R. K., McDonald, R. J., & Silva, A. J. (1998). The dorsal hippocampus is essential for context discrimination but not for contextual conditioning. *Behavioral Neuroscience*, *112*(4), 863–874. https://doi.org/10.1037/0735-7044.112.4.863

Furtak, S. C., Ahmed, O. J., & Burwell, R. D. (2012). Single Neuron Activity and Theta Modulation in Postrhinal Cortex during Visual Object Discrimination. *Neuron*, *76*(5), 976–988. https://doi.org/10.1016/j.neuron.2012.10.039

Furtak, S. C., Cho, C. E., Kerr, K. M., Barredo, J. L., Alleyne, J. E., Patterson, Y. R., & Burwell, R. D. (2009). The Floor Projection Maze: A novel behavioral apparatus for presenting visual stimuli to rats. *Journal of Neuroscience Methods*, *181*(1), 82–88. https://doi.org/10.1016/j.jneumeth.2009.04.023

Furtak, S. C., Wei, S.-M., Agster, K. L., & Burwell, R. D. (2007). Functional neuroanatomy of the parahippocampal region in the rat: The perirhinal and postrhinal cortices. *Hippocampus*, *17*(9), 709–722. https://doi.org/10.1002/hipo.20314

Gewirtz, J. C., McNish, K. A., & Davis, M. (2000). Is the hippocampus necessary for contextual fear conditioning? *Behavioural Brain Research*, *110*(1–2), 83–95. https://doi.org/10.1016/S0166-4328(99)00187-4

Holland, P. C., & Bouton, M. E. (1999). Hippocampus and context in classical conditioning. *Current Opinion in Neurobiology*, *9*(2), 195–202. https://doi.org/10.1016/S0959-4388(99)80027-0

Jacobson, T. K., Ho, J. W., Kent, B. W., Yang, F.-C., & Burwell, R. D. (2014). Automated Visual Cognitive Tasks for Recording Neural Activity Using a Floor Projection Maze. *Journal of Visualized Experiments*, *84*, 51316. https://doi.org/10.3791/51316

Jarrard, L. E., Davidson, T. L., & Bowring, B. (2004). Functional differentiation within the medial temporal lobe in the rat. *Hippocampus*, *14*(4), 434–449. https://doi.org/10.1002/hipo.10194

Knierim, J. J., Lee, I., & Hargreaves, E. L. (2006). Hippocampal place cells: Parallel input streams, subregional processing, and implications for episodic memory. *Hippocampus*, *16*(9), 755–764. https://doi.org/10.1002/hipo.20203

Komorowski, R. W., Manns, J. R., & Eichenbaum, H. (2009). Robust Conjunctive Item-Place Coding by Hippocampal Neurons Parallels Learning What Happens Where. *Journal of Neuroscience*, *29*(31), 9918–9929. https://doi.org/10.1523/JNEUROSCI.1378-09.2009

Lashley, K. S. (1938). The Mechanism of Vision: XV. Preliminary Studies of the Rat's Capacity for Detail Vision. *The Journal of General Psychology*, *18*(1), 123–193. https://doi.org/10.1080/00221309.1938.9709894

Maren, S., Aharonov, G., & Fanselow, M. S. (1997). Neurotoxic lesions of the dorsal hippocampus and Pavlovian fear conditioning in rats. *Behavioural Brain Research*, *88*(2), 261–274. https://doi.org/10.1016/S0166-4328(97)00088-0

Murray, E. A., Bussey, T. J., & Saksida, L. M. (2007). Visual Perception and Memory: A New View of Medial Temporal Lobe Function in Primates and Rodents. *Annual Review of Neuroscience*, *30*(1), 99–122. https://doi.org/10.1146/annurev.neuro.29.051605.113046

Naber, P. A., Witter, M. P., & Lopes da Silva, F. H. (2001). Evidence for a direct projection from the postrhinal cortex to the subiculum in the rat. *Hippocampus*, *11*(2), 105–117. https://doi.org/10.1002/hipo.1029

O'Keefe, J., & Conway, D. H. (1978). Hippocampal place units in the freely moving rat: Why they fire where they fire. *Experimental Brain Research*, *31*(4). https://doi.org/10.1007/BF00239813

O'Keefe, John. (1976). Place units in the hippocampus of the freely moving rat. *Experimental Neurology*, *51*(1), 78–109. https://doi.org/10.1016/0014-4886(76)90055-8

Shapiro, M. L., Tanila, H., & Eichenbaum, H. (1997). Cues that hippocampal place cells encode: Dynamic and hierarchical representation of local and distal stimuli. *Hippocampus*, *7*(6), 624–642. https://doi.org/10.1002/(SICI)1098-1063(1997)7:6<624::AID-HIPO5>3.0.CO;2-E

Shin, L. M., Shin, P. S., Heckers, S., Krangel, T. S., Macklin, M. L., Orr, S. P., Lasko, N., Segal, E., Makris, N., Richert, K., Levering, J., Schacter, D. L., Alpert, N. M., Fischman, A. J., Pitman, R. K., & Rauch, S. L. (2004). Hippocampal function in posttraumatic stress disorder. *Hippocampus*, *14*(3), 292–300. https://doi.org/10.1002/hipo.10183

Squire, L. R., Stark, C. E. L., & Clark, R. E. (2004). THE MEDIAL TEMPORAL LOBE. *Annual Review of Neuroscience*, *27*(1), 279–306. https://doi.org/10.1146/annurev.neuro.27.070203.144130

Wood, S. J., Proffitt, T., Mahony, K., Smith, D. J., Buchanan, J.-A., Brewer, W., Stuart, G. W., Velakoulis, D., McGORRY, P. D., & Pantelis, C. (2002). Visuospatial memory and learning in first-episode schizophreniform psychosis and established schizophrenia: A functional correlate of hippocampal pathology? *Psychological Medicine*, *32*(3), 429–438. https://doi.org/10.1017/S0033291702005275

CHAPTER 3

NOVEL OSCILLATORY "FLUTTER" EVENTS DURING A COMPLEX TASK

Valerie J. Estela[1], Sean G. Trettel[2], Tyler Barnes-Diana[2], Rebecca D. Burwell[1,2]

VJE performed all experiments contained in this chapter. SGT and TBD assisted with analyses of flutters. VJE wrote the chapter with input from RDB.

[1]Neuroscience Graduate Program, Brown University, Providence, Rhode Island 02912, USA
[2]Department of Cognitive, Linguistic and Psychological Sciences, Brown University, Providence, Rhode Island 02912, USA

Abstract

Currently, oscillation bands described for the cerebral cortex of rodents include a very broad theta band of 4-12 Hz and do not include a distinct range of frequencies for the alpha band. In humans, theta is generally defined as 4-8 Hz and alpha is defined as 8-12 Hz (Uhlhaas & Singer, 2010). Here, we describe a phenomenon in the rodent brain recorded in the hippocampus and postrhinal cortex, termed "flutters", that exhibit characteristics similar to alpha oscillations in the human brain. Flutters are 2-5 second episodes of increased power in the 9-12 Hz frequency band, peaking at ~10 Hz. They are different from Type 1 theta in that they occur only when the rat is nearly motionless, whereas Type 1 theta power positively correlates with running speed. Behaviorally, flutters occurred during three parts of a location bi-conditional task trial. They are most robust immediately after stimulus onset and after object selection, but they also sometimes occur between trials. Flutters appear to emerge as the animal moves from simple strategies in early trials to complex strategies in later trials. Together, these data suggest the need to update the defined oscillation bands in the rodent to include a novel oscillation that is analogous to attentional alpha in the human brain.

Introduction

Alpha rhythms (8–12 Hz) are the most predominant oscillations in the human brain, but their functional role remains controversial. Specifically, there seem to be contradictory reports about their proposed function. Historically, alpha was thought of as a correlate of a "ground state" or "cortical idling" that occurs during the absence of sensory input (Haegens et al., 2011; Pfurtscheller et al., 1996). According to this view, alpha oscillations are a passive mechanism that emerge when the brain is disengaged, whereas during sensorimotor or cognitive challenges they lose amplitude and are replaced by other neural mechanisms. Conversely, more recently alpha has been shown to be an active mechanism, becoming stronger when visual inputs are actively ignored, leading to a proposed top-down inhibitory role for alpha rhythms in attention (Klimesch et al., 1998; Worden et al., 2000; Jenson & Mazaheri, 2010; Jones et al., 2010; Bonnefond & Jenson, 2012; Sacchet et al., 2015; Sadaghiani & Kleinschmidt, 2016; Kizuk & Mathewson, 2017).

One way that alpha oscillations are studied are via event related synchronization and desynchronization (ERS/D). ERS/D has long been used in human EEG studies to assess the correlation of task-related events to changes in amplitude within different frequency bands when compared to a preceding reference interval (Neuper & Klimesch, 2006; Pfurtscheller & Aranibar, 1977; Pfurtscheller & Lopes da Silva, 2005). Using this method, the prevailing view was that ERD, or a decrease, of activity in the alpha band reflects an increase of excitability of neurons in the involved cortical areas, while ERS, or an increase in alpha activity, reflects a reduced state of active information processing in the underlying neuronal networks (Pfurtscheller & Lopes da Silva, 2005; Pfurtscheller,

1999; Pfurtscheller, Stancak, & Neuper, 1996). Recent evidence, however, also suggests that synchronization of alpha activity is a functional correlate of active cognitive task performance, presumably involving cognitive inhibition processes (Klimesch et al., 2007). Specifically, an information gating process has been suggested as a main function of alpha oscillations in cortical areas. Several studies have shown that cued spatial attention leads to decreased alpha amplitudes in parietal and occipital regions contralateral to the attended site in visual (Worden et al., 2000; Kelly et al., 2006; Thut et al., 2006) and multimodal (Foxe et al., 1998; Jones et al., 2010; Sacchet et al., 2015) tasks, while simultaneously showing an increase in alpha amplitudes contralateral to the distractor, or actively ignored, sites. Together, these suggest a function of alpha oscillations as a way to actively tune out certain stimuli and choose the stimuli to focus on.

Related to the idea of alpha oscillations serving to protect working memory maintenance against anticipated distracters, alpha oscillations have also been seen to differ based on working memory load and attentional demands. Several studies have reported a 'paradoxical' synchronization or increase in alpha activity during tasks requiring increased memory loads and/or attentional demands (Klimesch et al., 1999; Jensen et al., 2003; Sauseng et al., 2005; Cooper et al., 2003). For example, increases in alpha activity occur in association with internally versus externally directed attention (Cooper et al., 2003). In their study, Cooper and colleagues (2003) defined externally directed attention as that elicited by the presentation of visual, auditory, and haptic stimulus sequences, while internally directed attention was produced by the imagining of these stimulus sequences. EEG alpha activity in humans has also been found to correlate

with creative cognition in tasks designed to elicit divergent thinking, requiring the generation of original and creative ideas to solve problems (Arden et al., 2010; Dietrich & Kanso, 2010; Fink et al., 2007). An example of a divergent thinking task would be to require a participant to come up with as many unusual uses as possible for an everyday object such as a brick. Thus, there is evidence that increased alpha activity corresponds to internally directed processes and creative problem solving. Together, these suggest that alpha may be necessary for intentional deployment of selective attention.

These seemingly different observed functions of alpha oscillations might not be entirely separate or mutually exclusive, however. One thread that links these observations together is this idea of selective attention. Specifically, choosing what to ignore and what to focus on, with alpha oscillations serving as the medium for this communication within and between regions.

In humans, alpha is often defined as approximately 8-12 Hz, with theta defined as 4-8 Hz and (Lever et al., 2014). In rodents, the defined oscillation bands include delta (~0-4 Hz), theta (~4-12 Hz), beta (~12-30 Hz), and gamma (>30 Hz; Buzsaki, 2005). The theta frequency band is comparatively broad, and in rodents there is no distinct range of frequencies analogous to alpha in the human brain. Despite this lack of a defined alpha range in rodents, here we observed oscillations at approximately 10 Hz that we argue most closely resemble the described functions of alpha.

The original goals of the performed study were to examine theta and gamma oscillations in the HC and POR during the Location Bi-Conditional (locBCD) task to better understand how the regions interact during a complex spatial task. Serendipitously, during the data collection process, I observed a novel oscillation in the high theta

frequency band that did not show the expected characteristics of theta. Therefore, the goals of the following set of analyses were to better understand this phenomenon and determine any observed correlation with behavior and/or cognition. We herein refer to these high amplitude events that occurred at approximately 10 Hz as “flutters”.

Experimental procedures

Subjects

Subjects were 4 male Long-Evans rats (Charles Rivers Laboratories, Wilmington, MA). Rats were initially pair housed in a 12:12 hr light:dark cycle with ad libitum access to water. After surgery, rats were singly housed in paired cages with a porous divider in order to have contact with the former cage mate. After arriving in the colony, animals were handled several days per week until the beginning of behavioral training. Prior to training, rats were placed on a feeding schedule to maintain body weight at 85%–90% of free feeding weight. Because the task relied on light to be performed, animals were tested during the light portion of their light cycle to avoid disturbing the animals’ circadian rhythms. All procedures were in accordance with appropriate institutional animal care and use committee and NIH guidelines for the care and use of animals in research.

Apparatus

The floor projection apparatus described previously (Furtak et al., 2009; Jacobson et al., 2014) consisted of a bowtie shaped maze (~115 x 70 x 45 cm) in which images

were back-projected to the floor and the position of the animal was tracked via camera from above (Figure 3.1). This was used in conjunction with Cineplex v3 (Plexon, Inc.) for location tracking and Med-PC IV software (Med Associates, Inc.) for task automation based on location and delivery of intracranial stimulation (ICS) of the medial forebrain bundle for reward.

Behavioral Training

Animals are implanted prior to the start of behavioral training. The training paradigm began 7 days post-surgery with habituation to the room, habituation to the maze, and habituation to the connected cables. Optimization of ICS levels was then used to create a conditioned place preference for the start zones, simultaneously training the animals to stop in the correct zones and wait for a variable amount of time. Once stopping reliably, animals were trained to approach a 2D object that is presented on the floor following the variable wait period (900 - 1300ms) to receive a reward. Once approaching stimuli consistently, animals were then transitioned to a training pair of objects, and begin the process of learning the bi-conditional rule. Limits are set to ensure that observed preferences are minimized. Animals could not complete more than 5 trials on a given side of the maze without being forced to complete a trial on the opposite side. Similarly, correction trials were used to eliminate left/right side biases. Animals that demonstrated a preference for going to a particular side received correction trials that forced them to complete the same choice, with the correct answer on their non-preferred side. Finally, to avoid the possibility of using an alternating strategy, animals could only complete 10 trials in an alternating fashion before being forced to perform 2 trials on the

same side of the maze. After an animal reached criterion on a pair or no longer showed interest, they were subsequently presented with new pairs in following sessions. In all phases of shaping and training in which two objects were presented, the left versus right location of the correct stimulus was counterbalanced in randomized trials.

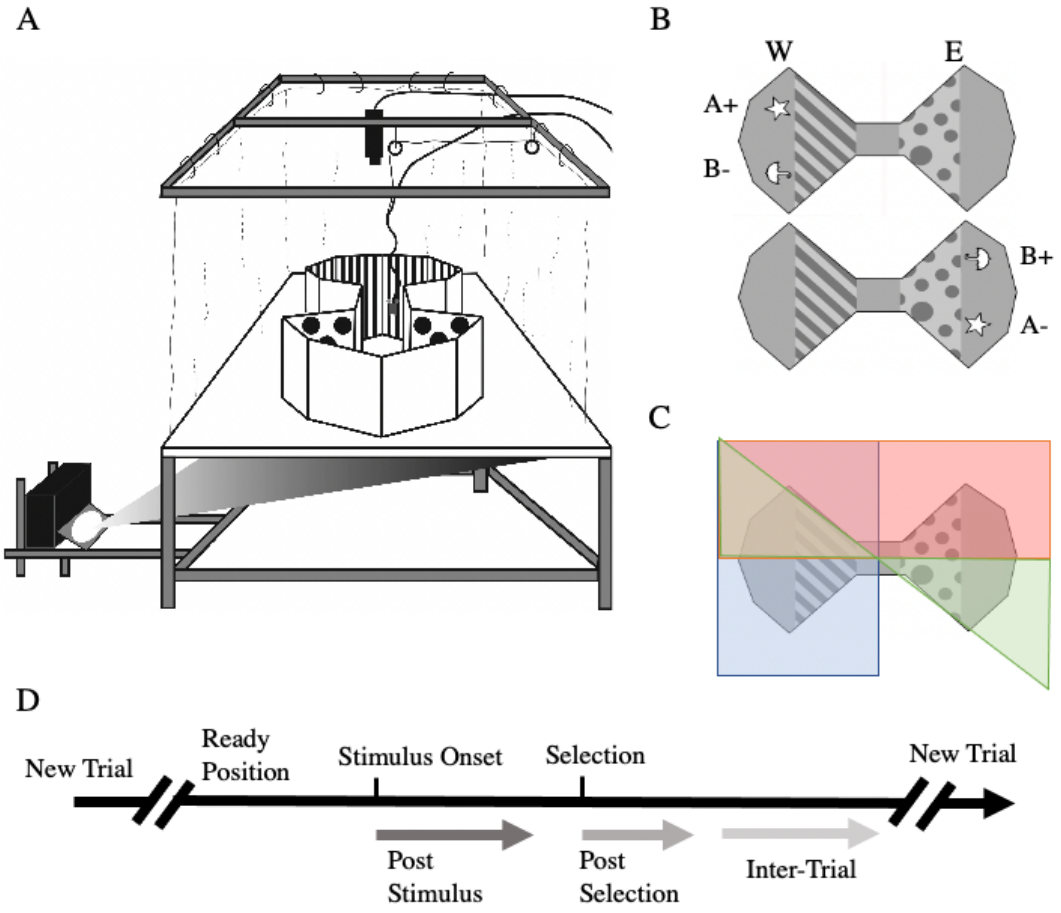

Figure 3.1. The Location Bi-conditional (locBCD) task. A. Schematic of the floor projection maze with the bowtie-shaped enclosure used for the task. B. Top down view of west vs. east trials. Trials were initiated when the rat stopped in the ready position (middle of the maze) and faced one side of the maze (either west or east). After a variable period, two objects appeared. One object was correct in the West (A+) and the other in the East (B+) regardless of left vs right location. The animal made a selection by approaching one of two objects. Correct choices were rewarded with intracranial stimulation of the medial forebrain bundle. C. Representative portions of the maze as analyzed; blue = allocentric West, red = allocentric North, green = egocentric right. D. Epochs examined within the locBCD task. Post Stimulus represents the time period following simulus onset until selection. Post Selection represents the 5 seconds immediately following object selection. Inter-Trial represents the time following Post Stimulus and before the start of the subsequent trial. Panel A adapted from Jacobson, et al., 2014, JOVE.

Surgery and Histology

Under isoflurane anesthesia electrodes were stereotaxically implanted targeting

POR (-0.1mm anterior to and 4.4mm lateral to lambda, 16°angle laterally) and HC (-3.6mm posterior to and 2.9mm lateral to bregma). An ICS electrode was implanted contralaterally to the HC bundle (-2.2 posterior to and 2.0 lateral to bregma). The implanted microdrive assembly was produced in-house and consisted of 24 individually drivable tetrodes (25 mm nichrome wires, A-M Systems, Inc., Carlsborg, WA). The electrodes were lowered 0.5 mm from the cortical surface and secured with dental cement, dental acrylic, and anchor screws. Rats were allowed 7 days to recover prior to behavioral training. At the end of the experiment, animals were given an overdose of Beuthanasia-D (100 mg/kg, i.p.), electrode tip placements were marked with a small lesion, the animals were perfused, and the brains were extracted and prepared for histology and subsequent localization of electrodes. The locations of electrode tips were reconstructed with a light microscope and localized in POR as defined by Burwell (2001). During recording, microdrivers were generally driven down slowly (~43.75μm/day) as the animal learned to perform the task. Total distance advanced ranged from 1.59mm to 2.91mm in HC and 3.32mm to 4.28mm in POR.

Electrophysiology

The Omniplex D Neural Data Acquisition (Plexon, Inc.) system was used to record neuronal activity during performance of the task. Single unit activity was filtered at 0.77 – 6000 Hz and digitized at 40 Hz. Waveforms were extracted by real-time thresholding (PlexControl, Plexon, Inc.) and stored for offline isolation using Offline Sorter (Plexon, Inc.). Timestamps and behavioral event markers were extracted using Neuroexplorer (Plexon, Inc.). Local field potential (LFP) activity was filtered at 0.7-170

Hz and digitized at 1 kHz. Power was obtained using multi-taper spectral analysis of the LFP (Neuroexplorer, Plexon, Inc.).

Analysis

Continuous data (LFPs) as well as timestamps for behaviorally relevant event markers were extracted and exported to Matlab (Mathworks, Natick, MA) from Neuroexplorer (NEX, Plexon, Inc.). For analysis of velocity, XY coordinates for each animal was collected at a rate of 30Hz based on location of LED's placed on the rats headcap. The animal's position was initially estimated from these XY coordinates. At each timestamp, position information was collected and averaged. Where position information was lacking (where no LED positions were recorded) the position was linearly interpolated from the preceding and post ceding data points. Once the position was estimated, a velocity vector was calculated by taking the difference of each two neighboring data values and creating a vector one less than the length of the position vector. To match this vector to the timestamps (which correspond to each position measurement) each timestamp corresponding to each velocity measurement was the average of the timestamps that corresponded to the position information used to calculate the velocity. As a simplified example, if the animal was at position 5 at second 1 and position 10 at second 2 the output would be 5 units/second as an instantaneous velocity at second 1.5. Once the velocities were calculated for each session, the velocities that directly preceded each flutter by 10 seconds, during each flutter, and followed each flutter (also a 10 second period) were extracted. The mean velocity magnitude was calculated for each flutter.

Before the flutters were accepted as an actual observed phenomenon, we determined what other sources these events might stem from such as physical sources of noise. Several potential sources were identified: grooming/scratching, chewing/bruxing, and physical banging of the implant on the walls of the maze. LFP's during grooming and scratching artifacts as well as physical banging of the implant on the walls of the maze were compared to observed flutters by examining timepoints in videos in which the physical acts were observed. When compared, we found that these types of physical noise created much larger amplitude events that were registered as all frequencies as compared to events that had a clear frequency of around 10 Hz. Chewing/bruxing artifacts were compared by allowing rats to forage for cocoa pebbles within the maze. While these artifacts had an amplitude more similar to the flutters, they also did not show a specific peak at 10 Hz, nor did they retain the characteristic elliptical shape that flutters tend to show. Finally, because we thought these flutters might represent alpha within the rodent, we checked to see if the rodents were closing their eyes during flutters, as eyes-closed resting has previously been strongly correlated with increased alpha in humans. It would be unusual for rodents to close their eyes, and upon examination of the videos, we can see that they do not appear to be doing so at any point during the observed events.

To detect the flutters in a given session, we created a detection algorithm. Prior to processing, the LFP during the 750 ms during ICS was zeroed out. The multi-taper spectrogram was then calculated from the processed LFP, using a 1 sec moving window, 10 ms step size, and taper parameters: [time-bandwidth product = 3, number of tapers = 5]. The spectrogram was z-scored within each frequency bin. The theta (6-12 Hz) band of the spectrogram was averaged across frequency, giving us a time-series vector with

average z-scored power as a function of time. Periods during which the average z-scored power was greater than 7.0 were removed, as these periods corresponded to either physical noise (e.g. drive hitting the wall) or chewing artifact. Periods in which the remaining averaged z-scored power was above 1.2 for at least one second were then considered as candidate alpha flutters. Each event was then inspected visually and compared to the video in order to eliminate false positives such as scratching/grooming artifact, high-amplitude noise not otherwise removed, or false positives from an overall lack of oscillatory activity.

Results

Histology

Implanted electrodes were localized via examination and measurement of Nissl-stained brain regions. A 500 μm x 500 μm grid was created based on the scale bar for the microscope images acquired, and overlaid on each section. Each column was numbered starting with the most medial box at 1. For HC slices, electrodes were localized within a 90º grid of columns as electrodes were implanted at a 0º angle, or 90º to the surface of the skull/brain. For POR slices, electrodes were localized within a 16º grid of columns as electrodes were implanted at a 16º angle to the surface of the skull/brain. Observed electrode locations were recorded for each individual section. Pictures of the implanted electrode bundle were then used to match tracks of electrodes based on anterior-posterior and medial-lateral relative locations. Hippocampal electrodes were located between -1.56 mm and -3.20 mm posterior to bregma and between 0.8 mm-2.5 mm lateral to the midline

(Figure 3.2A). Postrhinal electrodes were located between -7.38 mm and -9.24 mm posterior to bregma (Figure 3.2B).

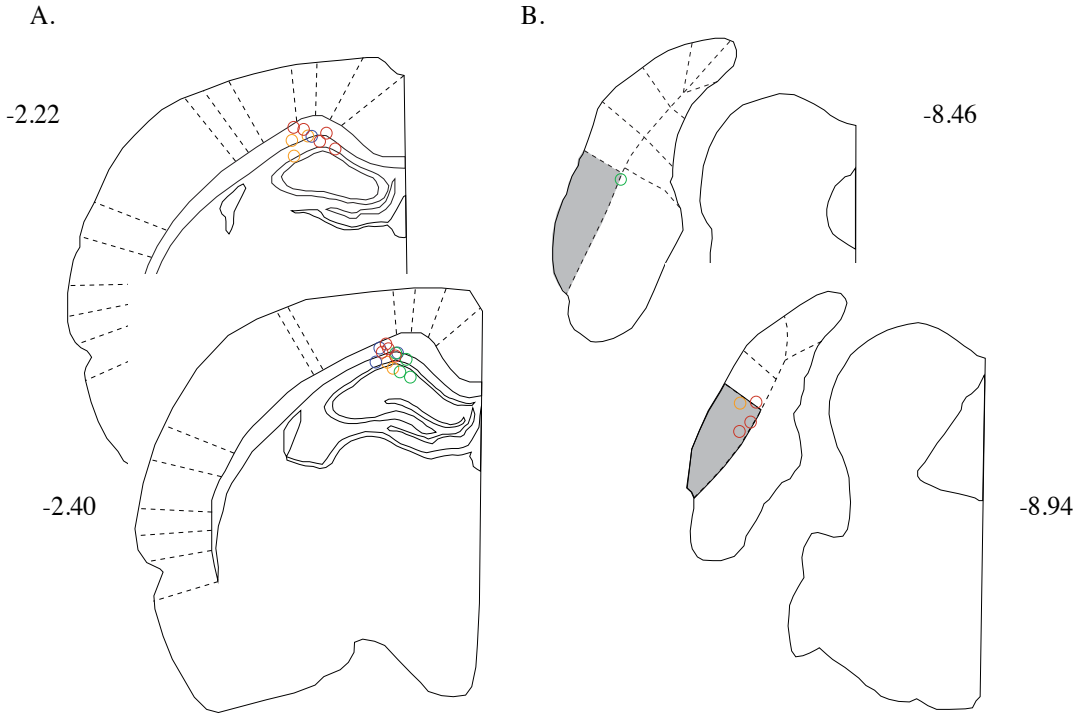

Figure 3.2. Estimated locations of implanted tetrodes. Tetrodes are color coded by animal. A. Histology from animals with dual-site HC and POR implants showing HC tetrodes. Coronal sections shown at Bregma - 2.22 mm and Bregma -2.40 mm. B. Histology from animals with dual-site HC and POR implants showing POR tetrodes. Coronal sections shown at Bregma – 8.46 mm and Bregma -8.94 mm. Red: 19-012, green: 19-013, blue: 19-014, orange: 19-015

Defining the Characteristics of Flutters

As previously stated, these novel flutter events were discovered during the course of alternate data collection. They were first observed in real time as animals were performing the task, and then subsequently isolated and analyzed for behavioral and cognitive correlates. Examples of what was observed in real-time as the animal was performing the task can be seen in Figure 3.3A, B, and F. Importantly, although the appearance of the flutters differed between electrodes that were in the HC and POR

bundles, both structures consistently showed clear events, with no events occurring in one region but not the other.

The first defining characteristic of this novel oscillation is its surprisingly distinct onset and offset. These oscillatory events produce a strikingly high amplitude pulse lasting an average of 2-5 seconds, although they ranged in duration from 0.9 s – 10.5 s. (Figure 3.3A, B). The onset and offset of these events were tapered, reaching their peak amplitude within 200-500 ms of starting and decreasing amplitude approximately 200-500 ms before ending.

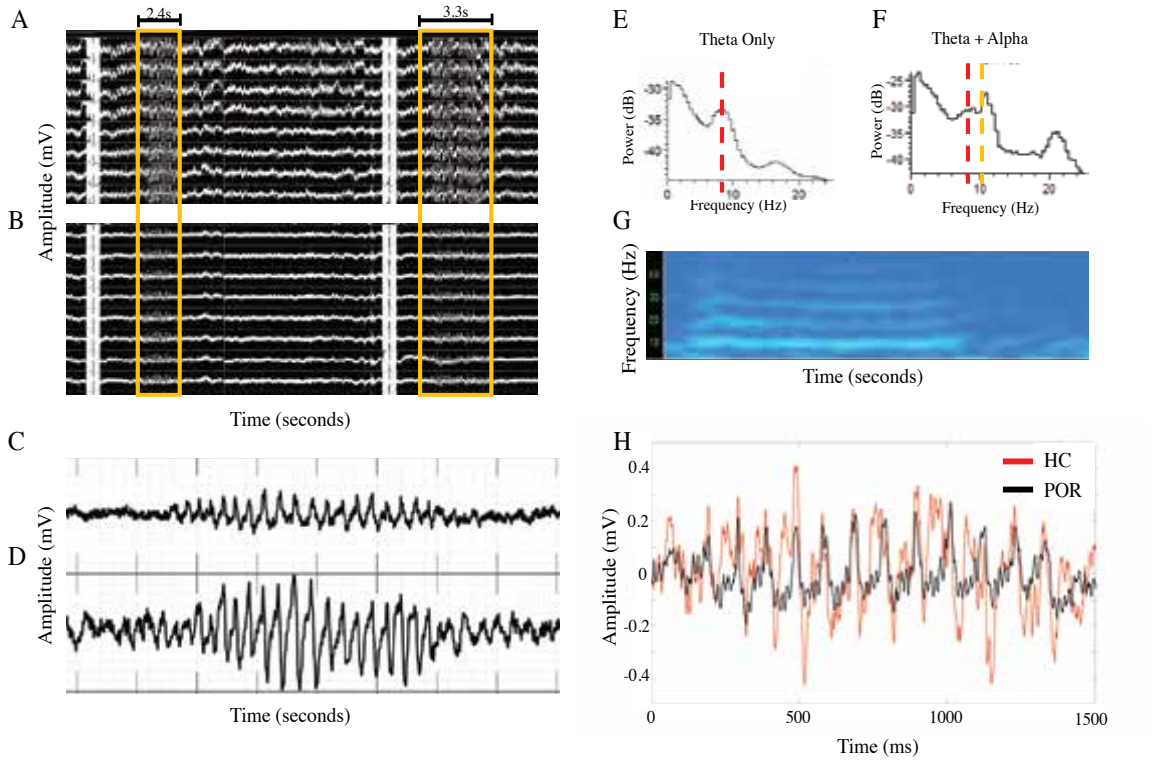

Figure 3.3. Example snapshots of flutters in real-time and within a single session. A. Example of two flutter occurrences, one 2.4 seconds in duration and one 3.3 seconds in duration, recorded from electrodes implanted in the HC. B. The same flutters shown in (A), here shown recorded from tetrodes located in the POR. Example of flutters detected post-collection in the HC (C) and POR (D). It can be seen that when the LFP for each region were filtered and normalized, flutters in the POR appeared larger than those observed in the HC. E. Example power spectral density of a rat performing the locBCD task when only theta was observed F. Example power spectral density of an animal performing the locBCD task in a session in which flutters were observed. G. Example of a real-time spectrogram generated as the animal produced a flutter event. H. Example flutter shown on a zoomed-in time-scale in both HC (red) and POR (black).

The second defining characteristic of these novel oscillations is their frequency. These events appear to be distinct from theta rhythms despite falling within the previously defined theta range (Figure 3.3E, F), as we can observe two peaks in the power spectral density suggesting a potential separation of frequencies. The flutters also had a well-defined presence on the real-time spectrogram at approximately 10 Hz, with obvious harmonics at ~10 Hz intervals above it (Figure 3.3G). Such defined events with specific and clear harmonics were confined to times when flutters occurred and were not seen at any other times, excluding the presence of mechanical noise. For this purpose,

mechanical noise consists of the rat scratching or knocking his head against the enclosure. Following detection of flutter events, time-locked videos were screened for mechanical noise and any false-positive flutter events detected during these time periods were removed prior to analysis.

The third defining characteristic of these novel oscillations is the velocity profile of the rat during the oscillatory event. Qualitatively, it was observed that the flutters only occurred when the rat was immobile, and the flutter ceased before the rat began moving again. Importantly, flutters did not occur every time the rat stopped running. Further, they did not always start immediately after the cessation of movement or end with the initiation of movement. Rather, flutters were seen to come and go, but only while the animal was immobile. This observation was quantitatively confirmed when the velocity of each rat during a flutter event was compared to the 20 seconds surrounding the event. Because the flutters were of variable length, each flutter was divided in half and the velocity of the rat during each half was examined. Velocities in the 10 seconds before and the 10 seconds after the flutters were distinctly higher than mean velocities during the first and second halves of the flutter time points (F1 and F2, Figure 3.4).

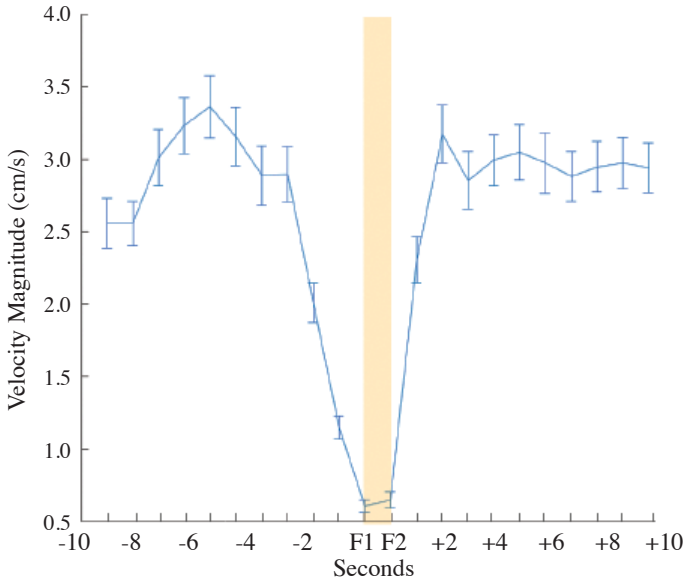

Figure 3.4. Velocity magnitude (cm/s) for the 10 seconds leading up to the flutters (-10 to 0), averaged velocity for the first half (F1) and second half (F2) of each flutter, and the 10 seconds following (0 to +10). Highlighted portion represents averaged flutters.

Finally, although the appearance of the flutters differed between electrodes that were in the HC and POR bundles, both structures consistently showed clear events, with no events observed in one region but not the other. A common question when examining oscillatory events is that of volume conduction. There are two main schools of thought when it comes to local field potential (LFP) recordings. The first school of thought, herein referred to as local-local field potentials (LLFPs), suggests that when an electrode is implanted, the recorded field potential is essentially a representation of the population activity of the neurons in a small, “local” area around the electrode. Therefore, how the neurons in the close vicinity (approximately 200–400 μm) of the electrode fire is directly reflected in the oscillatory activity recorded there (Katzner et al., 2009; Xing et al., 2009). The second school of thought, herein referred to as local-global field potentials (LGFPs), suggests that the local neuron activity creates a more "sub-threshold" or lower impact oscillatory activity, and that a "generator region", possibly a different region than the one being recorded, is responsible for the major oscillatory activity seen in the recorded LFP

(Herkenham and Nauta, 1977; Herreras, 2016). These two concepts are depicted with respect to volume conduction in Figure 3.5. If we assume we are recording LLFPs, then if an event is recorded (for example a flutter) in one region, it's possible that either A) it was generated in one region (X) and then volume conducted to also be recorded in another region (Y), or, B) it was independently generated in both regions based on that local population activity. If instead we assume we are recording LGFPs, then in this case, there might be either C) a generator region (Z) sending the signal to an intended region (X) and that signal that is received by X is then volume conducted to Y, or D) the generator region (Z) is sending the signal to both regions being recorded.

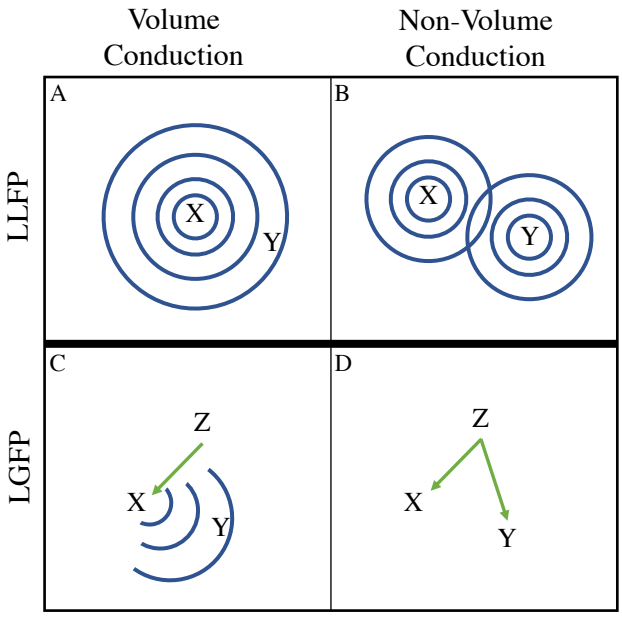

Figure 3.5. Depictions of local-local field potentials and local-global field potentials with respect to volume conduction. A. Neuronal acticity in region X generates an oscillatory event which is then volume conducted to region Y. B. Both region X and region Y independently generate an event from local neuronal activity. C. Region Z is a "generator" region for the oscillatory event/band and transmits that activity to region X, where it is subsequently volume conducted to region Y. D. Generator region Z transmits the event to both region X and Y.

In an effort to address the possibility of volume conduction that exists in both understandings of LFPs, we examined the peak times of the flutters in both the HC and POR as well as the phase differences between the oscillatory events in both regions. If the oscillatory event was being volume conducted and subsequently recorded in the other region, we might expect that the peak times in one region would be nearly identical to the

peak times in the other. Similarly, if the oscillatory event was volume conducted from one region to another, we might expect that the phase of the oscillations in each region would be stable with respect to each other.

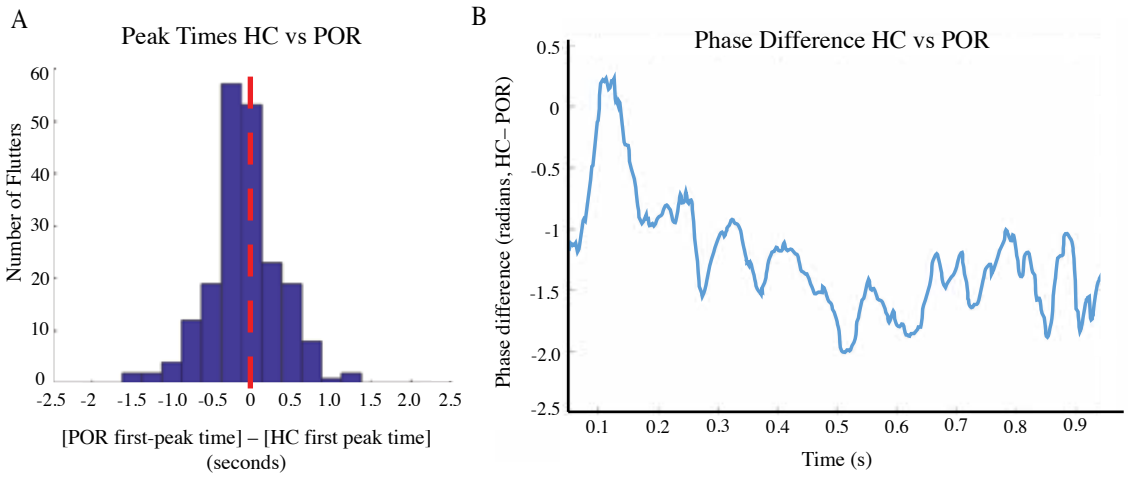

Figure 3.6. Peak differences and phase differences for flutters recorded from HC and POR. A. Time of the first peak of a POR flutter minus the time of the first peak of a HC flutter. POR flutters tend to have their first peak about 3ms before HC flutters. B. Phase differences in flutters in HC and POR are not consistent over time suggesting they are not volume conducted from one region to the other.

Instead, what we see is that the first peak of a POR flutter tends to happen approximately 3 ms before the first peak of a HC flutter (Figure 3.6A). We also see that if we examine the phase difference of the flutters between the two regions, we do not see a consistent difference over time but instead one that is fairly variable (Figure 3.6B). In this analysis, all flutters were collapsed across the occurrence in HC and POR, and the phase differences were subsequently examined. Together, these data suggest that the flutters are likely not being volume conducted from one of the recorded regions to the other. Based on this specific difference in peak times where the POR peaks before the HC, one potential explanation is that a generator region that is spatially closer to the POR is responsible for the generation of these flutter events, or one that preferentially transmits

posteriorly, such as the thalamus.

Behavioral Correlates of Flutters

To begin determining the behavior or behaviors that these novel flutters correlated with, and ultimately the neural purpose they serve, we examined the locBCD task from many angles. Specifically, we looked at the defined epochs in which the flutters were observed, the durations and number of occurrences of the flutters, the strategies the rodent used in an attempt to complete the task during trials with observed flutters, and the performance of the rodent throughout the task. Further, each of these were analyzed for differences both between and within sessions. Here, a session is defined as the set of trials performed on a given day. Therefore, when comparing across sessions we are comparing across all days of the experiment, split into Early, Mid, and Late sessions based on number of sessions completed. Early sessions included the first 7 sessions an animal ran, Mid sessions included the next 7 sessions the animal ran, and Late sessions included any remaining sessions. When comparing across trials, we are comparing the trials performed on a single day, with each session split equally into thirds based on the number of trials performed that day, creating Initial trials (first third of trials performed that day by that animal), Mid trials (second third of trials), and Ending trials (final third of trials performed that day).

Epoch analysis

To begin investigating the behavioral correlates of the flutters, we first identified

the epochs of an individual trial in which we found flutters. We were able to separate each trial into three distinct periods. The Post Stimulus epoch consists of the time from stimulus onset until selection, the Post Selection epoch begins at selection and includes the 5 seconds immediately following, and the Inter-Trial epoch begins at the end of the Post Selection epoch and ends at the start of the next trial (Figure 3.1C). Importantly, a flutter was counted in a specific epoch if it started within the time period that defined that epoch. When separated into these intervals, we see that 53% (184) of flutters occurred during the Post Stimulus epoch, 26% (89) occurred during the Post Selection epoch, and 21% (71) occurred during the Inter-Trial epoch (Figure 3.7A). These numbers were also broken down by animal (Figure 3.7B), and it can be seen that all animals follow approximately the same trend, having the majority of flutters occur during the Post Stimulus epoch.

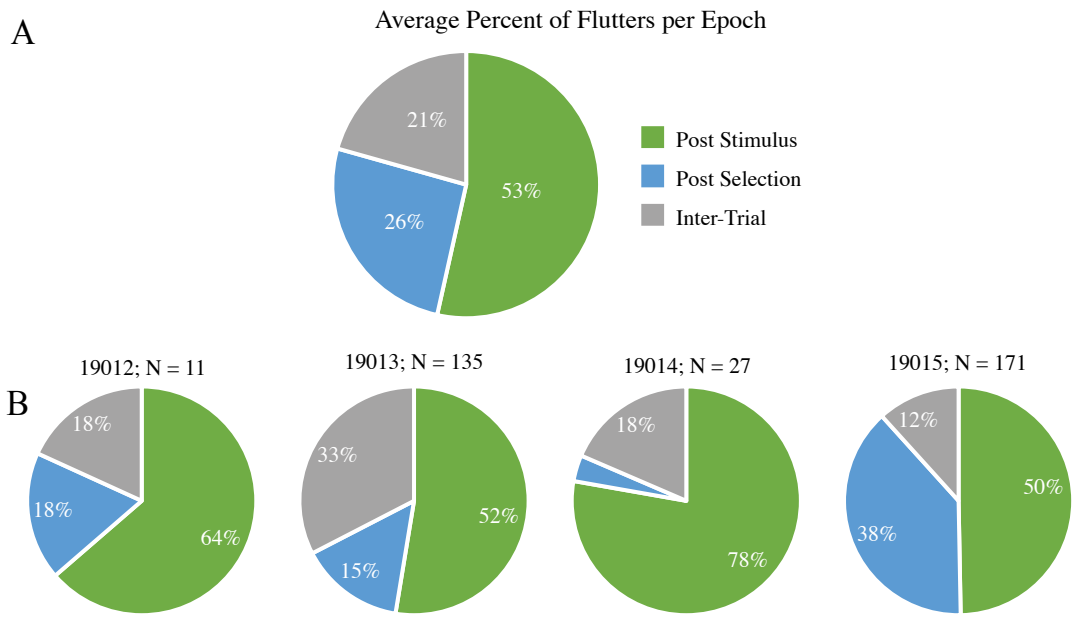

Figure 3.7. Distribution of flutter events across behavioral epochs. A. Flutters as observed in each of the three defined epochs averaged across all four animals. B. Flutters observed in each epoch split by individual animal

If we examine the patterns of occurrence of flutters across sessions (see Figure 3.8A), we can see that when normalized to the number of sessions in each group, the number of flutters that occurred in the Post Stimulus epoch went from 74% during Early Sessions down to 46% during Mid Sessions, and then back up to 77% during Late Sessions. Conversely, the occurrence of flutters went up between Early and Mid Sessions for both the Post Selection epoch (7% to 24%) and the Inter-Trial Interval (19% to 31%) before going back down in the Late Sessions (Post Selection Late = 10%, Inter-Trial Late = 13%). If we look across trials within a given session (see Figure 3.8B), we see that most flutters occurred within the Post Stimulus epoch across the entire session, with an additional increase during the Ending Trials (Post Stimulus: Initial = 49%, Mid = 49%, Ending = 67%). The number of flutters within the Post Selection epoch remained fairly

low, but increased throughout the session (Post Selection: Initial = 20%, Mid = 22%, Ending = 23%). Flutters occurring in the Inter-Trial interval started off occurring more than Post Selection flutters, but decreased in occurrence throughout the session (Inter-Trial: Initial = 31%, Mid = 29%, Ending = 10%).

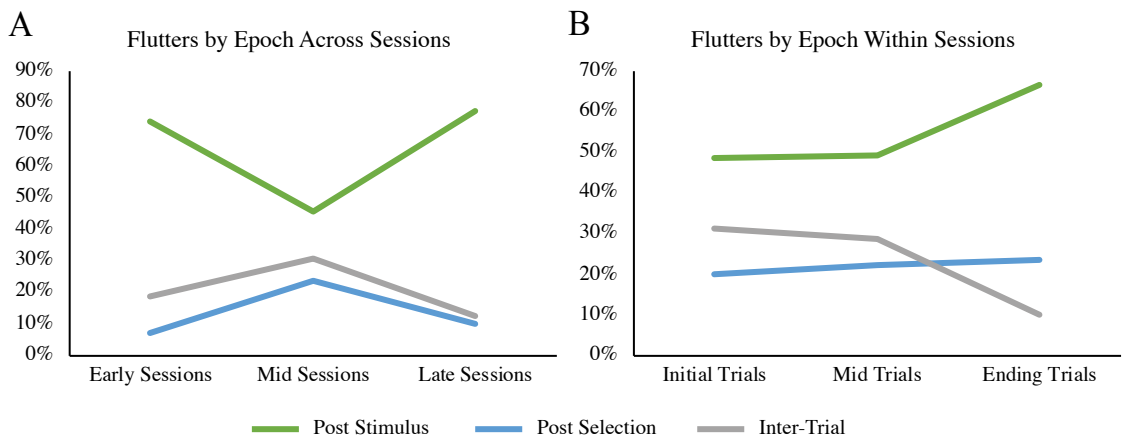

Figure 3.8. Flutters by epoch across and within sessions. A. Flutters in each of the three defined epochs across early, mid, and late sessions. Sessions in each group averaged across all four animals. B. Flutters in each of the three defined epochs across initial, mid, and ending trials within a given session. Trials in each group averaged across all four animals.

Flutter duration and flutter series analysis

During data collection, it was observed that the flutters were not uniform in either duration or consecutive bout number. Durations varied from .9 s – 10.5 s while consecutive bout numbers ranged from 1 – 10 flutters. Occurrences with more than one consecutive flutter were termed a "flutter series." Due to this variability, we analyzed the data for differences based on flutter duration and the number of flutters within a series.

We first separated the flutters into the most commonly occurring bins of 0-2 seconds, 2-5 seconds, 5-10 seconds, and >10 seconds. In doing this, we see that 29% (100) flutters fall within the 0-2 second length range, 60% (205) are between 2-5 seconds,

9% (31) are 5-10 seconds in length, and 2% (8) are longer than 10 seconds (Figure 3.9A). We then looked at how these durations differed across the previously defined three epochs and we found that the durations were generally consistent regardless of the epoch in which they occurred (Figure 3.9B). We can further break down durations by animal to see if there were differences in duration patterns across the animals (Figure 3.9C, D), and in doing this we see that most animals showed similar patterns (19012 average = 2.59 s, 19014 average = 1.89 s, 19015 average = 2.78 s), with animal 19013 (4.77 s) showing the highest average as well as the largest range of durations. Finally, we can look at how the flutter durations changed across sessions or over a given session. When we look across sessions, we see that durations were longest during the Mid Sessions (2.99 s) as compared to the Early (2.44 s) or Late Sessions (2.21 s; Figure 3.9E). When we look within sessions, we see that flutter duration appeared to get longer as the session went on, with the shortest durations during Initial Trials (2.29 s) and the longest durations during Ending Trials (3.30 s; Figure 3.9F).

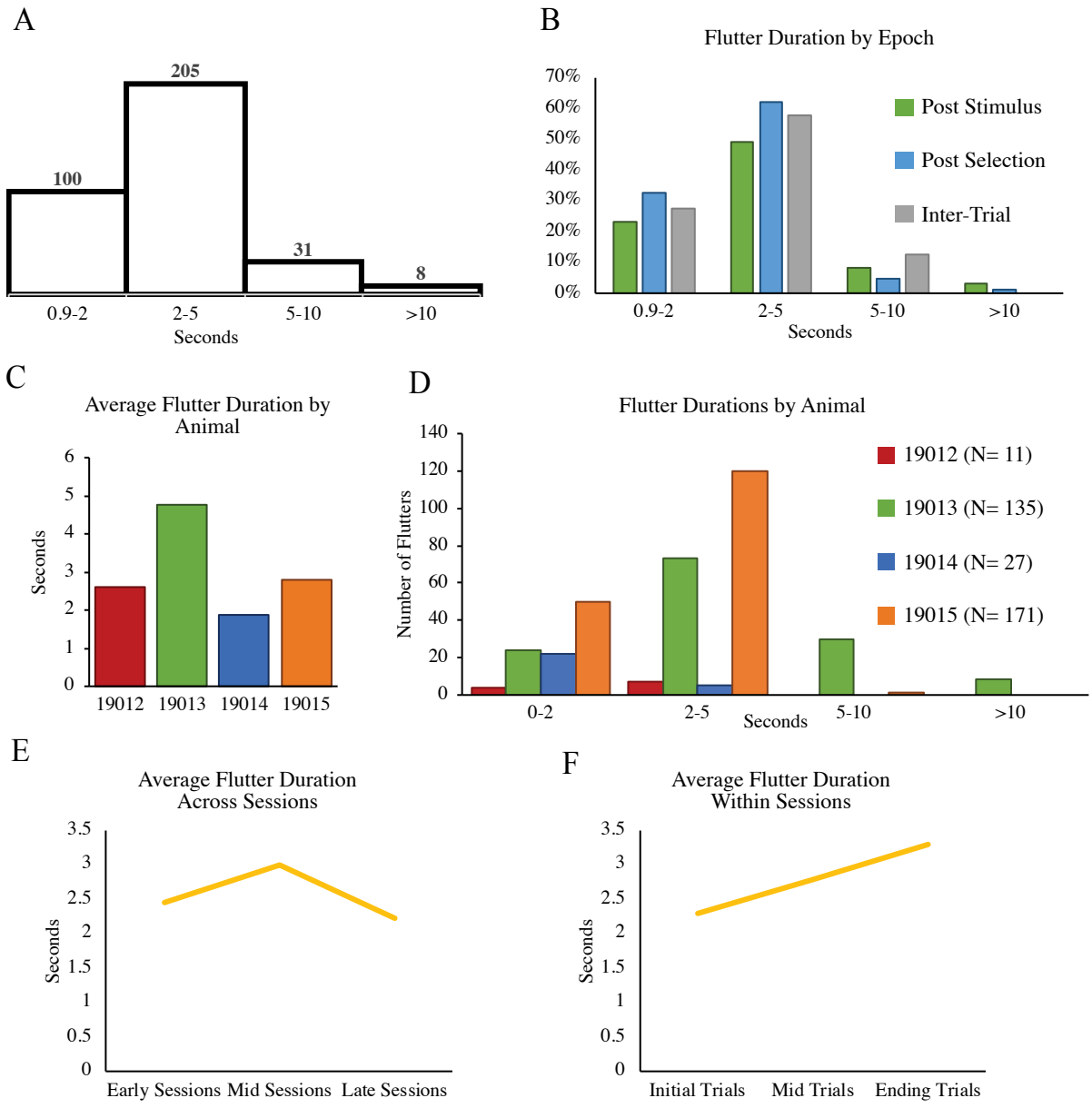

Figure 3.9. Flutter duration distribution by epoch, animal, and session. A. Histogram of flutter duration. B. Histogram of flutter duration broken down by the three previously defined epochs. C. Average flutter duration by animal. Animal numbers are 19012, 19013, 19014, and 19015. D. Histogram of flutter duration broken down by animal. E. Flutter duration averaged across all animals for each defined group of sessions: Early, Mid, and Late. F. Flutter duration averaged across all animals for each defined group of trials: Initial, Mid, and Ending.

Flutters occurred in bouts that ranged from a single flutter to 10 consecutive flutters. Fifty percent of the flutters that occurred (171 flutters) were a single bout event. Fifty percent of the recorded flutters (173) happened within a series and there was a total of 53 separate series. When we examined the distribution of the number of bouts that happened within each series, we found that 45% (24) of the series contained 2 bouts, 21% (11) contained 3 bouts, 17% (9) contained 4 bouts, and 15% (8) contained 5 or more bouts (Figure 3.10A). We further analyzed the occurrence of series within the three previously defined trial epochs. We found that 75% (40) of the series occurred within the Post Stimulus epoch, 6% (3) occurred in the Post Selection epoch, and 19% (10) occurred in the Inter-Trial epoch (Figure 3.10B). When we break down the occurrence of multiple bouts by animal, we see that there were differences in the proportion of single versus multiple bouts in different animals. Animal 19012 showed no flutters that occurred in a series (11 single), and animal 19015 had a much greater number of flutters occur individually (117 single, 20 multiple), whereas animals 19013 (36 single, 28 multiple) and 19014 (7 single, 3 multiple) had flutters appear individually and in series in closer proportions (Figure 3.10C). Finally, we can look at how the flutter bouts changed across sessions or over a given session. When we look across sessions, we see that multiple bouts happened most often during the Mid Sessions (40, 75%) as compared to the Early (9, 17%) or Late Sessions (4, 8%; Figure 3.10D). When we look within sessions, we see that multiple flutter bouts became more prevalent as the session went on, with the fewest series during Initial Trials (1, 2%) and the most during Ending Trials (41, 77%; Figure 3.10E).

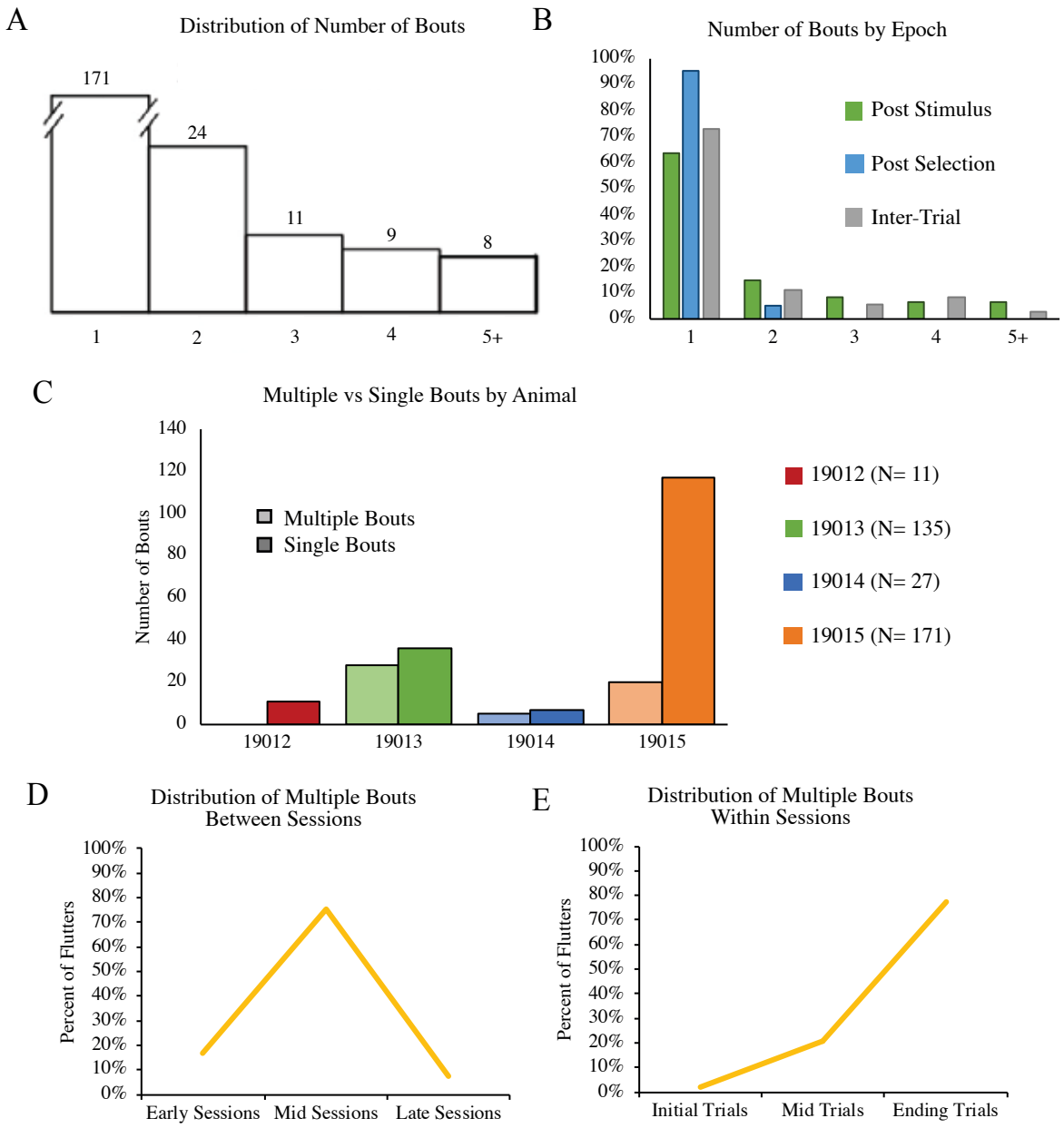

Figure 3.10. Flutter bout number distribution by epoch, animal, and session. A. Distribution of all flutters by bout number. B. Histogram of bout numbers broken down by the three previously defined epochs. C. Number of multiple compared to single bouts broken down by animal. D. Percent of flutters that occurred in multiple bouts averaged across all animals for each defined group of sessions: Early, Mid, and Late. E. Percent of flutters that occurred in multiple bouts averaged across all animals for each defined group of trials: Initial, Mid, and Ending.

Strategy analysis

In an effort to increase the number of intracranial stimulation rewards received, rats will go through a predictable series of strategies as they work towards determining

the correct rule. These strategies include focusing on an egocentric location, an allocentric location, or a particular object. In practice, an egocentric strategy looks like the rat making a selection on, for example, their right for several trials in a row regardless of the object that appears in that position, while in an allocentric strategy, the rat might make a selection in the north for several trials in a row, again regardless of the object that appears there. In an object strategy, the rat attempts a single discrimination rule by choosing one object on both the East and West sides of the maze, even though it is only correct in one of those sides. An animal was said to be using a specific strategy when that animal chose a particular object or relative location on three or more consecutive trials. For example, an animal was determined to be using an allocentric strategy if they made a selection in the North location on at least three consecutive trials. A designation of "multiple" was assigned if we were unable to dissociate a single strategy (for example, if the animal chose object 1 in the North for three consecutive trials, or in the transition from one strategy to another, for example if the animal went from a North strategy to a left strategy, and the final trial of the North strategy was also the first trial of the left strategy. Ultimately, because the task is biconditional based on the location in which objects are presented, all of these strategies will fail. Once an animal had exhausted these "simple" strategies, they tended to move on to more complex strategies. Qualitatively, this is the point where the flutters were first observed. Here, a putative complex strategy is assigned when no simple strategy can be attributed to the trial. To quantify this, we examined the correlation of flutter occurrence with the use of different strategies, or a "flutter associated strategy". As seen in Figure 3.6A, overall 9% (31) flutters correlated with a trial in which an animal was employing an allocentric strategy, 7% (25) correlated

with an egocentric strategy, 5% (17) correlated with an object strategy, 29% (99) correlated with overlapping strategies, and 50% (172) were determined to be putative complex strategies. This large proportion of the flutters associated with the lack of use of a previously defined "simple" strategy suggests that the animal was likely "on task" and actively engaged with determining the complex biconditional rule rather than attempting a simpler solution.

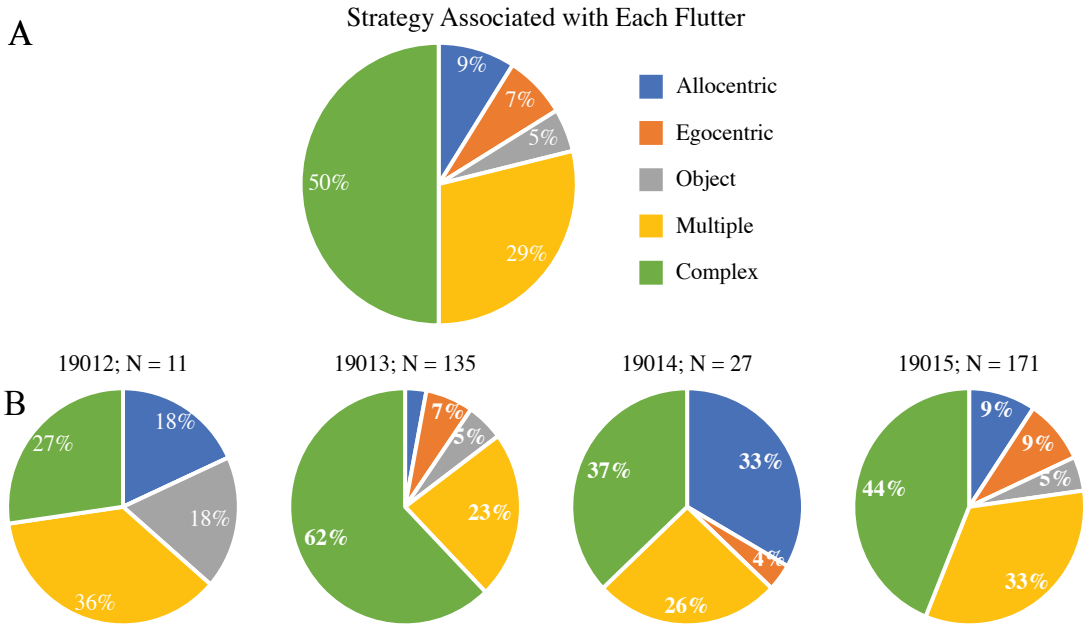

Figure 3.11. Distribution of flutter events across behavioral strategies. A. Percent of flutters associated with each strategy averaged across all four animals. B. Percent of flutters associated with each strategy split by individual animal

When this data is broken down by animal, we can see that 3 out of 4 of the animals show the majority of their flutters were associated with a putative complex strategy. The one animal who did not follow this trend instead had the most flutters (4 flutters; 36%)

associated with multiple strategies, and the second most flutters (3 flutters; 27%) associated with the putative complex strategy.

Figure 3.12. Strategy usage across and within sessions (all of the trials performed by an animal on a given day comprise a session). A. Flutter associated strategies across early, mid, and late sessions throughout the study. B. Strategy usage across all sessions (without consideration of flutters). C. Flutter associated strategies across initial, mid, and ending trials within a given session. D. Strategy usage across all trials (without consideration of flutters).

Interestingly, if we compare the strategies that were being employed during the occurrence of a flutter, or what we're calling here flutter-associated strategies, with the strategies that were employed in general both across and within sessions, we can see some specific differences (Figure 3.7). For these analyses, a session is defined as the set of trials performed on a given day. Therefore, when comparing across sessions we are comparing across all days of the experiment, split into Early, Mid, and Late sessions based on number of sessions completed. Early sessions included the first 7 sessions an animal ran, Mid sessions included the next 7 sessions the animal ran, and Late sessions

included any remaining sessions. When comparing across trials, we are comparing the trials performed on a single day, with each session split equally into thirds based on the number of trials performed that day, creating Initial trials (first third of trials performed that day by that animal), Mid trials (second third of trials), and Ending trials (final third of trials performed that day). Using these distinctions, we can see that when looking at strategy usage alone, strategy usage did not differ widely either across sessions (Figure 3.7B) or across trials (Figure 3.7D), with animals predominately using multiple strategies, and/or switching strategies often throughout all sessions and trials. However, if we look at the strategies employed during the occurrence of a flutter, we see a different pattern. First, if we look across sessions, we can see that the majority of flutters were associated with a complex strategy across Early, Mid, and Late sessions (Figure 3.7A). If we examine trials on which flutters occurred within sessions (Figure 3.7C), we see that during the Initial trials of a session, the flutters that were recorded were most often associated with multiple strategies, but this changed starting with the Mid trials. In the middle of a session, flutters started to become more often associated with a complex strategy, and this persisted until the end of the session, through Ending trials. These differences in general strategy usage compared to flutter-associated strategy usage suggests that flutters are correlated with the complex thought needed to complete this unusually difficult task.

Performance analysis

Because this was a very difficult task for the rats to learn, their averaged performance when looking either across or within trials appears to stay around chance

(Figure 3.11A, B) and has no apparent correlation with the occurrence of flutters. However, because the task was difficult, the performance needs to be examined in more nuanced ways. One way we attempted to do this was to examine performance and flutter correlation with the presentation of new, changed, or repeat objects. Throughout the task, objects were presented in pairs, with one or two pairs being presented in a given session. In previous successful tasks such as the context bi-conditional task that is also used in the lab, one pair of objects would be presented until the rule was learned for that pair. Then, a second pair would be presented until the rule was transferred. Finally, the two pairs would be presented together in a set, with each pair being shown approximately equally, pseudo-randomly interspersed throughout the session. When training animals on this task, the location bi-conditional task, we found that rats began to get bored of a given pair before the rule appeared to be fully "learned" as demonstrated by reaching trials to criterion (TTC, at least 10 correct in the previous 12 consecutive trials). Therefore, within this task, objects were presented either when the animal reached TTC three or more times in a session, or when they appeared to no longer be interested in the pair enough to continue performing the task. Interestingly, when an animal seemed to begin to understand the rule, as shown by reaching TTC, upon being switched to another pair, the rule did not appear to transfer as has been seen in other paradigms. Instead, a similar pattern of trying different strategies was observed with each new presentation. To examine if our observed flutters correlated with presentation of different objects and thus perhaps novelty or general motivation, we separated them into "new" which is the first presentation of a given object pair, "old", a pair that was used in the previous session, or "changed", a pair that has been seen before, but was not seen in the previous session.

When we look at the presentation of these groups of objects with respect to accuracy, TTC, and flutter occurrence, we see no obvious correlation (Figure 3.11C-F, black dots).

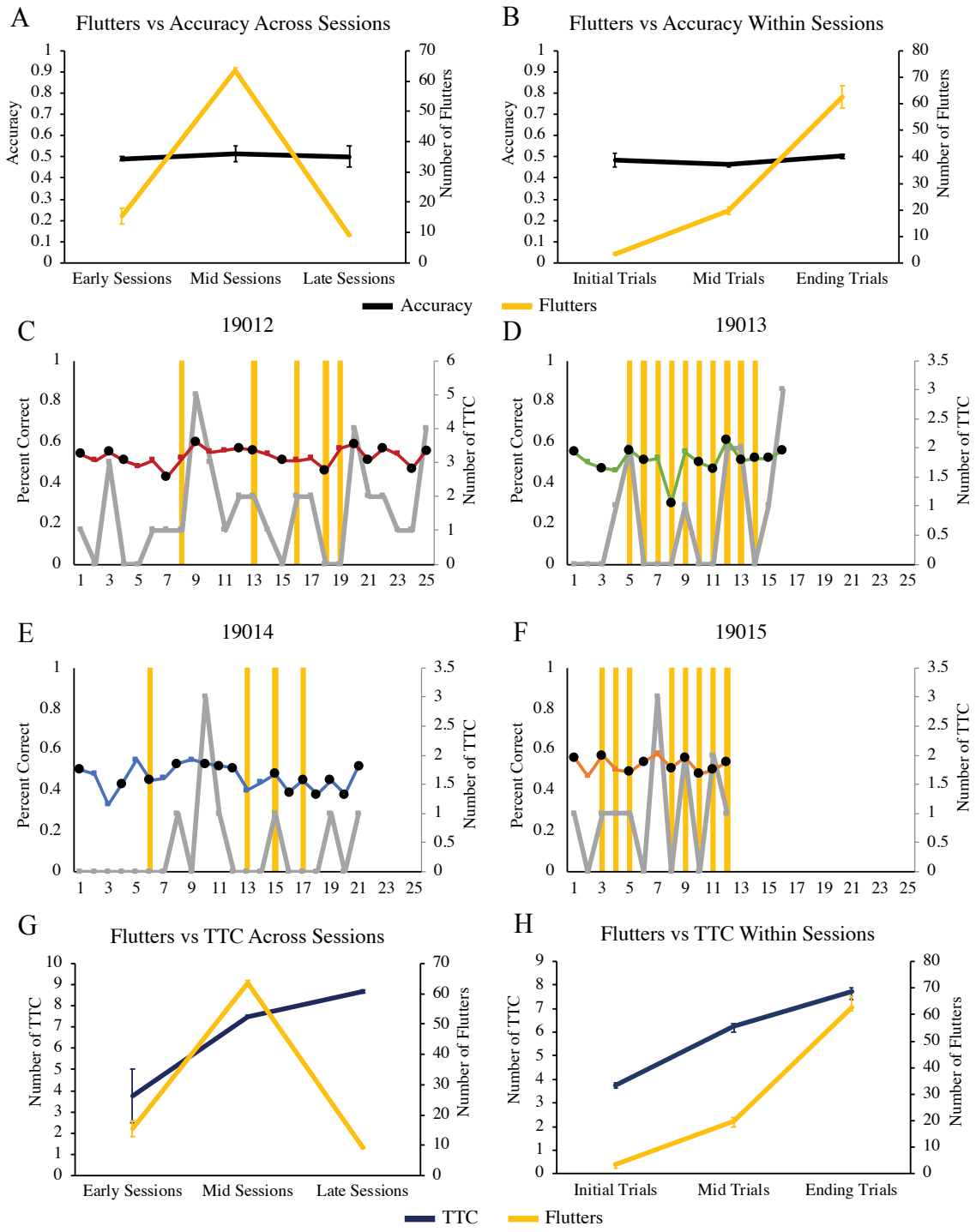

Figure 3.13. Accuracy, Trials to Criterion, and Flutters. A. Average accuracy and number of flutters that occurred averaged across all animals for each defined group of sessions: Early, Mid, and Late. B. Average accuracy and number of flutters that occurred averaged across all animals for each defined group of trials: Initial, Mid, and Ending. C - F. Accuracy of each animal (line colored by animal) plotted with presentation of new or changed objects (black dots) number of trials to criterion reached within that session (grey line), and days on which flutters occurred (yellow bars). G. Number of Trials to Criterion (TTC) and number of flutters that occurred averaged across all animals for each defined group of sessions: Early, Mid, and Late. H. Number of TTC and number of flutters that occurred averaged across all animals for each defined group of trials: Initial, Mid, and Ending. All error bars = SEM.

If we instead look at the number of TTC with respect to flutter occurrence, while the number of TTC in a given session does not seem to correlate with whether or not flutters were seen on that day (Figure 3.11C-F, G), when we look within a session, we see that both the occurrences of flutters and the number of TTC reached within a session increase as the session goes on, with the lowest number of both flutters and TTC occurring during Initial trials (Initial flutters = 3.5, Initial TTC = 3.75), rising during the Mid trials (Mid flutters = 19.75, Mid TTC = 6.25), and finishing with the highest numbers in the Ending trials (Ending flutters = 62.75, Ending TTC = 7.75). Therefore, although flutters do not appear to directly correlate with better average performance, they do appear to correlate with better acute performance.

Discussion

In an effort to characterize these novel events, we aimed to answer two main questions: 1. What are the defining characteristics of this oscillation? And 2. How do the flutters correlate with behaviorally relevant aspects of the task? We observed that these oscillatory events previously undescribed in the rodent peak at about 10 Hz and occur when the animal is immobile. In contrast, Type 1 theta (generally defined as 6-10 Hz) is highly correlated with running speed. In addition, in our hands HC and POR theta consistently peak at about 8.5 Hz, clearly differing from the current observed phenomenon. Importantly, the proposed functional correlates of these 10 Hz oscillatory events in rodents are consistent with putative functions of alpha recently reported in humans.

Comparison with theta

Theta oscillations (human: 4-8 Hz, rat: 6-12 Hz) are often described as representing the "on-line" state of the hippocampus. The extracellular currents underlying theta waves are thought to be generated mainly by entorhinal input, CA3 projections to CA1 (Schaffer collaterals), and voltage-dependent calcium currents in pyramidal cell dendrites in conjunction with drive from the medial septum. The theta rhythm itself is believed to be critical for temporal coding and decoding of active neuronal ensembles, especially for the purpose of memory. Two types of theta have been described in the rodent: Type 1 theta (6-12 Hz) is highly correlated with movement while Type 2 theta (4-9 Hz) is more closely associated with immobility as well as anxiety and arousal (Bland, 1986). The vast majority of studies looking at theta focus on the hippocampal theta rhythm and its role in navigation and spatial memory, thus focusing predominantly on Type 1 movement-associated theta (6-12 Hz).

Our observed phenomenon would fall within the previously defined Type 1 movement-related theta range, although it has been proposed that distinguishing theta into mutually exclusive categories in this way may be overlooking more nuanced differences among the ranges contained within theta (Benedek et al., 2011). This movement-related theta, however, has been linked to several proposed behaviors, including arousal (Green & Arduini, 1954), sensorimotor processing (Whishaw & Venderwolf, 1973), navigation (O'Keefe & Nadel, 1978), and learning and memory (Hasselmo, 2005). Both navigation and learning and memory functions would potentially line up with our observations of when this oscillatory event occurred, although neither would fully account for them. With navigation, we see that the use of

allocentric and egocentric strategies does not specifically correlate with the occurrence of flutters, although they do sometimes coincide. The function of theta in learning and memory poses a possible explanation for the occurrences of these oscillatory events, as the animal is performing a demanding memory-based task. We see flutters emerging as a session progresses, and while we do not see this correlating specifically with accuracy in the task either within or between sessions, we do see a correlation with the number of trials to criterion reached, specifically within a given session (Figure 3.11).

Comparison with previously observed 10-12 Hz oscillations

Previously, another phenomenon also termed "flutter" was described with similar characteristics except for several points. Nerad and Bilkey (2004) described flutters that occurred between 10-12 Hz and were found in the rat hippocampus and rhinal cortex (perirhinal and entorhinal cortices). These flutters were described to be at the border of theta and alpha and appeared to be "of non-theta origin" as they were seen to occur simultaneously with theta. It was described that these flutters typically lasted for approximately 1 second, although on occasion there were continuous bursts of >5 seconds. These characteristics match well with our observed phenomenon, but there are several key differences. First, the Nerad and Bilkey 10-12 Hz flutters were specifically associated with movement and were not present during immobility. In contrast, our observed oscillations had the opposite velocity profile, only being seen when the animal was not moving and ending prior to or simultaneously with the onset of movement. Second, the 10-12 Hz flutters described by Nerad and Bilkey were associated with the familiarity of a given environment, disappearing when the animal was placed into a novel

environment. To examine if our observed oscillations exhibited a similar correlation, we recreated the task that was used in the original paper using the familiar bow-tie enclosure from the locBCD task and a novel bow-tie enclosure that differed in both visual and olfactory cues. When animals were allowed to forage within these environments in the same method described in the original paper, we saw no flutters in either environment.

Comparison with Alpha

Recently, studies have ceased talking about alpha as a passive mechanism occurring only in the absence of other cognitive function and have started suggesting that alpha oscillations are an active mechanism of selective attention that become stronger when select visual inputs are actively ignored, working memory loads and/or attentional demands are higher, or attention is selectively directed "inward" (Klimesch et al., 1998; Worden et al., 2000; Jenson & Mazaheri, 2010; Jones et al., 2010; Bonnefond & Jenson, 2012; Sacchet et al., 2015; Sadaghiani & Kleinschmidt, 2016; Kizuk & Mathewson, 2017). Together, these suggest a top-down role for alpha rhythms in attention, where phase and/or amplitude of alpha oscillations lead to the selective focus on, or ignoring of, given stimuli. As a step further, several studies have found that increased alpha correlates with active internal processing and creative cognition in tasks designed to elicit divergent thinking, which require generation of original and creative ideas to solve problems (Benedek et al., 2011; Arden et al., 2010; Dietrich & Kanso, 2010; Fink et al., 2007).

These concepts line up especially well with the observations surrounding our novel flutter oscillatory events. Animals will go through a predictable series of strategies as they work towards determining the correct rule. These strategies include focusing on

an egocentric location, an allocentric location, or a particular object. However, once they have exhausted these simple strategies, the animal begins to try more complex strategies. For example, the next strategy that is usually employed is one of alternating objects. This strategy is very close to correct and can be employed successfully for a number of trials, but to ensure that it is not mistaken for the rule, there are limits in place to force the animal to repeat a given side/object pair after a certain number of alternations. This alternating strategy, however, is a more creative, or "divergent", way of approaching the task than a rodent otherwise employs, as is the successful completion of the correct bi-conditional rule. Therefore, seeing an oscillatory event that correlates with creative or divergent thinking at this point in the task would provide an attractive explanation.

Another interesting connection between the observed flutters and the recently suggested behavioral correlates of increased alpha is the suggestion of a relationship to internally directed attention and/or an inhibition of other processes. This is particularly relevant in light of the complete cessation of movement as well as the apparent drowning out of other oscillatory activity that is seen during the course of the flutters. An explanation of internally directed attention in combination with the inhibition of other signals would thus align extremely well with these observations.

Proposed Function of Flutter Oscillations

Based on the similarities observed between our flutter events and alpha oscillations in humans, I propose that a likely function that these flutters serve is one of inter-region communication for the purpose of selective attention. While it is often suggested that slower oscillations (delta, theta, alpha, lower beta) allow synchronization

of neuronal activity over large, spatially distant networks and faster oscillations (higher beta, gamma, ripple) coordinate neuronal firing more locally (Valera et al., 2001; Kim et al., 2017), there are currently many theories about how oscillations in general affect neuronal processes. These include (but are not limited to) the "communication through coherence" theory (Fries, 2005), that suggests that communication between two neuronal groups mechanistically depends on coherence between them, and the "temporal correlation hypothesis" (Singer & Gray, 1995) that suggests that the discharges of neurons become synchronous if they participate in the encoding of related information. It is exceedingly likely that oscillations within the brain serve several complex functions that include both of these theories and many more, and that differ both situationally and inter-regionally. Our data did not show increased coherence or phase locking to alpha (see chapter 2), but one theory our data does potentially support is that of the "intake-rejection hypothesis" (Cole and Ray, 1985). This hypothesis differentiates between sensory 'intake' processes, or externally directed attention to take in stimuli, and non-sensory 'rejection' processes, or internally directed attention such as mental imagery and working memory tasks. The rejection aspect of the theory suggests that in order to facilitate internal attention, one needs to inhibit or 'reject' incoming sensory information. Several studies found increased alpha power in rejection tasks such as mental imagery and mental arithmetic especially at parietal sites (Ray and Cole, 1985a, Ray and Cole, 1985b). Based on our results showing that flutters happen more often when complex strategies are being employed as well as during the clear inhibition of movement, I propose that these alpha events are hallmarks of complex internally directed thought that are further functioning to communicate across regions and inhibit sensory intake.

Possible Origin of Flutter Oscillations

Exactly how and where cortical oscillations are generated is still widely unknown, but there are several possibilities. One possibility stems from the observation of these flutter events in the HC. Theta-rhythmic bursting of medial septum neurons is thought to drive HC theta oscillations in rats specifically during waking motor activity (Vertes and Kocsis, 1997; Buzsáki, 2002). This source is unlikely, however, as we have shown that these flutters are distinct from and seen in parallel with theta. Another possible source of these events is the local neuronal activity within the recorded regions, similar to the finding of the generation gamma rhythms by local neuronal circuits in the medial entorhinal cortex (Middleton et al., 2008). These locally generated oscillations were specifically dependent on the influence of fast spiking inhibitory interneurons in the region. A local generation of these alpha events within either the POR or HC is possible, with a higher probability that it would come from the POR based the timing of the peaks in each region, but this possibility is also unlikely due to the previously reported low numbers of interneurons within the POR (Sugden, 2015; Beaudin et al., 2012; de Curtis and Paré, 2004). The most likely source of these alpha events are the feedback loops generated by thalamocortical networks within the regions (Hughes & Crunelli, 2005). In this scenario, high-threshold rhythmic burst firing that occurs in a subset of thalamocortical neurons would work in conjunction with gap junctions between these specialized cells to drive alpha rhythms. Because we see these large amplitude alpha events in 2 distinct regions, and because these events most closely match the proposed function of alpha in humans, this generator is most likely.

Summary

Rodent tasks are generally designed to be easily trained, quickly learned, and performed with a high degree of accuracy; they are rarely designed to require complex creative problem solving. We suggest that our novel location bi-conditional task, which proved to be more difficult for rodents to learn than originally anticipated, provided a unique learning environment not typically used in rodent electrophysiology studies allowing the discovery of novel oscillatory events. In summary, based on both the physical attributes of the observed novel oscillatory flutter events as well as the associated behavioral correlates, these events are most similar to the alpha oscillation as defined in humans. This is the first demonstration of what appears to be attentional alpha in the rodent brain. In light of this finding, we argue that the defined oscillation bands in the rodent should be updated to include a band specific to alpha.

References

Altunkaynak, B. Z., Altunkaynak, E., Unal, D., & Unal, B. (2009). A novel application for the cavalieri principle: A stereological and methodological study. *The Eurasian Journal of Medicine*, *41*(2), 99–101.

Arden, R., Chavez, R. S., Grazioplene, R., & Jung, R. E. (2010). Neuroimaging creativity: A psychometric view. *Behavioural Brain Research*, *214*(2), 143–156. https://doi.org/10.1016/j.bbr.2010.05.015

Benedek, M., Bergner, S., Könen, T., Fink, A., & Neubauer, A. C. (2011). EEG alpha synchronization is related to top-down processing in convergent and divergent thinking. *Neuropsychologia*, *49*(12), 3505–3511. https://doi.org/10.1016/j.neuropsychologia.2011.09.004

Bertone-Cueto, N. I., Makarova, J., Mosqueira, A., García-Violini, D., Sánchez-Peña, R., Herreras, O., Belluscio, M., & Piriz, J. (2020). Volume-Conducted Origin of the Field Potential at the Lateral Habenula. *Frontiers in Systems Neuroscience*, *13*, 78. https://doi.org/10.3389/fnsys.2019.00078

Bland, B. H. (1986). The physiology and pharmacology of hippocampal formation theta rhythms. *Progress in Neurobiology*, *26*(1), 1–54. https://doi.org/10.1016/0301-0082(86)90019-5

Bonnefond, M., & Jensen, O. (2012). Alpha Oscillations Serve to Protect Working Memory Maintenance against Anticipated Distracters. *Current Biology*, *22*(20), 1969–1974. https://doi.org/10.1016/j.cub.2012.08.029

Buzsáki, G. (2002). Theta Oscillations in the Hippocampus. *Neuron*, *33*(3), 325–340. https://doi.org/10.1016/S0896-6273(02)00586-X

Cole, H. W., & Ray, W. J. (1985). EEG correlates of emotional tasks related to attentional demands. *International Journal of Psychophysiology*, *3*(1), 33–41. https://doi.org/10.1016/0167-8760(85)90017-0

Cooper, N. R., Croft, R. J., Dominey, S. J. J., Burgess, A. P., & Gruzelier, J. H. (2003). Paradox lost? Exploring the role of alpha oscillations during externally vs. internally directed attention and the implications for idling and inhibition hypotheses. *International Journal of Psychophysiology*, *47*(1), 65–74. https://doi.org/10.1016/S0167-8760(02)00107-1

Csicsvari, J., Jamieson, B., Wise, K. D., & Buzsáki, G. (2003). Mechanisms of Gamma Oscillations in the Hippocampus of the Behaving Rat. *Neuron*, *37*(2), 311–322. https://doi.org/10.1016/S0896-6273(02)01169-8

Dietrich, A., & Kanso, R. (2010). A review of EEG, ERP, and neuroimaging studies of creativity and insight. *Psychological Bulletin*, *136*(5), 822–848. https://doi.org/10.1037/a0019749

Fink, A., Benedek, M., Grabner, R., Staudt, B., & Neubauer, A. (2007). Creativity meets neuroscience: Experimental tasks for the neuroscientific study of creative thinking. *Methods*, *42*(1), 68–76. https://doi.org/10.1016/j.ymeth.2006.12.001

Foxe, J. J., Simpson, G. V., & Ahlfors, S. P. (1998). Parieto-occipital approximately 10 Hz activity reflects anticipatory state of visual attention mechanisms. *Neuroreport*, *9*(17), 3929–3933. https://doi.org/10.1097/00001756-199812010-00030

Fries, P. (2005). A mechanism for cognitive dynamics: Neuronal communication through neuronal coherence. *Trends in Cognitive Sciences*, *9*(10), 474–480. https://doi.org/10.1016/j.tics.2005.08.011

Furtak, S. C., Cho, C. E., Kerr, K. M., Barredo, J. L., Alleyne, J. E., Patterson, Y. R., & Burwell, R. D. (2009). The Floor Projection Maze: A novel behavioral apparatus for presenting visual stimuli to rats. *Journal of Neuroscience Methods*, *181*(1), 82–88. https://doi.org/10.1016/j.jneumeth.2009.04.023

Girardeau, G., Benchenane, K., Wiener, S. I., Buzsáki, G., & Zugaro, M. B. (2009). Selective suppression of hippocampal ripples impairs spatial memory. *Nature Neuroscience*, *12*(10), 1222–1223. https://doi.org/10.1038/nn.2384

Gray, C. M., & Singer, W. (1989). Stimulus-specific neuronal oscillations in orientation columns of cat visual cortex. *Proceedings of the National Academy of Sciences*, *86*(5), 1698–1702. https://doi.org/10.1073/pnas.86.5.1698

Gray, Charles M., König, P., Engel, A. K., & Singer, W. (1989). Oscillatory responses in cat visual cortex exhibit inter-columnar synchronization which reflects global stimulus properties. *Nature*, *338*(6213), 334–337. https://doi.org/10.1038/338334a0

Green, J. D., & Arduini, A. A. (1954). HIPPOCAMPAL ELECTRICAL ACTIVITY IN AROUSAL. *Journal of Neurophysiology*, *17*(6), 533–557. https://doi.org/10.1152/jn.1954.17.6.533

Haegens, S., Nacher, V., Luna, R., Romo, R., & Jensen, O. (2011). -Oscillations in the monkey sensorimotor network influence discrimination performance by rhythmical inhibition of neuronal spiking. *Proceedings of the National Academy of Sciences*, *108*(48), 19377–19382. https://doi.org/10.1073/pnas.1117190108

Herreras, O. (2016). Local Field Potentials: Myths and Misunderstandings. *Frontiers in Neural Circuits*, *10*. https://doi.org/10.3389/fncir.2016.00101

Jacobson, T. K., Ho, J. W., Kent, B. W., Yang, F.-C., & Burwell, R. D. (2014). Automated Visual Cognitive Tasks for Recording Neural Activity Using a Floor Projection Maze. *Journal of Visualized Experiments*, *84*, 51316. https://doi.org/10.3791/51316

Jadhav, S. P., Kemere, C., German, P. W., & Frank, L. M. (2012). Awake Hippocampal Sharp-Wave Ripples Support Spatial Memory. *Science*, *336*(6087), 1454–1458. https://doi.org/10.1126/science.1217230

Jensen, O. (2002). Oscillations in the Alpha Band (9-12 Hz) Increase with Memory Load during Retention in a Short-term Memory Task. *Cerebral Cortex*, *12*(8), 877–882. https://doi.org/10.1093/cercor/12.8.877

Jensen, Ole, & Mazaheri, A. (2010). Shaping Functional Architecture by Oscillatory Alpha Activity: Gating by Inhibition. *Frontiers in Human Neuroscience*, *4*. https://doi.org/10.3389/fnhum.2010.00186

Jones, S. R., Kerr, C. E., Wan, Q., Pritchett, D. L., Hämäläinen, M., & Moore, C. I. (2010). Cued spatial attention drives functionally relevant modulation of the mu rhythm in primary somatosensory cortex. *The Journal of Neuroscience: The Official Journal of the Society for Neuroscience*, *30*(41), 13760–13765. https://doi.org/10.1523/JNEUROSCI.2969-10.2010

Kajikawa, Y., & Schroeder, C. E. (2011). How Local Is the Local Field Potential? *Neuron*, *72*(5), 847–858. https://doi.org/10.1016/j.neuron.2011.09.029

Kelly, S. P., Lalor, E. C., Reilly, R. B., & Foxe, J. J. (2006). Increases in Alpha Oscillatory Power Reflect an Active Retinotopic Mechanism for Distracter Suppression During

Sustained Visuospatial Attention. *Journal of Neurophysiology*, *95*(6), 3844–3851. https://doi.org/10.1152/jn.01234.2005

Kim, B., Kocsis, B., Hwang, E., Kim, Y., Strecker, R. E., McCarley, R. W., & Choi, J. H. (2017). Differential modulation of global and local neural oscillations in REM sleep by homeostatic sleep regulation. *Proceedings of the National Academy of Sciences*, *114*(9), E1727–E1736. https://doi.org/10.1073/pnas.1615230114

Kizuk, S. A. D., & Mathewson, K. E. (2017). Power and Phase of Alpha Oscillations Reveal an Interaction between Spatial and Temporal Visual Attention. *Journal of Cognitive Neuroscience*, *29*(3), 480–494. https://doi.org/10.1162/jocn_a_01058

Klimesch, W, Doppelmayr, M., Russegger, H., Pachinger, T., & Schwaiger, J. (1998). Induced alpha band power changes in the human EEG and attention. *Neuroscience Letters*, *244*(2), 73–76. https://doi.org/10.1016/S0304-3940(98)00122-0

Klimesch, Wolfgang. (1999). EEG alpha and theta oscillations reflect cognitive and memory performance: A review and analysis. *Brain Research Reviews*, *29*(2–3), 169–195. https://doi.org/10.1016/S0165-0173(98)00056-3

Klimesch, Wolfgang, Sauseng, P., & Hanslmayr, S. (2007). EEG alpha oscillations: The inhibition–timing hypothesis. *Brain Research Reviews*, *53*(1), 63–88. https://doi.org/10.1016/j.brainresrev.2006.06.003

Lever, C., Kaplan, R., & Burgess, N. (2014). The Function of Oscillations in the Hippocampal Formation. In D. Derdikman & J. J. Knierim (Eds.), *Space,Time and Memory in the Hippocampal Formation* (pp. 303–350). Springer Vienna. https://doi.org/10.1007/978-3-7091-1292-2_12

Middleton, S., Jalics, J., Kispersky, T., LeBeau, F. E. N., Roopun, A. K., Kopell, N. J., Whittington, M. A., & Cunningham, M. O. (2008). NMDA receptor-dependent switching between different gamma rhythm-generating microcircuits in entorhinal cortex. *Proceedings of the National Academy of Sciences*, *105*(47), 18572–18577. https://doi.org/10.1073/pnas.0809302105

Nerad, L., & Bilkey, D. K. (2005). Ten- to 12-Hz EEG Oscillation in the Rat Hippocampus and Rhinal Cortex That Is Modulated by Environmental Familiarity. *Journal of Neurophysiology*, *93*(3), 1246–1254. https://doi.org/10.1152/jn.00199.2004

Neuper, C., Klimesch, W., & Neuper-Klimesch (Eds.). (2006). *Event-related dynamics of brain oscillations* (1. ed). Elsevier.

O'Keefe, J., & Conway, D. H. (1978). Hippocampal place units in the freely moving rat: Why they fire where they fire. *Experimental Brain Research*, *31*(4). https://doi.org/10.1007/BF00239813

Pfurtscheller, G., & Aranibar, A. (1977). Event-related cortical desynchronization detected by power measurements of scalp EEG. *Electroencephalography and Clinical Neurophysiology*, *42*(6), 817–826. https://doi.org/10.1016/0013-4694(77)90235-8

Pfurtscheller, G., & Lopes da Silva, F. H. (1999). Event-related EEG/MEG synchronization and desynchronization: Basic principles. *Clinical Neurophysiology*, *110*(11), 1842–1857. https://doi.org/10.1016/S1388-2457(99)00141-8

Pfurtscheller, G., Neuper, C., Brunner, C., & da Silva, F. L. (2005). Beta rebound after different types of motor imagery in man. *Neuroscience Letters*, *378*(3), 156–159. https://doi.org/10.1016/j.neulet.2004.12.034

Pfurtscheller, G., Stancák, A., & Neuper, Ch. (1996). Event-related synchronization (ERS) in the alpha band — an electrophysiological correlate of cortical idling: A review. *International Journal of Psychophysiology*, *24*(1–2), 39–46. https://doi.org/10.1016/S0167-8760(96)00066-9

Ramadan, W., Eschenko, O., & Sara, S. J. (2009). Hippocampal Sharp Wave/Ripples during Sleep for Consolidation of Associative Memory. *PLoS ONE*, *4*(8), e6697. https://doi.org/10.1371/journal.pone.0006697

Ray, W., & Cole, H. (1985). EEG alpha activity reflects attentional demands, and beta activity reflects emotional and cognitive processes. *Science*, *228*(4700), 750–752. https://doi.org/10.1126/science.3992243

Ray, W. J., & Cole, H. W. (1985). EEG activity during cognitive processing: Influence of attentional factors. *International Journal of Psychophysiology*, *3*(1), 43–48. https://doi.org/10.1016/0167-8760(85)90018-2

Sacchet, M. D., LaPlante, R. A., Wan, Q., Pritchett, D. L., Lee, A. K. C., Hämäläinen, M., Moore, C. I., Kerr, C. E., & Jones, S. R. (2015). Attention drives synchronization of alpha and beta rhythms between right inferior frontal and primary sensory neocortex. *The*

Journal of Neuroscience: The Official Journal of the Society for Neuroscience, *35*(5), 2074–2082. https://doi.org/10.1523/JNEUROSCI.1292-14.2015

Sadaghiani, S., & Kleinschmidt, A. (2016). Brain Networks and α-Oscillations: Structural and Functional Foundations of Cognitive Control. *Trends in Cognitive Sciences*, *20*(11), 805–817. https://doi.org/10.1016/j.tics.2016.09.004

Sauseng, P., Klimesch, W., Freunberger, R., Pecherstorfer, T., Hanslmayr, S., & Doppelmayr, M. (2006). Relevance of EEG alpha and theta oscillations during task switching. *Experimental Brain Research*, *170*(3), 295–301. https://doi.org/10.1007/s00221-005-0211-y

Singer, W., & Gray, C. M. (1995). Visual Feature Integration and the Temporal Correlation Hypothesis. *Annual Review of Neuroscience*, *18*(1), 555–586. https://doi.org/10.1146/annurev.ne.18.030195.003011

Thut, G. (2006). -Band Electroencephalographic Activity over Occipital Cortex Indexes Visuospatial Attention Bias and Predicts Visual Target Detection. *Journal of Neuroscience*, *26*(37), 9494–9502. https://doi.org/10.1523/JNEUROSCI.0875-06.2006

Uhlhaas, P. (2009). Neural synchrony in cortical networks: History, concept and current status. *Frontiers in Integrative Neuroscience*, *3*. https://doi.org/10.3389/neuro.07.017.2009

Valera, F. J., Toro, A., Roy John, E., & Schwartz, E. L. (1981). Perceptual framing and cortical alpha rhythm. *Neuropsychologia*, *19*(5), 675–686. https://doi.org/10.1016/0028-3932(81)90005-1

Varela, F., Lachaux, J.-P., Rodriguez, E., & Martinerie, J. (2001). The brainweb: Phase synchronization and large-scale integration. *Nature Reviews Neuroscience*, *2*(4), 229–239. https://doi.org/10.1038/35067550

Whishaw, I. Q., & Vanderwolf, C. H. (1973). Hippocampal EEG and behavior: Change in amplitude and frequency of RSA (Theta rhythm) associated with spontaneous and learned movement patterns in rats and cats. *Behavioral Biology*, *8*(4), 461–484. https://doi.org/10.1016/S0091-6773(73)80041-0

Worden, M. S., Foxe, J. J., Wang, N., & Simpson, G. V. (2000). Anticipatory biasing of visuospatial attention indexed by retinotopically specific alpha-band

electroencephalography increases over occipital cortex. *The Journal of Neuroscience: The Official Journal of the Society for Neuroscience*, *20*(6), RC63.

CHAPTER 4

CONCLUSIONS: FUNCTIONAL DIFFERENTIATION OF THE HIPPOCAMPUS AND POSTRHINAL CORTEX DURING ASSOCIATIVE LEARNING

Abstract

In the included set of studies, I examined the neural correlates of associative learning in the hippocampus and postrhinal cortex. Both regions have crucial learning-phase specific roles in the formation of associations with context. To examine the functions of these regions during different phases of learning, it was necessary to design a task that provided an environment in which learning was both discrete, such that we could quantifiably measure the stages of learning, as well as ongoing, such that the learning phases could be recreated multiple times with the presentation of a new discrimination. To accomplish this, we developed a novel location bi-conditional discrimination task that provided the opportunity to observe associative learning using a complex, context-guided rule. Using this task, we were able to dissociate the functions of the hippocampus and the postrhinal cortex in rule learning and in associative learning. Briefly, we found that the POR represents the conjunction of an object with a particular location before the learning of an association has occurred, suggesting that here, this conjunction is a signature of context representation. We also discovered alpha-like oscillations, or "flutters", that were previously undescribed in the rodent brain. These flutters mostly closely resemble attentional alpha as recently described in the human brain, suggesting the need to update the oscillatory bands defined in the rodent.

Introduction

Associative learning is a necessary component of survival and growth. Both the hippocampus (HC) and the postrhinal cortex (POR) are important for the formation of associations with context. Generally, the POR is considered part of the "spatial" pathway that feeds location and context-based information to the HC. The HC is then suggested to bind together item information from the perirhinal cortex (PER) with spatial information from the POR to form a representation of the context, and then also to use this representation to associate items with a particular context. We propose, however, that the POR plays more of a role in the representation of the context than previously attributed to it. Our overarching hypothesis is that the POR uses information from multiple sources to form representations of environmental contexts, monitors those contexts for changes, and updates context representations when changes occur. Other regions then use these representations of contexts for multiple purposes, for example, forming context frames, identifying objects and items, associative learning, episodic memory, as well as a variety of context guided behaviors. A specific example is hippocampal dependent associative learning, such as the association of a particular item with a particular location (Eichenbaum et al., 2007). Komorowski et al., (2009) showed that as animals are learning to associate items in context, cells with place correlates take on object correlates. Thus, in the HC item-location conjunctive coding emerged with learning. This sort of conjunctive coding is thought to be a signature of representations of the spatial layout of objects and features of in the local environmental context. One prediction of our overarching hypothesis is that conjunctive coding supporting context representations in the POR

should be present before conjunctive coding supporting associative learning in the HC emerges.

To examine the functions of these regions during different phases of learning, we recorded single units and local field potentials in a complex location bi-conditional discrimination (locBCD) task that provided the opportunity to observe associative learning using a complex, context-guided rule. Using this task, we were able provide evidence for a functional differentiation of the HC and POR in the representation of context and in context-guided associative learning.

This dissertation examined two main arenas in which the functions of HC and POR can be distinguished during learning: single-unit firing patterns and oscillatory activity.

Task-related epoch and location responses differ between HC and POR

A trial starts after the animal has waited a variable amount of time in the middle of the maze and triggered stimulus onset. During the stimulus onset epoch, the animal must detect the presented visual stimuli, spatially orienting itself within the task to ensure use of the appropriate location-based rule. During the selection epoch, the animal has to process and integrate the collected relevant visual and spatial information to choose which target to approach, direct its attention to the target, and move to make the correct choice in order to be rewarded. These stimulus onset and selection epochs provide opportunities to examine how the HC and POR represent different timeframes within a trial as well as how location-based reference frames are utilized in each area to complete the task.

In our examination of single unit activity during the locBCD task, we found that HC and POR cells showed specific yet different responses to the epochs surrounding stimulus onset and selection. During the peri-stimulus epoch, 28% of cells recorded in the HC represented stimulus onset compared to only 15% of cells recorded in the POR (X^2 = 9.1275, $p<0.05$). Conversely, cells in the POR represented the interaction of stimulus onset and trial outcome more than the HC with 11% in the POR compared to only 4% in the HC (X^2 = 5.0236, $p<0.05$; see Table 2.1). While subtle, this statistically significant difference is the first indication that the POR is representing contextually relevant conjunctions earlier than the HC. Further, these differences between regions were driven predominantly by the pyramidal cells of the regions. HC pyramidal cells showed a significantly higher occurrence of response to stimulus onset compared to the POR (X^2 = 9.6646, $p<0.05$) while the POR had significantly more pyramidal cells that responded to the interaction of stimulus presentation and outcome of the trial (X^2 = 9.5929, $p<0.05$).

In the location analysis, we found that, whereas the HC had more location representations overall, when assessed by reference frames, the POR had significantly more allocentric-only representations, whereas the HC had more allocentric-egocentric interactions. Further, we found that these differences were also predominately driven by the pyramidal cells in each region (allocentric and egocentric: X^2 = 55.86, $p<0.0001$; allocentric only: X^2 = 12.55, $p<0.001$; Table2.2; Figure 2.7A, C). This finding for the HC is not surprising as allocentric-egocentric interactions are likely a large component of place cells' robustly punctate characteristic, and both allocentric and egocentric spatial information processing is necessary for navigation. The greater allocentric-specific representation in the POR is also interesting. It suggests that while both allocentric and

egocentric references frames are necessary to move around and behave appropriately in the environment, allocentric spatial information is more important for stable representations of context that can be monitored for changes over time.

Object-location conjunction formation differs between HC and POR

The locBCD task permitted examination of HC and POR neuronal responses to the presented objects, the behaviorally relevant locations, and the conjunction of an object in a particular location. The formation of an object-location conjunction, in which a neuron responds more to an object in a particular location than to either the object or the location alone, could be an indication of multiple things. First, this conjunctive coding could represent the formation of an association between object and location. This is likely the case in the conjunctions that have been previously observed in the HC (Komorowski et al., 2009), especially considering that they were found to emerge with the learning of the association. Alternatively, the formation of an object-location conjunction could be indicative of a mechanism through which complex representations, such as the representation of a context, are formed prior to the full learning of an association.

To examine what object-location conjunctions represented in each area, we initially blocked the training sessions of the locBCD task into early, mid, and late sessions to compare the occurrence of object-location conjunctions between the HC and POR by day. Based on Komorowski et al. (2009) showing that item-place, or object-location, correlates emerged with the learning of an association in the HC combined with those of Burwell and Hafeman (2003) showing that the POR remaps quickly when the environment changes, we expected to see conjunctions in the POR in earlier sessions than

we saw them in the HC. This would support the view that conjunctive coding in the POR supports context representations that must be present before context can be associated with an item or object. This is not, however, what was found (see Figure 2.11). Instead, we found that in early sessions and mid sessions, the HC had significantly more conjunction correlates than the POR [early: HC: 40%, POR: 16%, $X^2 = 14.29$, $p<0.05$; mid: HC: 49%, POR: 25%, $X^2 = 11.29$, $p<0.05$]. Further, we found that when the cells of each region are separated by cell type, we see that the patterns observed in the overall data were mainly driven by pyramidal cells, although there was a strong response from POR FS cells (Figure 2.11B, D). This response was not significantly greater than that of the HC FS cells, likely due to the low numbers of total FS cells recorded.

Initially this result was surprising. We had expected that because the POR appeared to form representation of the contextual environment more immediately than the HC, and because the task took multiple sessions to learn the rule, that the division of sessions in this manner would show conjunctions in POR sooner than they were seen in the HC. It is likely, however, that learning the rules of the task, which were complex, would be necessary before we could observe leaning the object-context associations. Therefore, once we took into account that most of the features of the local physical environment were completely stable across many sessions, and that the same objects were used for a high number of sessions, we reasoned that these highly familiar objects might not trigger a remapping of the current context. If that were the case, we might not see conjunctive coding in support of context representations. On that basis, we decided to examine the sessions in which novel object pairs were presented. These novel object sessions provided the potential to 1) identify conjunctions in support of updating the

current context, and 2) to observe the levels of conjunctive coding in the absence of associative learning. Further, this analysis more closely matches that which was done by Komorowski and colleagues (2009) as they examined conjunction emergence within single sessions as opposed to across multiple sessions.

When only sessions with novel pairs were examined and trials within each session were split into "initial" and "ending" trials, we do, in fact, see a striking difference in the timing of conjunction emergence in the POR and HC (see Figure 2.12). In the first half of the session, or early trials, 40% of the POR cells recorded showed object-location conjunctions, compared to 5% of HC cells ($X^2 = 20.92$, $p<0.0001$). Further, in this analysis, the fast spiking cells of the POR showed an extremely strong response to the presentation of novel objects with respect to forming object-location conjunctions. This provides strong evidence that, consistent with our hypothesis, the POR represents object-location conjunctions in the local physical environment on a faster time scale than the HC, along with the suggestion that these quick remappings may be dependent on fast spiking cells within the region. These findings are consistent with the view that POR is monitoring the current context for changes, and provides further evidence that object-location conjunctions in the HC support associative learning.

Novel oscillatory events discovered in the HC and POR

During the examination of the relative timing of conjunction emergence in the POR compared to the HC, novel oscillatory events were observed that spanned both the HC and POR electrode bundles. Before the flutters were accepted as an actual observed phenomenon, we first established what other sources these events might stem

from such as physical noise. Several potential sources were identified: grooming/scratching, chewing/bruxing, and physical banging of the implant on the walls of the maze. Methodically, each of these potential sources were eliminated. We next examined the possibility of volume conduction leading to the observation of the events in both the HC and the POR. To do this, we examined the peak times of the flutters in both regions as well as the phase differences between the oscillatory events in both regions. If the oscillatory event was being volume conducted and subsequently recorded in the other region, we might expect that the peak times in one region would be nearly identical to the peak times in the other. Similarly, if the oscillatory event was volume conducted from one region to another, we might expect that the phase of the oscillations in each region would be stable with respect to each other. As shown in Figure 3.6, neither of these are the case. Instead, when the peak times are examined between regions, we see that the first peak of a POR flutter tends to happen approximately 3 ms before the first peak of a HC flutter (Figure 3.6A). We also see that if we examine the phase difference of the flutters between the two regions, we do not see a consistent difference over time but instead one that is fairly variable (Figure 3.6B). Together, these data suggest that the flutters are likely not being volume conducted from one of the recorded regions to the other. Based on this specific difference in peak times where the POR peaks before the HC, one potential explanation is that a generator region that is spatially closer to the POR is responsible for the generation of these flutter events, or one that preferentially transmits posteriorly, such as the thalamus.

In characterizing these novel oscillations, we determined three main features. First, we found that flutters consist of a relatively high amplitude pulse lasting an average

of 2-5 seconds and ranging in duration from .9 s – 10.5 s. These events appeared to begin and end with ramping, reaching their peak amplitude within 200-500 milliseconds of starting and decreasing amplitude approximately 200-500 milliseconds before ending. Second, we observed that these events appear to be distinct from theta despite falling within the previously defined theta range for rodents. Specifically, they had a well-defined presence on the real-time spectrogram at approximately 10 Hz, with harmonics at 10 Hz intervals, and we were able to observe 2 peaks in the power spectral density suggesting a potential separation of frequencies. Third, the flutters were associated with a clearly defined immobility-based velocity profile that specifically differs from the movement-related theta that has previously defined this frequency range.

Flutters occurred during three distinct epochs of each trial. The first epoch, Post Stimulus, consisted of the time from stimulus onset to the time immediately before choice. The Post Selection epoch consisted of the time immediately following selection to 5 seconds after selection. The Inter-Trial epoch consisted of the time following the Post Selection interval until the triggering of a new trial (see Figure 3.1). Within these epochs, we found that 53% of the flutters occurred in the Post Stimulus epoch, 26% occurred in the Post Selection epoch, and 21% occurred in the Inter-Trial epoch.

Further, we examined the duration and bout numbers of the flutters for behavioral relevance. We found that the average flutter duration was 2-5 seconds (Figure 3.9A). Flutter duration did not appear to correlate with the particular epoch in which it occurred. When we examined flutter duration across and within sessions, we found that flutter duration peaked during Mid Sessions, and that they increased throughout a given session (Figure 3.9E, F). When we examined number of bouts, we found that most flutters

occurred in individual bouts, but if there were multiple bouts, 2 bouts were most likely (Figure 3.10A), and series distribution mimicked overall flutter distribution between the epochs. When we examined number of bouts across and within sessions, we found that bout numbers again peaked during Mid Sessions, and that again they increased throughout a given session (Figure 3.10D, E).

We also examined the use of simple versus complex strategies in correlation with the occurrence of the flutters. In an effort to increase the number of intracranial stimulation rewards received, rats will go through a predictable series of strategies as they work towards determining the correct rule. These strategies include focusing on an egocentric location, an allocentric location, or a particular object. Here, we found that 5% of flutters occurred when the animal was employing an object-based strategy, 16% while the animals was employing a location-based strategy (9% allocentric, 7% egocentric), 29% of flutters occurred while the animal appeared to be using multiple strategies, and 50% when the animal was using a putative complex strategy. This large proportion of the flutters associated with the lack of use of a defined simple strategy suggests that the animal was likely "on task" and actively engaged with determining the complex rule rather than attempting a simpler solution.

We further examined strategy associated flutter occurrence across and within sessions. When we look at strategy usage regardless of flutter occurrence, we see that strategy usage did not differ widely either across sessions (Figure 3.7B) or across trials (Figure 3.7D), with animals predominately using multiple strategies, and/or switching strategies often throughout all sessions and trials. However, if we look at the strategies employed during the occurrence of a flutter, we see a different pattern. First, if we look

across sessions, we can see that the majority of flutters were associated with a complex strategy across Early, Mid, and Late sessions (Figure 3.7A). If we examine trials on which flutters occurred within sessions (Figure 3.7C), we see that during the Initial trials of a session, the flutters that were recorded were most often associated with multiple strategies, but this changed starting with the Mid trials. In the middle of a session, flutters started to become more often associated with a complex strategy, and this persisted until the end of the session, through Ending trials. These differences in general strategy usage compared to flutter-associated strategy usage suggests that flutters are correlated with the complex thought needed to complete this unusually difficult task.

Finally, we looked at flutter occurrence with respect to performance. Because this was a very difficult task for the rats to learn, their averaged performance when looking either across or within trials appears to stay around chance (see Figure 3.11A, B) and has no apparent correlation with the occurrence of flutters. If we instead look at the number of TTC with respect to flutter occurrence, while the number of TTC in a given session does not seem to correlate with whether or not flutters were seen on that day (see Figure 3.11C-F, G), when we look within a session, we see that both the occurrences of flutters and the number of TTC reached within a session increase as the session goes on, with the lowest number of both flutters and TTC occurring during Initial trials and finishing with the highest numbers in the Ending trials. Therefore, although flutters do not appear to directly correlate with better average performance, they do appear to correlate with better acute performance.

The described features of these novel flutter events are consistent with the most recently described functions of alpha oscillations in humans. The similarities include the observations that increases in alpha power can be viewed as a functional correlate of active cognitive task performance, specifically as an active mechanism of selective attention (Klimesch et al., 2007), and that increases in alpha activity happen in correlation to internally directed attention (Cooper et al., 2003). EEG alpha activity in humans has also been found to correlate with creative cognition in tasks designed to elicit divergent thinking, which require generation of original and creative ideas to solve problems (Arden et al., 2010; Dietrich & Kanso, 2010; Fink et al., 2007).

When these novel flutter events observed in the complex locBCD task are considered in the framework of the proposed functions of alpha, we find exciting potential interpretations. The locBCD task was difficult for the rats to learn, requiring adaptation of both the location cues and the reward paradigm to facilitate the acquisition of two location-specific rules simultaneously. This increase in difficulty level differs from canonical rodent learning and memory tasks as rodent tasks are generally designed to be easily trained, quickly learned, and performed with a high degree of accuracy; therefore, they rarely require overly complex or creative problem solving. We believe this change in difficulty level, combined with the recording of the HC and POR, facilitated the discovery of these previously undescribed oscillation events. Based on the nature of the task, we suggest that flutter is attentional alpha.

Currently defined oscillation bands in rodents	Proposed oscillation bands in rodents	Currently defined oscillation bands in primates
Delta = 1-4 Hz	Delta = 1-4 Hz	Delta = 1-4 Hz
Theta = 4 – 12 Hz	Theta = 4 – 10 Hz	Theta = 4 – 7 Hz
	Alpha = 9 – 13 Hz	Alpha = 8 – 12 Hz
Beta = 12 – 30 Hz	Beta = 13 – 30 Hz	Beta = 13 – 30 Hz
Slow Gamma = 35 – 55 Hz	Slow Gamma = 35 – 55 Hz	Slow Gamma = 35 – 55 Hz
Fast Gamma = 65 – 100 Hz	Fast Gamma = 65 – 100 Hz	Fast Gamma = 65 – 100 Hz

Figure 4.1. Currently defined oscillation bands in the rodent and primate compared to our proposed set of oscillation bands. Theta would shift down, ending at 10Hz to ensure all of cortical theta was captured. Alpha would slightly overlap with theta to ensure all flutters were caught regardless of individual differences.

Our findings suggest the need to update the defined oscillation bands in the rodent to include a defined alpha band, therefore we suggest the shift of theta to 4-10 Hz, with alpha as 9-13 Hz (Figure 4.1). These specific values of theta were chosen based on the average frequency we see movement- and attention-correlated theta in the rodent, which is typically 8.5 Hz. The values for alpha were determined based on the range of frequencies around ~10 Hz that were observed between animals.

Early- and late-stage learning in the HC and POR

Together, this single unit and oscillation data indicate that there are interesting patterns with respect to early- and late-stage learning within the HC and POR. First, it's clear that the POR is particularly important in the early stages of learning, forming object-location conjunctions well before they are seen with the learning of an association in the HC. Our interpretation is that POR conjunctive coding is a reflection of the

updating of the current context. This is consistent with our hypothesis that the POR rapidly and automatically updates the spatial layout of objects and features of the local context. These representations are likely then used by other regions, including the HC, to support the learning of associations and the formation of episodic memories.

Other brain regions likely interact with the POR and the HC in the service of episodic memory. For example, one question not often asked is how, from all the information available at any given time, is only a subset of information selected to be encoded in episodic memory. Likely candidates for subserving this attentional function are the retrosplenial cortex (RSC), the posterior parietal cortex (PPC), and the lateral posterior nucleus of the thalamus, also called the pulvinar. Studies from our lab have provided evidence that these regions, which are highly interconnected with each other and with the POR, are involved in both allocentric and egocentric spatial reference frame processing, as well as in visuo-spatial attention (Hwang & Burwell, 2020, Yang et al., 2017; Yang & Burwell, 2020). I would expect this pattern to hold in both non-human primates and humans, as extensive functional homology has been demonstrated between the POR and the PHC. Taken together, these findings across regions suggest a broader network that may support complex cognitive functions that require problem solving, rule learning, selection, abstraction, and integration (Figure 4.3). Each of these regions should be examined for attentional alpha in a complex task like the locBCD task which involves simultaneous learning of hierarchical rules, associative learning, and context-guided behavior

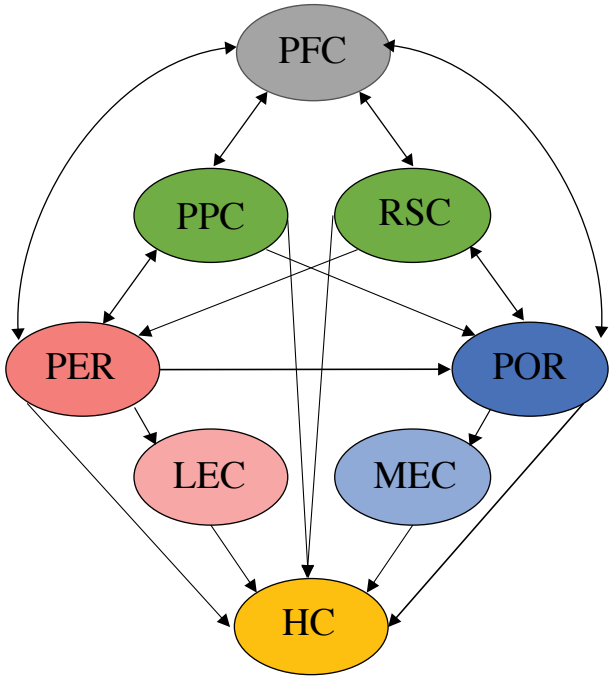

Figure 4.2. A proposed circuit for supporting the capacity to use divergent thinking to solve complex problems. Prefrontal cortex (PFC) in grey provides hierarchical cognitive control; Posterior parietal cortex (PPC) and retrosplenial cortex (RSC) participate in attention and selection; perirhinal cortex (PER) and lateral entorhinal cortex (LEC) process content and topological space; the postrhinal cortex (POR) and medial entorhinal cortex (MEC) process context and euclidian space; and the hippocampus (HC) is involved in associative learning and episodic memory. Each of these regions should be examined for attentional alpha in a complex task like the locBCD task which involves simultaneous learning of hierarchical rules, associative learning, and context-guided behavior.

Future Work

Future experiments to provide more in-depth analysis to fully characterize these novel oscillations would be beneficial, as would additional experiments to recreate and further examine the situations and environments in which they are generated. Expanding the brain regions in which these flutters are studied would also be an interesting avenue. If our hypothesis is correct, and these flutters represent internally directed attention to allow creative thinking, this likely takes the form of cognitive inhibition of other processes during the duration of the flutter. The use of silicone probes with multiple depth channels would provide a larger picture of the regions in which these flutters occur

simultaneously, while optogenetic inhibition of the flutter frequency would provide a causational connection between the flutters and the performance of the task. We have provided an interesting snapshot into a previously undescribed phenomenon, but more extensive and more targeted probing will allow us to fully elucidate the purpose of these neural mechanisms.

Summary

Our observations are consistent with the interpretation that creative strategies employed to learn complex associations are accompanied by an increase in alpha-like flutters. We propose that these flutters are an indication of internally directed attention for the purpose of creative thinking. To our knowledge, this is the first compelling evidence that rodents exhibit attentional alpha similar to attentional alpha described in humans.

References

Arden, R., Chavez, R. S., Grazioplene, R., & Jung, R. E. (2010). Neuroimaging creativity: A psychometric view. *Behavioural Brain Research*, *214*(2), 143–156. https://doi.org/10.1016/j.bbr.2010.05.015

Benedek, M., Bergner, S., Könen, T., Fink, A., & Neubauer, A. C. (2011). EEG alpha synchronization is related to top-down processing in convergent and divergent thinking. *Neuropsychologia*, *49*(12), 3505–3511. https://doi.org/10.1016/j.neuropsychologia.2011.09.004

Burwell, R. D., & Hafeman, D. M. (2003). Positional firing properties of postrhinal cortex neurons. *Neuroscience*, *119*(2), 577–588. https://doi.org/10.1016/s0306-4522(03)00160-x

Cooper, N. R., Croft, R. J., Dominey, S. J. J., Burgess, A. P., & Gruzelier, J. H. (2003). Paradox lost? Exploring the role of alpha oscillations during externally vs. internally directed attention and the implications for idling and inhibition hypotheses. *International Journal of Psychophysiology*, *47*(1), 65–74. https://doi.org/10.1016/S0167-8760(02)00107-1

Dietrich, A., & Kanso, R. (2010). A review of EEG, ERP, and neuroimaging studies of creativity and insight. *Psychological Bulletin*, *136*(5), 822–848. https://doi.org/10.1037/a0019749

Eichenbaum, H., Yonelinas, A. P., & Ranganath, C. (2007). The medial temporal lobe and recognition memory. *Annual Review of Neuroscience*, *30*, 123–152. https://doi.org/10.1146/annurev.neuro.30.051606.094328

Fink, A., Benedek, M., Grabner, R., Staudt, B., & Neubauer, A. (2007). Creativity meets neuroscience: Experimental tasks for the neuroscientific study of creative thinking. *Methods*, *42*(1), 68–76. https://doi.org/10.1016/j.ymeth.2006.12.001

Klimesch, W., Sauseng, P., & Hanslmayr, S. (2007). EEG alpha oscillations: The inhibition–timing hypothesis. *Brain Research Reviews*, *53*(1), 63–88. https://doi.org/10.1016/j.brainresrev.2006.06.003

Komorowski, R. W., Manns, J. R., & Eichenbaum, H. (2009). Robust Conjunctive Item-Place Coding by Hippocampal Neurons Parallels Learning What Happens Where. *Journal of Neuroscience*, *29*(31), 9918–9929. https://doi.org/10.1523/JNEUROSCI.1378-09.2009

Yang, F.-C., & Burwell, R. D. (2020). Neuronal Activity in the Rat Pulvinar Correlates with Multiple Higher-Order Cognitive Functions. *Vision*, *4*(1), 15. https://doi.org/10.3390/vision4010015

Yang, F.-C., Jacobson, T. K., & Burwell, R. D. (2017). Single neuron activity and theta modulation in the posterior parietal cortex in a visuospatial attention task: POSTERIOR PARIETAL CORTEX: PERCEPTION TO ACTION. *Hippocampus*, *27*(3), 263–273. https://doi.org/10.1002/hipo.22691